SOME KINETIC PROPERTIES OF LIQUID HELIUM AT VERY LOW TEMPERATURES

A Thesis submitted

for the Degree of

Doctor of Philosophy

in the

University of Oxford

by

G. A. Brooker, M.A.

BODLEIAN LIBRARY OXFORD
DEPOSITED
THESIS
VII.1.65

Trinity Term,

1964.

Pembroke College

Oxford

ACKNOWLEDGEMENTS

It is a pleasure to record here my sincere thanks to

Professor B. Bleaney for extending to me the facilities of the Clarendon Laboratory;

Professor L. Fox for extending to me the use of the Mercury Computer at the Oxford University Computing Laboratory;

Dr. J. Wilks, my supervisor, for his generous encouragement and assistance;

Dr. B. E. Keen, Dr. D. S. Betts, and Dr. P. M. Richards for many valuable discussions;

the Department of Scientific and Industrial Research for a Research Studentship.

CONTENTS

Abstract

Chapter 1: Introduction

1. 1

2. Possible Measurements 8

3. Measurement of Acoustic Impedance 10

4. Theoretical Analysis 12

Chapter 2: Experimental

1. Introduction 14

2. Theory of the Measurement 16

3. Production of High-frequency Sound 19

4. Propagation Effects 27

5. Microwave Cavities 31

6. Cryogenics 33

7. Electronics 35

8. Crystal Testing 37

9. Improving the Sensitivity 41

Chapter 3: Theory of Sound Propagation in Liquid He^3

1. Landau's Theory 47

2. Oscillations in He^3: general 53

3. Dispersion of Sound 59

4. The Number of Solutions 63

Chapter 4: The Acoustic Impedance of Liquid He^3

1. Introduction 71

2. The Kinetic Equation 72

3. Boundary Condition 74

4. Solution of the Kinetic Equation 77

5. Physical Interpretation 88

Chapter 5: Extending the Theory

1. 93

2. Estimates of F_2 96

3. Calculation of the Acoustic Impedance: Including F_2 98

4. Numerical Analysis 104

5. Results 118

Chapter 6: Discussion

1. 123

2. The Transport Coefficients 125

3. The Specific Heat 127

4. Transverse Waves 130

5. The Kapitza Boundary Resistance 131

6. Conclusions 135

References

ABSTRACT

The theoretical picture of liquid helium 3 which is currently accepted is due to Landau (1957 a). According to this theory, the propagation of sound in He^3 should show a new phenomenon, called zero sound, if the liquid is excited at a high acoustic frequency and at low temperatures. This thesis describes theoretical and experimental investigations into this phenomenon.

We have attempted a measurement of the acoustic impedance of liquid He^3 at a frequency of 10 000 Mc/s. In the method of measurement adopted, a travelling sound wave is reflected up and down inside a quartz crystal immersed in liquid He^3. The acoustic impedance of the liquid is found by measuring the loss of energy from the crystal due to the radiation of sound out into the liquid. In order to obtain useful accuracy, it is necessary to obtain a crystal in which the sound wave can be reflected back and forth at least 250 times. Preliminary experiments performed with various crystals showed that it was not hard to obtain a crystal which would give 100 echoes, but that obtaining a larger number presented unexpected difficulties. Various attempts were made to improve the performance of the apparatus, but the experiment was eventually abandoned as our theoretical analysis appeared to be more promising.

For the theoretical work, we have analysed measurements of the acoustic impedance of liquid He^3 at a frequency of 1000 Mc/s which have been made by Keen, Matthews, and Wilks (1965). The theoretical expressions used are an extension of those given by Bekarevich and Khalatnikov (1961), who give expressions related to the acoustic impedance as part of a calculation of the Kapitza thermal boundary resistance. Using the same assumptions as Bekarevich and Khalatnikov, we find that the acoustic impedance Z divided by the density ρ should rise from 185 m/s to about 190 m/s when the temperature is reduced through $0{\cdot}09^{\circ}K$. The experimentally observed rise in Z/ρ is 19 ± 6 m/s, so the theory appears to underestimate the change in Z/ρ , and we have considered how the theory should be modified to account for the discrepancy.

In the theory of a Fermi liquid due to Landau (1957 a), the forces of interaction between the particles of the liquid are taken into account by introducing certain parameters F_0, F_1, F_2, . . . which are determined from experimental measurements. Bekarevich and Khalatnikov include only two parameters (F_0, F_1) as these are the ones most easily derived from experiment. We have been able to estimate a third parameter (F_2), and have used this to obtain revised values of the acoustic impedance. These values of Z/ρ are still a little smaller than the experimental points, but we regard the agreement as satisfactory. We conclude that the experimental results of Keen, Matthews, and Wilks are consistent with

Landau's theory of a Fermi liquid, and provide valuable support for the existence of zero sound.

CHAPTER 1

Introduction

1.1

The two isotopes of helium, He^3 and He^4, are the only substances which can exist as liquids at temperatures approaching absolute zero. Of these isotopes, He^3 forms only about one part in 10^6 of natural helium, so most investigations of liquid helium have been done on He^4. However, during the last 16 years, a gradually increasing supply of artificial He^3 (formed as the decay product of tritium) has become available, and many of the properties of liquid He^3 have now been measured.

The electronic structure of a helium atom is the same for both isotopes, except that the reduced mass of the electrons differs slightly in the two cases, due to the difference in nuclear mass. This implies that the van der Waals forces between He^3 atoms and between He^4 atoms should be almost identical. Therefore at first sight, one would expect He^3 and He^4 to behave in very similar ways in the liquid state, with only simple factors like 4/3 relating the properties of one isotope to those of the other. However, in liquid helium, the de Broglie wavelength of an atom is greater than the mean atomic spacing, and consequently it is not permissible to describe the liquid by treating the atoms as individuals. It is neces-

sary to give a quantum-mechanical description by constructing a wave-function for the liquid. In doing this, one has to note that He^4 is composed of bosons, so that the atoms obey Bose-Einstein statistics, while He^3 atoms have spin $\frac{1}{2}$, and so are fermions obeying Fermi-Dirac statistics. Thus, in spite of the similarity in the interatomic forces, the wave functions representing liquid He^3 and liquid He^4 are quite different.

The properties of liquids He^3 and He^4 observed experimentally do indeed show considerable differences. For example He^4 becomes superfluid when cooled below $2{\cdot}17^{\circ}K$, while He^3 is a normal fluid down to the lowest temperature so far investigated ($0{\cdot}006^{\circ}K$). It is therefore clear that the quantum statistics is all-important to any theoretical account of the properties of liquid helium.

To see how far the properties of liquid He^3 can be accounted for in terms of Fermi-Dirac statistics, it is natural to compare He^3 with a perfect Fermi-Dirac gas, as this is the simplest model which takes account of the statistics.

In a Fermi gas, the probability that a quantum level of energy ε shall be occupied is

$$n(\varepsilon) = \frac{1}{e^{\frac{\varepsilon-\mu}{kT}} + 1} \qquad (1.1)$$

where μ is the Fermi energy, k is Boltzmann's constant, and T is the absolute temperature. The momentum of an atom of energy μ is called

the Fermi momentum, and it is given by

$$\frac{p_F^2}{2m} = \mu \qquad \text{or} \qquad p_F = \hbar (3\pi^2 N)^{1/3} \tag{1.2}$$

where m is the mass of a He^3 atom, and N is the number of atoms per unit volume. Then the Fermi temperature, defined by $kT_F = \mu$ is given by

$$T_F = \frac{p_F^2}{2mk} . \tag{1.3}$$

Using the known value of the density of He^3 (about 0·082 gm/cc below $1^\circ K$), one finds $T_F = 4{\cdot}95^\circ K$. Therefore one should be able to apply the theory of a degenerate Fermi gas at temperatures well below $5^\circ K$, say at $1^\circ K$ and below. In this temperature range, the specific heat of a Fermi gas is given by

$$C = \frac{k^2 p_F m}{3\hbar^3} T = 0{\cdot}225\ T \text{ joule cm}^{-3}\ {}^\circ K^{-1} \tag{1.4}$$

where C is the thermal capacity per unit volume. The magnetic susceptibility is given by

$$\chi = \frac{3N\beta^2}{2kT_F} \tag{1.5}$$

where β is the magnetic moment of a He^3 atom. χ is independent of temperature. The velocity of sound c is given by

$$c = \frac{p_F}{\sqrt{3}\,m} = 95{\cdot}4 \text{ metres sec}^{-1} \tag{1.6}$$

which is also independent of temperature.

The transport properties of a Fermi gas may be estimated as well if we assume a relaxation time for collisions between atoms. The Pauli principle acts to suppress collisions in which atoms try to enter states which are already occupied. The effect of this is that two atoms cannot collide unless they can find two vacant quantum states of suitable energy for them to go into after collision. Calculation shows that effectively suitable states may only be found within about kT of the Fermi energy, so the probability of finding an empty quantum level is proportional to T. As two are needed for a collision to occur, the collision probability $1/\tau$ is proportional to T^2. By simple kinetic theory arguments, one can derive expressions for the viscosity η, thermal conductivity κ, and diffusion coefficient D:

$$\eta = \frac{2}{3} N k T_F \tau \qquad \propto T^{-2}$$

$$\kappa = \frac{2}{3} \frac{k T_F}{m} C\tau \qquad \propto T^{-1}$$

$$D = \frac{2}{3} \frac{k T_F}{m} \tau \qquad \propto T^{-2}.$$

A comparison of these results with the measured properties of liquid He^3 shows large numerical discrepancies. The specific heat is proportional to temperature only below $0{\cdot}04^{\circ}K$ (Anderson, Salinger, Steyert, and Wheatley (1961), Strongin, Zimmerman, and Fairbank (1961), Brewer and Keyston (1961)) and it has a value about 2 - 5 times larger than that for a Fermi gas. The velocity of sound

in liquid He^3 is 185 m/s (Laquer, Sydoriak, and Roberts (1959)), which is larger than that of a Fermi gas by a factor of 1·75, and the magnetic susceptibility does not depart from Curie's law ($\chi \propto T^{-1}$) until about 0·2°K, instead of at about 2°K, as would be expected. The transport properties all have the expected temperature dependences, but only below 0·1°K, and all require different values for the constant τT^2.

It is clear from this comparison of liquid He^3 with a perfect gas that the behaviour of He^3 is considerably influenced by interactions between the atoms, though the correct prediction of temperature dependences below 0·1°K confirms the effect of the statistics. Unfortunately one cannot allow for the interactions in any simple way, for example by introducing an "effective mass" m*, as the value of m*/m needed to account for the magnetic susceptibility is about 10, while for the specific heat it is about $2\frac{1}{2}$, and for the velocity of sound 0·57 (Bernardes and Brewer (1962)).

Attempts have been made to calculate the properties of liquid He^3 by taking into account the interaction forces from first principles (e.g. Brueckner and Gammel (1958)), but the most successful theory is due to Landau (1957a,b, 1959). In Landau's theory, two interacting particles in the liquid are assumed to have an energy of interaction which depends on their momenta and spins. The gross features of this interaction are found by comparing the predictions of the theory with experiment, rather than by calculation. If

parameters describing the interaction are derived by fitting the specific heat, magnetic susceptibility, and velocity of sound to the measured values, the theory predicts values for the kinetic coefficients which agree rather well with experiment (Hone (1962)). This agreement forms the best justification of the theory so far available. Landau's theory can also account for the fact that its predictions fail above about $0{\cdot}1^{\circ}K$, so that on the whole the situation is satisfactory, though much theoretical work remains to be done before the empirically determined interaction can be accounted for by calculation from first principles.

If sound of low frequency $\omega/2\pi$ is propagated in liquid He^3, it has a velocity $c = 183$ m/s, and an absorption which can be accounted for entirely in terms of viscous damping. In this respect He^3 is a normal liquid. However, there is a relaxation time $\tau \propto T^{-2}$ for liquid He^3 just as there is for a Fermi gas (though τT^2 has different magnitudes for the two cases), and the propagation of sound is modified when $\omega\tau$ becomes of the order of 1. One would expect by analogy with a Fermi gas that for sufficiently large $\omega\tau$, the propagation of sound should become impossible, since a sound wave cannot propagate in a gas when the wavelength is of the same order as the mean free path. On this picture, the velocity and absorption of sound should both rise until $\omega\tau$ reaches a critical value (actually about 4·5 - see Fig. 18 of this thesis), at which point sound propagation should cease. It is one of the important predictions of Landau's theory

that liquid He^3 should not behave as described above, because the interactions between the particles can support a wave motion even when the period of the motion is short compared with the relaxation time ($\omega\tau \gg 1$). This wave motion carried by the interactions is called zero sound.

In principle, there can be several kinds of wave which propagate in He^3 when $\omega\tau \gg 1$, and these waves are distinguished by the polarization of the wave about the direction of propagation. The simplest wave of this type is a longitudinal motion, and the name "zero sound" is usually taken to refer to this mode only. We shall discuss the different waves in chapter 3 of this thesis, where it will be shown that a zero sound wave gives rise to oscillations in pressure, so it should be possible to detect it by means of ordinary acoustic apparatus. Zero sound is distinguished from ordinary sound by having a different velocity and attenuation.

The simplest transverse mode which can propagate for $\omega\tau \gg 1$ can be shown to give rise to an oscillating shear stress in liquid He^3. This wave, which we shall call "transverse zero sound", should therefore also be detectable with suitable acoustic apparatus. According to the theory, transverse zero sound can exist only if the forces of interaction between the particles of He^3 are sufficiently strong. The information at present available leaves it an open question whether or not transverse zero sound is to be expected in liquid He^3 under the vapour pressure, but since the effective inter-

action increases with pressure, this motion should occur for pressures of a few atmospheres.

1.2 Possible Measurements

The most natural ultrasonic experiments to perform as tests for the existence of zero sound are measurements of the velocity and attenuation of sound. Both these measurements involve considerable technical difficulties, as we shall now show. We have calculated the attenuation of sound from Landau's theory, to obtain figures relevant to the design of ultrasonic apparatus. The results of a calculation for a frequency of 9·4 Gc/s (the actual frequency used in our experiment) are shown in Fig. 1. The lower curve shows the values obtained using Landau's theory in its simplest form. The upper curve includes a quantum-mechanical correction to allow for the destruction of phonons by collisions among the particles (Landau (1957b)). The absorption is only plotted for temperatures below $0{\cdot}1^{\circ}K$, because Landau's theory does not apply for higher temperatures. It may be seen from the graph that the absorption of zero sound is of the order of 10^4 cm^{-1}, so the amplitude of a zero sound wave falls by a factor e in a distance of 1 micron. The wavelength of sound in He^3 at a frequency of 9·4 Gc/s is about 200 Å, so if a measurement of the absorption were made, it would be necessary to place an acoustic source and receiver about 1 micron apart, with their faces parallel to within about 100 Å. The transit time of the sound signal between

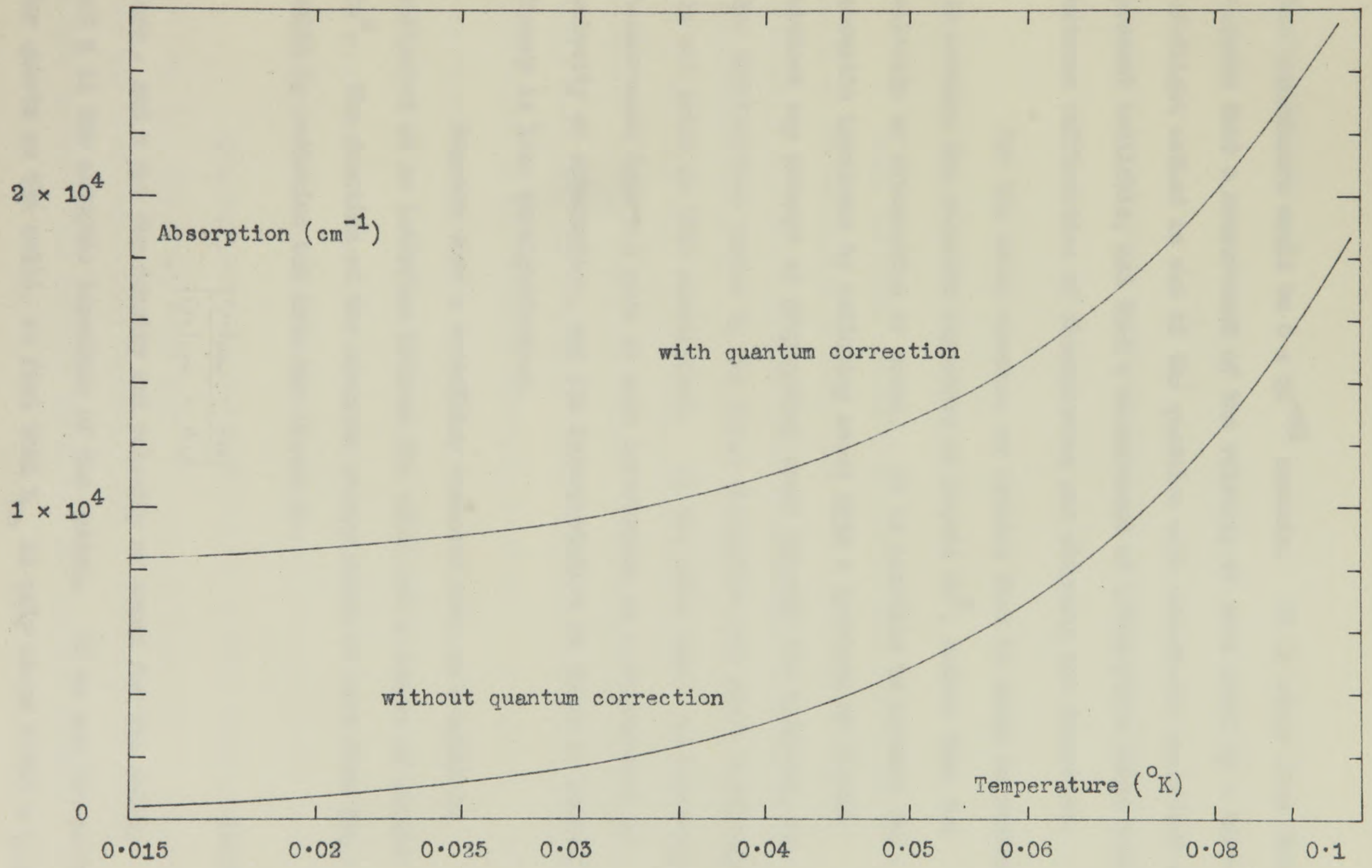

Fig. 1. Absorption of Zero Sound at 9·4 Gc/s. ($F_0 = 7{\cdot}1320$; $F_1 = 3{\cdot}6$; $F_2 = 0$)

the transducers would be 5×10^{-11} seconds. It is clear from these figures that a measurement of the velocity of zero sound by a time-of-flight method is out of the question with electronic apparatus at present available, and that a measurement of attenuation would involve extreme difficulties of dimensioning and aligning the apparatus.

For the above reasons, we decided that it would be preferable to measure the acoustic impedance of liquid He^3, rather than the velocity or attenuation of sound. It is possible to measure the acoustic impedance by radiating sound into a specimen of liquid without any attempt at propagating sound through the specimen, so the difficulties caused by the large absorption and short wavelength do not arise in this measurement. On the other hand, an impedance measurement does not give so much information as a measurement of velocity or attenuation, and its interpretation in terms of Landau's theory is less straightforward.

Suppose that a travelling acoustic wave in a solid is reflected at an interface between the solid and a sample of liquid He^3. The fraction of the acoustic energy which is lost from the solid by radiation out into the liquid is

$$\alpha = 1 - \left| \frac{(\rho c)_{solid} - Z_{He}}{(\rho c)_{solid} + Z_{He}} \right|^2 . \qquad (1.7)$$

Here ρ and c are the density and velocity of sound for the solid, and Z is the acoustic impedance of the helium. If we use the values for quartz as the solid, we find that Z_{He} is only about $0{\cdot}001 \times (\rho c)_{solid}$,

so α reduces to

$$\alpha \simeq 4 \frac{\mathrm{Re}\, Z_{He}}{(\rho c)_{solid}} \sim 0{\cdot}004.$$

Therefore by measuring α one can find the acoustic impedance of liquid He^3.

1.3 Measurement of Acoustic Impedance

Abel, Anderson, and Wheatley (1961) have shown from measurements of the absorption of sound that $\tau T^2 \sim 1{\cdot}7 \times 10^{-12}$ sec $^{\circ}K^2$. This means that if a sample of He^3 is cooled to $0{\cdot}04^{\circ}K$, one can make measurements up to an $\omega\tau$ of about 70 by using a frequency of 10 000 Mc/s, or up to about 7 by using a frequency of 1000 Mc/s. When the work described in this thesis was started, a measurement at 1000 Mc/s was being developed, and eventually (Keen, Matthews, and Wilks (1965)) gave values of the acoustic impedance up to an $\omega\tau$ of about 9. It was considered desirable to extend these measurements to larger values of $\omega\tau$. As it would have been rather hard to achieve this increase by reducing the temperature, we decided to work at a higher frequency $\omega/2\pi$, and chose to use a frequency of about 10 000 Mc/s.

The apparatus used for measuring α is shown diagrammatically in Fig. 2. The sound waves were set up in a quartz rod by subjecting one end to an oscillating electric field. A resonant microwave cavity provided this electric field, and was fed with microwave

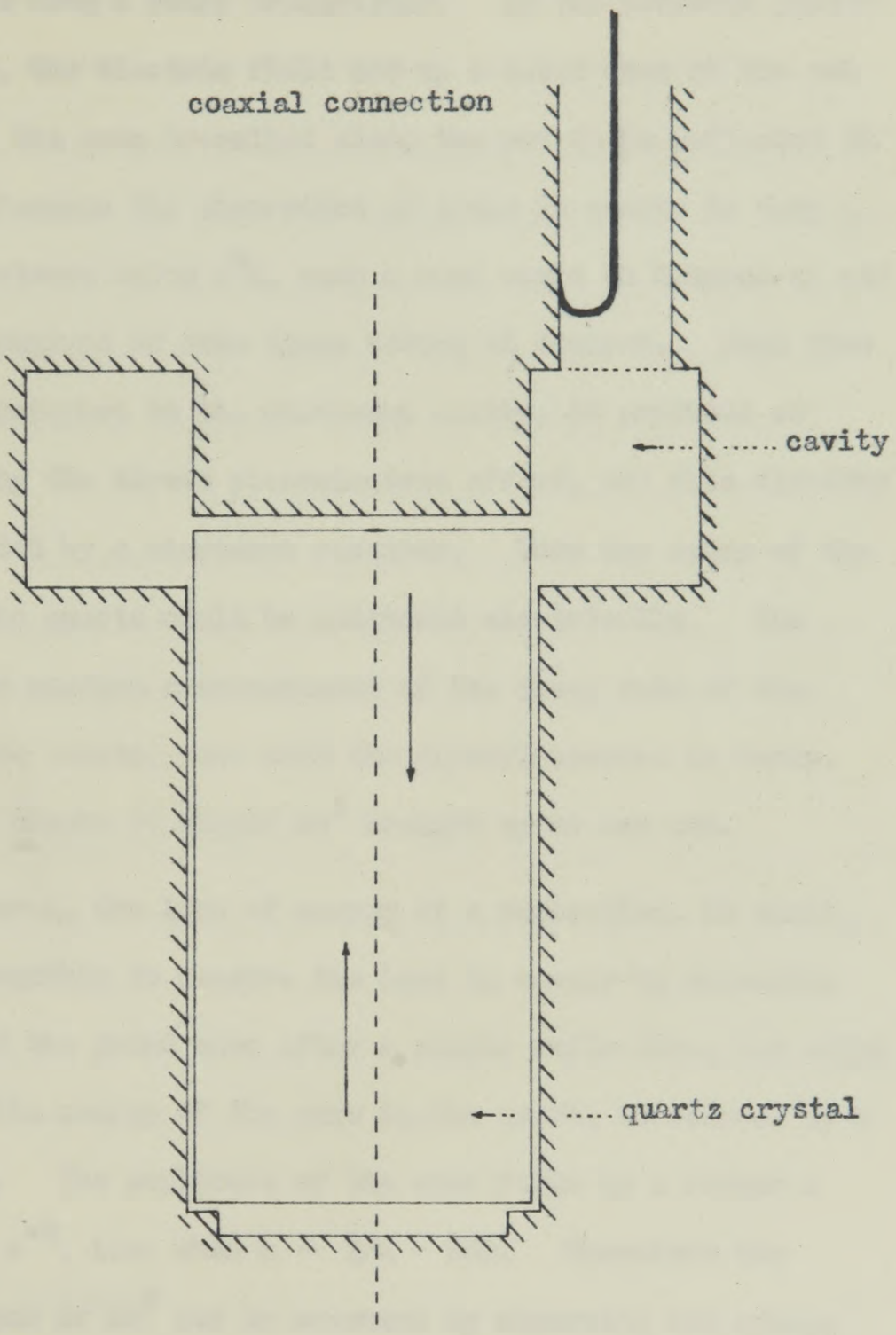

Fig. 2. Microwave Cavity (Diagrammatic)

energy in pulses from a radar transmitter. By the converse piezoelectric effect, the electric field set up a sound wave at the end of the rod, and the wave travelled along the rod to be reflected at the far end. Because the absorption of sound in quartz is very small at temperatures below $4^{\circ}K$, such a wave could be bounced up and down the rod a hundred or more times before it decayed. Each time the sound wave returned to the microwave cavity, it produced an electric field by the direct piezoelectric effect, and this electric field was detected by a microwave receiver. Thus the decay of the sound wave in the quartz could be monitored electrically. The intention was to perform a measurement of the decay rate of the sound wave in the quartz, once with the crystal mounted in vacuo, and once with a sample of liquid He^3 brought up to one end.

Because a, the loss of energy at a reflection, is small, it would be impossible to measure the loss in energy by measuring the amplitude of the sound wave after a single reflection, but after n reflections, the energy of the wave in the quarts is reduced by a factor $(1 - a)^n$. The amplitude of the wave falls by a factor e when $(1 - a)^n = e^{-2}$, i.e. when $n \simeq 2/a \sim 500$. Therefore the acoustic impedance of He^3 can be measured by observing the change in decay-rate of the acoustic wave in the quartz crystal, provided that the decay of the wave due to causes other than acoustic radiation is relatively small. As a rough estimate, one ought to have a crystal in which the 500th echo is measurable if one is to make measurements

with liquid on only one end of the crystal. If liquid is placed on both ends of the crystal, only 250 echoes need be measurable.

It was found that it was not difficult with our apparatus to observe about 50 echoes (i.e. 100 double reflections) in a reasonably good crystal, and by selecting crystals, 100 echoes could be obtained without excessive difficulty. However the amplitude was by then 3 or 4 orders of magnitude below the initial amplitude of the sound wave, an effect which is attributed not to absorption, but to distortion of the wavefront by imperfections in the polishing of the crystal. Various attempts were made to obtain a larger number of echoes, and a discussion of these is given in chapter 2 of this thesis.

It was found that achieving a decay pattern containing more than 100 echoes involved unexpected difficulties, and in consequence we decided that it would be more profitable to concentrate on a theoretical analysis of the acoustic impedance, which had been proceeding in parallel with the experimental work.

1.4 Theoretical Analysis

It was uncertain at the time when this work was started what was the relation between the acoustic impedance of liquid He^3 and the velocity of zero sound. For ordinary sound, the acoustic impedance Z is known to be given by

$$Z = \rho c \qquad (1.8)$$

where ρ is the density of the liquid, and c is the velocity of sound. The properties of zero sound are rather different from those of ordinary sound; consequently we could not be sure whether equation (1.8) would still hold with c replaced by the velocity of zero sound. This situation has now been clarified by Bekarevich and Khalatnikov (1961), who calculate a complicated expression for the acoustic impedance in the zero sound region.

We have slightly extended Bekarevich and Khalatnikov's calculation by putting the result into a form which is correct for all values of $\omega\tau$, instead of being valid for the limit $\omega\tau \to \infty$ only. A numerical evaluation of the resulting expression, carried out with the aid of an electronic computer, shows that there is reasonable agreement between the theory and the experimental results of Keen, Matthews, and Wilks. The agreement is not perfect however, for the change in acoustic impedance between the sound and zero sound regions is underestimated by a factor of about 2; this lies outside the experimental error. In order to see whether this discrepancy can be accounted for within Landau's theory, we have made a further extension to the analysis by removing an approximation used in calculating the acoustic impedance. The results of this analysis are discussed in chapter 5 of this thesis.

CHAPTER 2

Experimental

2.1 Introduction

In chapter 1, we gave the reasons for attempting to conduct an acoustic impedance measurement at a frequency of about 10 000 Mc/s. In this chapter we describe the procedures which were adopted for performing the experiment.

We have described the principle of an impedance measurement in chapter 1, but recapitulate briefly here for clarity. A plane travelling sound wave is set up in a solid rod, and is reflected up and down the rod several hundred times. The acoustic impedance of liquid He^3 is found by measuring the decay of this wave caused by surrounding the rod with a sample of liquid He^3. Now, in order to reflect a sound wave many times within a solid rod, it is necessary to use a material with a very small absorption coefficient. It is also desirable that the solid should be piezoelectric, as this facilitates the generation of the sound wave. The number of materials which satisfy these conditions is not large, and we decided upon quartz as an obvious choice. In order to generate compression waves in quartz, with the energy flow normal to the wavefront, it is necessary to use the quartz rod in the form of a single crystal cut with the X-axis along the axis of the rod. A sound wave can be generated

in such a crystal by applying an oscillating electric field normal to one end of the rod.

The appropriate configuration of electric field is conveniently obtained by using a microwave cavity, as shown diagrammatically in Fig. 2. The cavity is fed with microwave energy from a radar transmitter for a period of 1/4 μs. As a pulse of this length contains 2500 periods of oscillation, the frequency is well-defined. In 1/4 μs, a sound wave in quartz travels only about 1·4 mm, so a localized wave-packet is set up which travels down the rod. For a crystal 12 mm long, the time taken by this wave-packet to travel down the rod and return to the microwave cavity is 4·2 μs. This time is sufficient for switching devices in the radar set to connect the microwave apparatus to a sensitive receiver. A 1/4 μs pulse of energy is produced in the microwave cavity every time the sound wave is reflected at the end of the crystal which lies in the cavity. Thus the radar receiver registers a signal every 4·2 μs after the initial excitation of the crystal. These signals, which are fed to an oscilloscope for examination, give an indication of the amplitude of the sound wave in the crystal, and gradually become smaller as the sound wave decays. The decay is caused by absorption in the quartz, mounting losses, by an inevitable small amount of energy fed into the radar receiver, and by radiation out into the liquid He^3 surrounding the crystal. The amount of energy radiated out can be determined by performing two measurements, one with the crystal mounted in vacuo,

and one with it partly covered by liquid.

Because the absorption of sound in liquid He^3 is very large, there is no possibility of any energy radiated into the helium being reflected back onto the crystal and modifying the measured value of the acoustic impedance: for all practical purposes the crystal radiates out into a semi-infinite medium, even if the specimen is only a few microns thick.

2.2 Theory of the Measurement

The condition for observing zero sound, $\omega\tau \gg 1$, is equivalent to saying that the mean free path of particles in liquid He^3 is greater than the wavelength of the disturbance. Therefore "the displacement of an element of the liquid" has no meaning when we look at elements whose linear dimensions are of the order of the wavelength. In other words, the liquid does not obey hydrodynamics. It follows that we are not entitled to assume that the displacement of the liquid is of the simple form $e^{i(kx - \omega t)}$, and it will be shown later (s 4.5) that in fact this assumption is false. Equation (1.7) which gives the fraction of the energy radiated into the liquid, is usually derived on the assumption that a displacement of the form $e^{i(kx - \omega t)}$ is valid for both media. We now show that equation (1.7) remains true for the more general conditions of the present experiment.

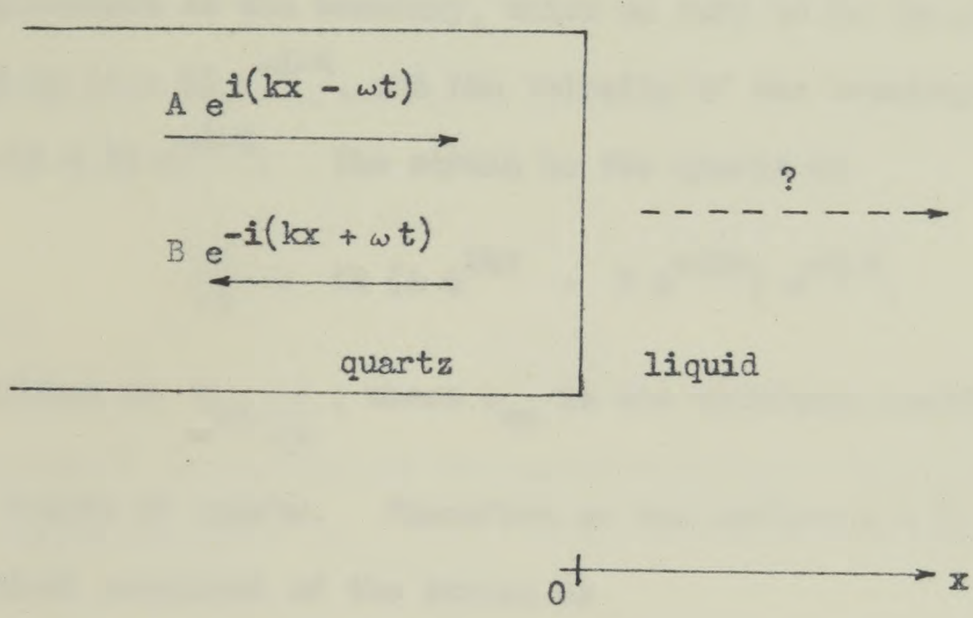

Fig 3. Radiation of Acoustic Energy.

Consider a plane wave travelling through a quartz rod and reflected at one end, so that some energy is radiated out into a surrounding liquid as shown in Fig. 3. Let the displacements of incident and reflected waves be $Ae^{i(kx - \omega t)}$ and $Be^{-i(kx + \omega t)}$, so that the displacement $\xi(x)$ in the crystal is

$$\xi(x) = (A e^{ikx} + B e^{-ikx}) e^{-i\omega t}.$$

The displacement at the boundary, which we take to be the plane $x = 0$, is given by $(A + B) e^{-i\omega t}$, and the velocity of the boundary is $v = -i\omega(A + B) e^{-i\omega t}$. The strain in the quartz is

$$\frac{\partial \xi}{\partial x} = ik (A e^{ikx} - B e^{-ikx}) e^{-i\omega t},$$

so the stress is $c_{xx} \frac{\partial \xi}{\partial x}$, where c_{xx} is the stiffness coefficient for the X-axis of quartz. Therefore at the surface $x = 0$, the longitudinal component of the stress is

$$\Pi_{xx} = i k c_{xx} (A - B) e^{-i\omega t}.$$

Now the acoustic impedance of a medium is generally defined by

$$Z = \frac{\text{pressure}}{\text{particle velocity}} = \frac{-\Pi_{xx}}{v},$$

when a plane travelling disturbance is radiated into the semi-infinite medium. (We have introduced a negative sign in the definition of Z because in elastic theory a stress is conventionally regarded as positive when it tends to give rise to a positive strain, so that

Π_{xx} represents a tensile stress rather than a pressure.) In the present problem, particle velocity has no meaning within the liquid, but it is meaningful at the boundary, where it is just the velocity of the quartz surface. Therefore the acoustic impedance of the liquid is

$$Z_{He} = \frac{-ik c_{xx} (A - B) e^{-i\omega t}}{-i\omega (A + B) e^{-i\omega t}} = \frac{k}{\omega} c_{xx} \frac{(A - B)}{(A + B)} .$$

The velocity of sound in quartz is given by

$$c = \sqrt{\frac{c_{xx}}{\rho}} , \quad \text{so that} \quad \frac{k}{\omega} c_{xx} = \frac{c_{xx}}{c} = \rho c .$$

Therefore

$$Z_{He} = \rho c \frac{(A - B)}{(A + B)} .$$

The fraction of the energy in the quartz which is lost as a result of the reflection is

$$a = \frac{|A|^2 - |B|^2}{|A|^2} = 1 - \left|\frac{B}{A}\right|^2 = 1 - \left|\frac{(\rho c)_{quartz} - Z_{He}}{(\rho c)_{quartz} + Z_{He}}\right|^2 . \qquad (1.7)$$

Thus we recover the usual expression for the fraction of the energy radiated.

2.3 Production of High-frequency Sound

We now discuss various points of design in the apparatus, as the success of the experiment can depend greatly on these details.

In our experiments, the sound wave in a quartz crystal is set up by applying an oscillating electric field to one end of the crystal. We shall now calculate the efficiency with which electrical energy is converted into acoustic energy. The argument is a simplification of that given by Jacobsen (1960 a).

The equation which gives the relation between stress, strain, and electric field in an anisotropic medium is

$$T_{ij} = c_{ijk\ell}\, u_{k\ell} - e_{ijk}\, E_k , \qquad (2.1)$$

where T_{ij} is the stress, u_{ij} is the strain, E_i is the electric field vector, c_{ijkl} is the elastic stiffness tensor, and e_{ijk} is the piezoelectric tensor which relates the stress to the electric field at constant strain. We use the customary convention of tensor analysis that repeated suffixes are to be summed over. The equation of motion for the crystal is

$$\rho\, \ddot{\xi}_i = \frac{\partial T_{ij}}{\partial x_j} + P_j \frac{\partial E_i}{\partial x_j} \qquad (2.2)$$

where $\partial T_{ij}/\partial x_j$ represents the force on an element due to differences of stress between its opposite sides, and $P_j\, \partial E_i/\partial x_j$ gives the electrostatic force on an element whose electric polarization is P_i.

ξ_i is the local value of the displacement of an element from its equilibrium position. We reject the last term of (2.2) because it is quadratic in the electric field (quartz is not ferroelectric) and we shall only keep linear terms. The strain u_{ij} is related to the displacement ξ_i by

$$u_{ij} = \frac{1}{2}\left(\frac{\partial \xi_i}{\partial x_j} + \frac{\partial \xi_j}{\partial x_i} \right). \tag{2.3}$$

Eliminating T_{ij} and u_{ij} between these three equations, one can derive the equation

$$\rho \ddot{\xi} = \frac{\partial}{\partial x_j}\left(c_{ijkl} \frac{\partial \xi_k}{\partial x_l} \right) - \frac{\partial}{\partial x_j}(e_{ijk} E_k). \tag{2.4}$$

If now we consider the practical problem in which we propagate a plane longitudinal wave along the X-axis, (2.4) reduces to

$$\rho \ddot{\xi}_1 = \frac{\partial}{\partial x}\left(c_{1111} \frac{\partial \xi_1}{\partial x} \right) - \frac{\partial}{\partial x}(e_{11k} E_k)$$

or

$$\rho \ddot{\xi}_1 = \frac{\partial}{\partial x}\left(c_{xx} \frac{\partial \xi_1}{\partial x} \right) - \frac{\partial}{\partial x}(e_{xx} E_1) \tag{2.5}$$

where we have dropped unnecessary subscripts, and used the fact that $e_{112} = e_{113} = 0$ for quartz.

In deriving (2.5) we have been careful not to assume that the medium is uniform, for in the case of a uniform medium under the influence of a spatially uniform electric field, (2.5) reduces to

$$\ddot{\xi} = \frac{c_{xx}}{\rho} \frac{\partial^2 \xi}{\partial x^2} \tag{2.6}$$

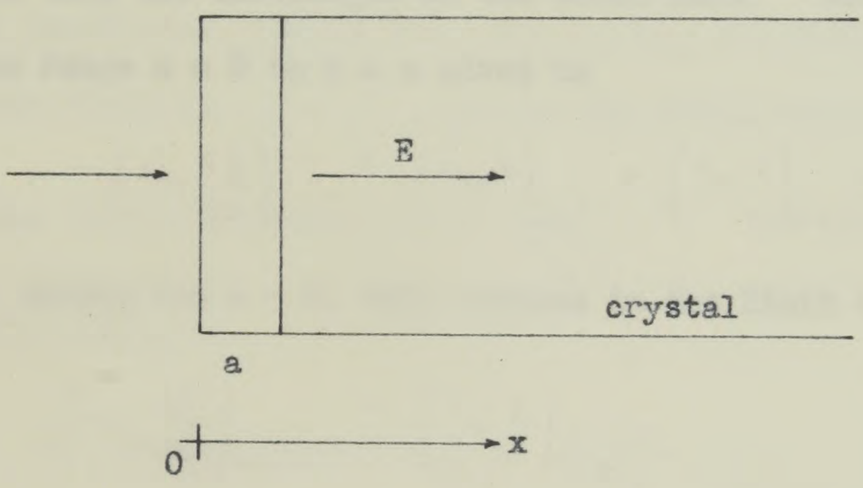

Fig. 4. Generation of Sound in a Crystal.

which does not contain the electric field E, and so does not describe the generation of a sound wave by the field. Therefore the generation of sound by piezoelectric effects relies on the non-uniformity of $e_{xx}E$.

Consider a sample of quartz subject to a spatially uniform electric displacement (E is discontinuous at the surface) as shown in Fig. 4, and assume that at the surface of the crystal c_{xx} and e_{xx} fall from their bulk values to zero over a distance a, which will be very much less than the wavelength of the sound wave. Integrating (2.5) over the range x = 0 to x = a gives us

$$\left(c_{xx} \frac{\partial \xi}{\partial x} \right)_{x=a} - \left(c_{xx} \frac{\partial \xi}{\partial x} \right)_{x=0} - \left(e_{xx} E \right)_{x=a} + \left(e_{xx} E \right)_{x=0} = O(a).$$

If there is a vacuum for x < 0, this reduces in the limit $a \to 0$ to

$$\left[c_{xx} \frac{\partial \xi}{\partial x} \right]_{x=0+} = \left[e_{xx} E \right]_{x=0+} . \qquad (2.7)$$

From (2.6), the motion of the crystal for x > 0 is given by

$$\xi = B e^{i(kx - \omega t)} \qquad \text{where} \qquad \frac{\omega}{k} = \sqrt{\frac{c_{xx}}{\rho}} .$$

The boundary condition (2.7) gives us the value of B, so if $E = E_0 e^{-i\omega t}$ (note that E_0 is the value of the electric field inside the crystal),

$$\xi = - i \frac{e_{xx} E_0}{c_{xx} k} e^{i(kx - \omega t)} . \qquad (2.8)$$

Jacobsen (1960 a) derives an expression similar to (2.8) by a rather longer method, and goes on to show that when the electric field is

not uniform inside the crystal, the additional source of sound produced by the $e_{xx} \frac{\partial E}{\partial x}$ term is always negligible when frequencies in the microwave region are used.

The electric field driving the crystal is produced in practice by a microwave cavity (Fig. 5a). Let us suppose for the purpose of calculating the energy stored in the cavity that all the electric field lies in the crystal. Then if the crystal has area A and the field penetrates into it like exp (-x/l), the energy stored in the electric field is $\frac{\varepsilon E_o^2}{16\pi} A \frac{l}{2}$, and so the total energy stored in the electric and magnetic fields is $\frac{\varepsilon E_o^2 A l}{16\pi}$. The power supplied to the cavity is

$$P_{in} = (\text{energy stored}) \times \frac{\omega}{Q} = \frac{\varepsilon E_o^2 A l}{16\pi} \frac{\omega}{Q}.$$

The power passing down the crystal in the form of sound is

$$S = \tfrac{1}{2} c_{xx} \frac{|B|^2}{2} k^2 c A = \frac{c_{xx}}{4} \frac{e_{xx}^2 E_o^2}{c_{xx}^2} c A,$$

where c is the velocity of sound in quartz. Therefore the fraction of the microwave power entering the cavity which is converted into sonic energy is

$$\frac{S}{P_{in}} = \frac{e_{xx}^2 E_o^2 c A}{4 c_{xx}} \cdot \frac{16\pi Q}{\varepsilon E_o^2 A l \omega} = 2 K^2 Q \frac{\lambda}{l}$$

where λ is the wavelength of sound in the quartz, and $K^2 = \frac{e_{xx}^2}{\varepsilon c_{xx}}$.

The distance l through which the electric field penetrates into the quartz rod is determined by the fact that the metal tube within which the quartz lies acts as a circular waveguide beyond its cut-off frequency. For the TM_{01} mode, which is the dominant mode set up in this case, $l = 0{\cdot}21\ D$, where D is the diameter of the crystal.

Therefore $$\frac{S}{P_{in}} = 9{\cdot}5\ K^2 Q \frac{\lambda}{D} = 6{\cdot}05 \times 10^{-3}\ Q \frac{\lambda}{D}. \qquad (2.9)$$

It might appear from this that there is a theoretical advantage in using crystals of small diameter. We have however assumed that nearly all the electric field of the cavity lies in the crystal; this desirable condition can only be satisfied for a limited range of diameters, so the practicable variation in D is not large. For a crystal 6 mm in diameter, and a frequency of 9·4 Gc/s,

$$\frac{S}{P_{in}} = 6{\cdot}15 \times 10^{-7}\ Q. \qquad (2.10)$$

Equation (2.10) can be put into a form more useful for design calculations if we define

$$Q_c = \omega \times \frac{\text{energy stored in cavity}}{\text{rate of energy loss into crystal}} = 1{\cdot}6 \times 10^6.$$

Then $$\frac{S}{P_{in}} = \frac{Q}{Q_c} \qquad (2.11)$$

where Q is the quality factor of the cavity as loaded by the crystal. Thus if the quality factor of the unloaded cavity is Q_o,

$$\frac{1}{Q_{L2}} = \frac{1}{Q_o} + \frac{1}{Q_c}$$

and Q_{L2} is the quantity to be used in the numerator of (2.11)

Now (2.11) is exactly analogous to the relation which one has for a cavity loaded by an external circuit:

$$\frac{\text{power lost up transmission line}}{\text{total power lost from cavity}} = \frac{Q_{L1}}{Q_E}$$

where $$\frac{1}{Q_{L1}} = \frac{1}{Q_o} + \frac{1}{Q_E},$$

and Q_E measures the rate of energy loss into the external circuit. It is therefore possible to construct an analogy between the crystal, which carries energy away from the cavity in the form of sound waves, and a transmission line, which carries away electrical energy. With this analogy, we can discuss the performance of a cavity which contains a crystal, and which also has one coupling loop to an electrical transmission line (Fig. 5). This corresponds to the situation in an actual cavity used for an experiment. Consider first the case where the cavity is fed with power from the electrical system, and produces sound in an otherwise undisturbed crystal (Fig. 5 a). An electromagnetic wave in the transmission line is in general partially reflected when it reaches the cavity, so that the fraction of the available power which enters the cavity is

$$\frac{4 Q_E Q_{L2}}{(Q_E + Q_{L2})^2}.$$

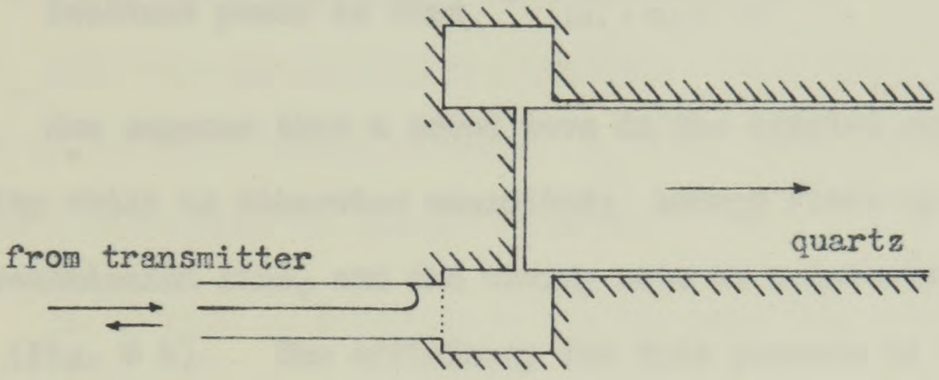

Fig. 5a. Generation of Sound.

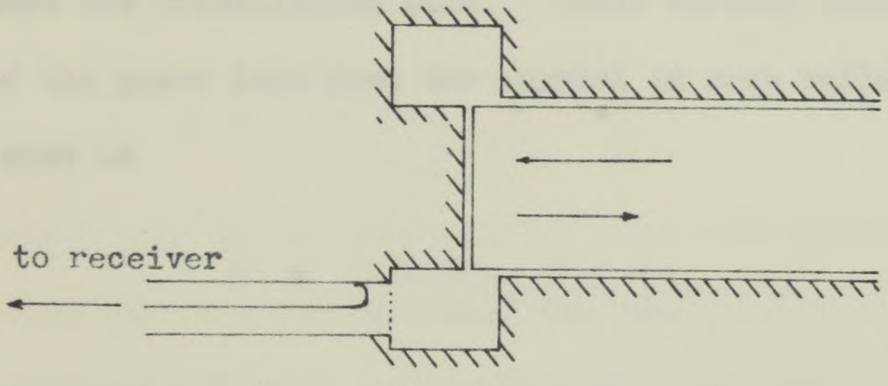

Fig. 5b. Detection of Sound.

A fraction Q_{L2}/Q_c of this is converted into acoustic power in the crystal, so the efficiency of sound generation is

$$\frac{\text{power entering crystal}}{\text{incident power in line}} = \frac{4 Q_E Q_{L2}}{(Q_E + Q_{L2})^2} \frac{Q_{L2}}{Q_c}.$$

Now suppose that a sound wave in the crystal arrives at the cavity which is otherwise unexcited; energy flows up the electrical transmission line, and the cavity acts as a detector of acoustic signals (Fig. 5 b). The efficiency for this process is the same as for generation, so

$$\frac{\text{power entering transmission line}}{\text{incident power in crystal}} = \frac{4 Q_E Q_{L2}}{(Q_E + Q_{L2})^2} \frac{Q_{L2}}{Q_c}.$$

When a sound wave arrives at the cavity in this way, a fraction β of its energy is converted into electrical energy, and of this a fraction Q_{L1}/Q_E enters the transmission line. Hence working backwards, the fraction of the power lost from the crystal at each reflection of the sound wave is

$$\beta = \frac{4 Q_E Q_{L2}}{(Q_E + Q_{L2})^2} \frac{Q_{L2}}{Q_c} \frac{Q_E}{Q_{L1}}. \qquad (2.12)$$

This fraction must be small, otherwise the sound wave in the crystal will die away due to the extraction of energy by the cavity. To obtain a simple estimate, let us assume that the electrical transmission line is matched to a copper cavity with a Q_o of 5000. Then $Q_E = Q_{L2}$ and $Q_{L2} \doteq Q_o$ since $Q_c \gg Q_o$, so that

$$\beta = \frac{2\,Q_o}{Q_c} = 6{\cdot}15 \times 10^{-5}.$$

The generation and reception efficiencies are both $Q_o/Q_c = \frac{1}{2}\beta$. Thus if a power P_o is fed into the transmission line, an acoustic power $P_o\,\beta/2$ is generated in the crystal. When this wave is detected by the same cavity, a power $P_o\,\beta^2/4$ is received, making the overall efficiency of the cavity $\beta^2/4$.

It is also of interest to see how much improvement can be gained by increasing Q_o, for example by using a superconducting cavity. The power lost from the crystal on each reflection of the sound wave can be large in this case if the transmission line is still matched to the cavity. We suppose that this situation is avoided by overcoupling the line to the cavity so that β is held to the same value as was obtained before. Then the fraction of the power lost from the crystal at each reflection is

$$\beta = \frac{4\,Q_E\,Q_c}{(Q_E + Q_c)^2} \simeq \frac{4\,Q_E}{Q_c}\,. \qquad (2.13)$$

All this energy goes up the transmission line into the receiver, so the generation and reception efficiencies are now both β. If an electrical power P_o is used to generate sound, an acoustic power $P_o\,\beta$ is generated, which on subsequent detection gives a power $P_o\,\beta^2$. Therefore the overall efficiency of a superconducting cavity is only a factor 4 better than that of an ordinary cavity, if the comparison is made under the assumption of a constant loss of acoustic power

from the crystal at each reflection.

2.4 Propagation Effects

In practice, one does not observe a perfectly exponential decay of a sound wave in a quartz crystal when detecting echoes by the piezoelectric effect. When the acoustic wave arrives at the detecting end of the crystal, the wavefront may not be plane and parallel to the face of the crystal. The amplitude of the electric field set up in the microwave cavity is proportional to the total amplitude of the sound wave summed over the surface, and if the wavefront is badly distorted, the total amplitude may be considerably smaller than it would be for a plane wavefront.

There are several mechanisms which can cause the acoustic wavefront in a crystal to become distorted. Consider first the effect of misaligning the crystal, so that the pure mode axis is not normal to the end faces of the crystal. The propagation of sound along such a crystal has been considered by Waterman (1959). The effect of misalignment is to cause the acoustic energy to flow in a direction which makes a small angle with the axis of the crystal, as shown in Fig. 6. In isolation this effect is not too serious, provided that most of the acoustic beam succeeds in reaching the far end of the crystal, for on reflection at the far end, the wave is returned along its path. The main effect is therefore to reduce the useful

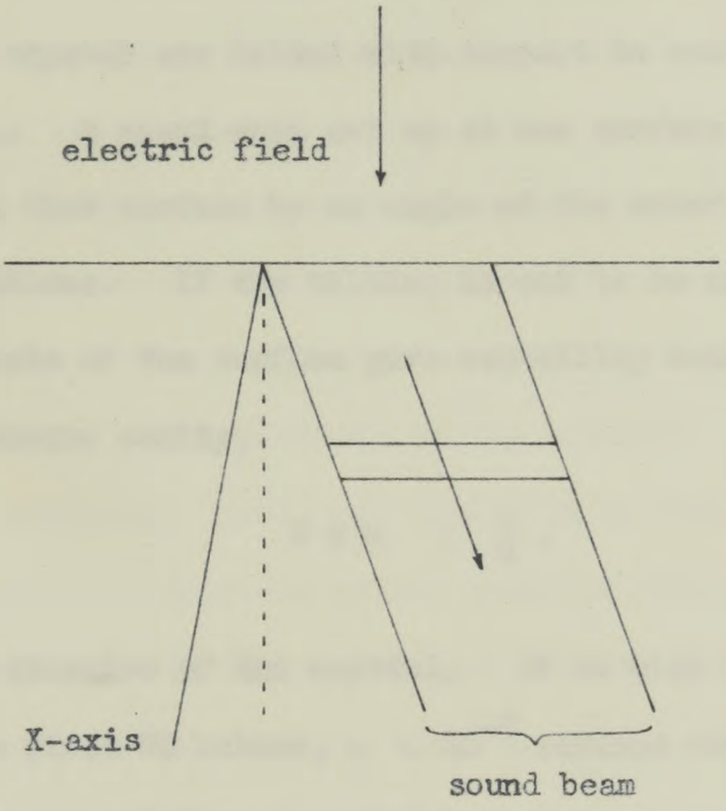

Fig. 6. Off-axis Propagation

cross-sectional area of the crystal.

A more serious error in the production of a crystal suitable for hypersonic measurements occurs if the ends of the crystal are not flat and parallel. To consider a simple example, suppose that the end faces of a crystal are tilted with respect to each other through a small angle α. A sound wave set up at one surface becomes tilted with respect to that surface by an angle of the order of $2n\alpha$ after n double reflections. If the tilting is not to be so severe that different elements of the surface give cancelling contributions when exciting a microwave cavity,

$$2 n \alpha \lesssim \frac{\lambda}{D},$$

where D is the diameter of the crystal. If we wish to avoid cancellations for the first 50 echoes, $\alpha \lesssim 10^{-6}$ radians for a frequency of 10^{10} c/s, and a crystal diameter of 6 mm.

Carr and Strandenberg (1962) have shown that the variation of signal with α is mathematically very similar to the case of the diffraction of light at a circular aperture. A zero response occurs when $2n\alpha = 1{\cdot}22\ \lambda/D$, and the first subsidiary maximum occurs when $2n\alpha = 1{\cdot}63\ \lambda/D$, but then the power received is a factor 0·0175 below that which could be received were the wavefront parallel to the end of the crystal. The angle of tilt of the wavefront is increased if a misalignment of the crystal occurs as well as non-parallelism, for then the propagation is affected by the acoustical birefringence of

the crystal. (Strictly, if the two end faces of a crystal are not parallel, at least one is not normal to the pure mode axis, so a separation of the effects of misalignment and non-parallelism is somewhat arbitrary.)

A further mechanism which can lead to a distorted wavefront is the fact that waves propagated in a finite specimen do not propagate in the same way as they do in an infinite medium. The effect is rather difficult to work out for an anisotropic substance like quartz, but one can obtain a rough approximation from the behaviour of an isotropic specimen. The solutions to the equation of motion have been given by Pochhammer (1876) and discussed by McSkimin (1956). The result obtained is that the normal modes of vibration of the specimen are expressed in terms of Bessel functions of the radial co-ordinate, and each mode travels down the rod with a slightly different velocity. The phenomenon is analogous to the propagation of electromagnetic waves in a circular waveguide. Any disturbance to the specimen can be represented as a sum of these normal modes, but the shape of the wavefront changes with time as the different modes get in and out of phase. If each normal mode propagates like $e^{i(kx - \omega t)}$ with its own value of k, we have

$$k^2 = \frac{\omega^2}{c^2} - h^2$$

where h is the solution of a complicated expression, but is given approximately for $\lambda/D \ll 1$ by $J_0(hD/2) = 0$. Therefore the two

lowest modes are characterized by $hD/2 = 2{\cdot}405$ and $hD/2 = 5{\cdot}52$, so

$$k_1^2 = \frac{\omega^2}{c^2} - \frac{4{\cdot}81^2}{D^2}, \qquad k_2^2 = \frac{\omega^2}{c^2} - \frac{11{\cdot}04^2}{D^2},$$

and

$$k_1^2 - k_2^2 = \frac{11{\cdot}04^2 - 4{\cdot}81^2}{D^2}.$$

As $k \sim 1/\lambda$, while $h \sim 1/D$, we can approximate this to

$$k_1 - k_2 = \frac{11{\cdot}04^2 - 4{\cdot}81^2}{D^2\ 2k}.$$

These two waves become out of phase after travelling a distance l given by $(k_1 - k_2)\, l = 2\pi$, so

$$l = \frac{2\pi\ D^2\ 2k}{11{\cdot}04^2 - 4{\cdot}81^2} = 0{\cdot}8\ \frac{D}{\lambda}\ D.$$

For a specimen 6 mm diameter × 12 mm long, $l = 786\ D$ which means that the first two guided wave modes get out of phase after the wave has made about 200 double journeys along the crystal. This calculation applies to an isotropic medium, and takes no account of mode conversion which can occur when the wave is reflected at the ends of the specimen. Nevertheless, it does indicate that at a frequency of 10^{10} c/s, guided wave modes should be relatively unimportant as a source of distorted wavefronts.

It is clear from the above discussion that an experiment which involves reflecting a sound wave many times between the same two end surfaces of a crystal gives results which are very sensitive to slight defects in these surfaces. In fact this sensitivity is

similar to that used in investigating very small details of crystal surfaces by the multiple reflection of light waves (e.g. Tolansky (1960)). Nevertheless, Jacobsen (1960 b) has reported obtaining 400 echoes in a crystal at a frequency of 10 Gc/s.

2.5 Microwave Cavities

A typical microwave cavity as used for testing crystals is shown in Fig. 7. The cavity was constructed from two pieces of tellurium copper, which were clamped together to form a hollow coaxial structure. The central post of the cavity was made to have the same diameter as the crystal, which was usually 6 mm. The proportions of the cavity were then determined by the frequency required and by convenience of construction. Since the object of the cavity is to provide a large electric field, one requires the cavity to give a maximum electric field for a given power supplied. If the r.m.s. voltage between the post and the wall of the crystal holder is V, a shunt impedance R_{sh} can be defined such that the power supplied to the cavity is V^2/R_{sh}. It follows that one should proportion the cavity so as to achieve a maximum shunt impedance. Moreno (1948) states that the shunt impedance is a maximum when the length of the post is approximately equal to the difference between the inner and outer radii of the coaxial structure. This relation was always approximately satisfied for our cavities.

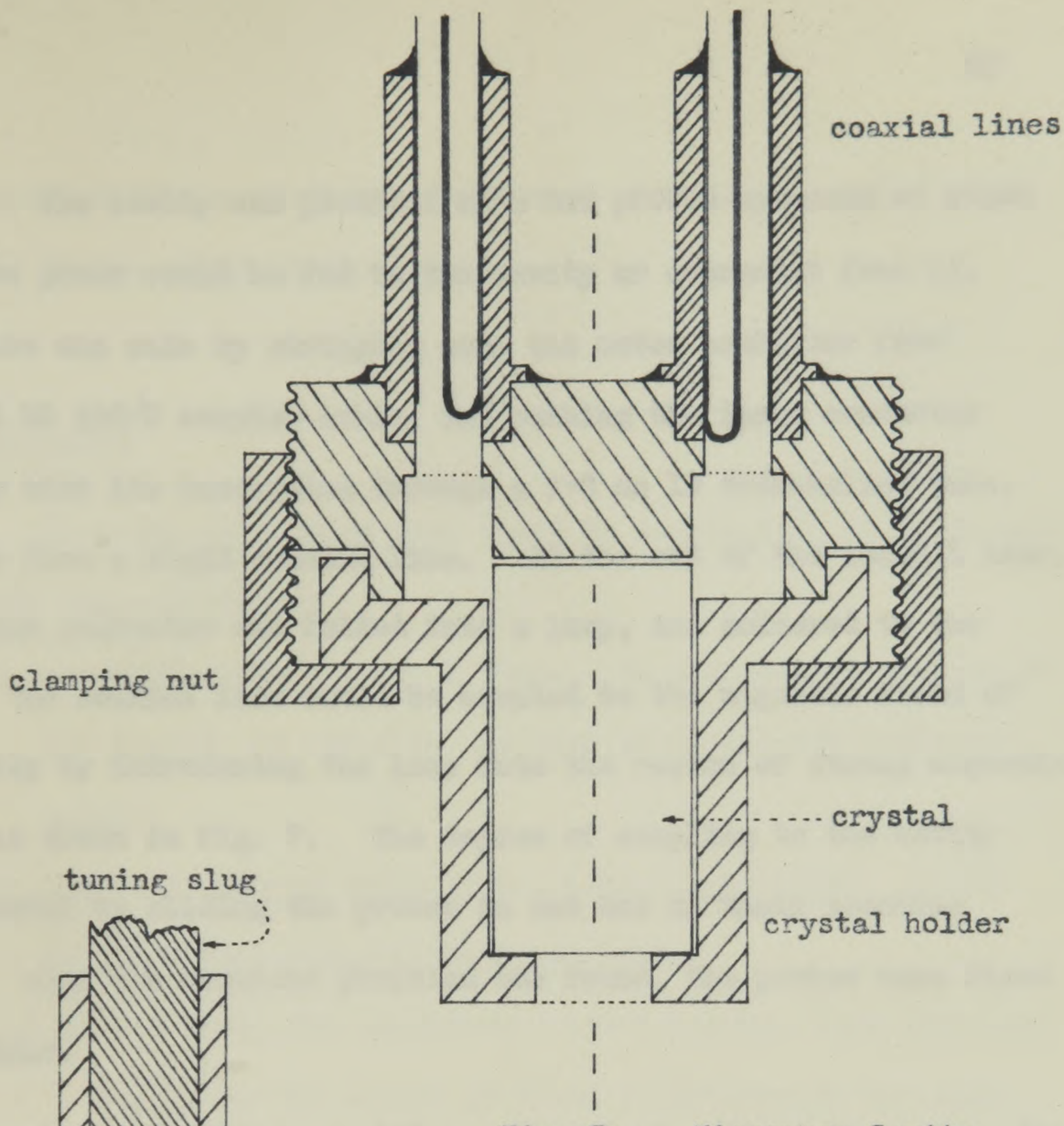

Fig. 7a. Microwave Cavity

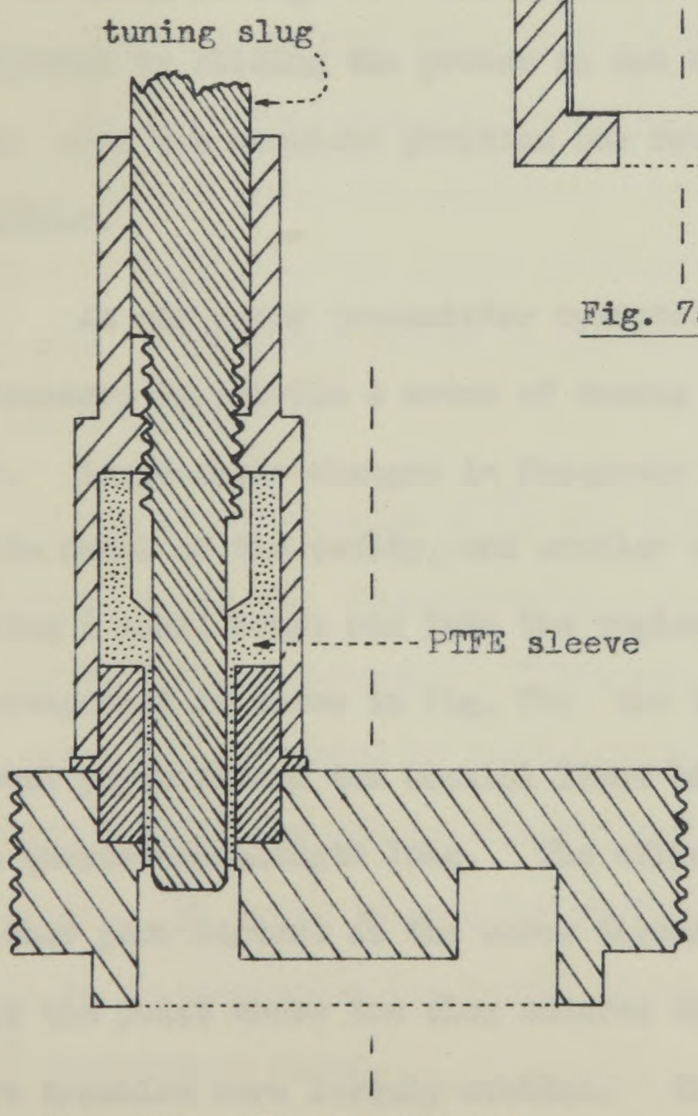

Fig. 7b. Tuning Mechanism.

The cavity was provided with two probes by means of which microwave power could be fed to the cavity or extracted from it. Each probe was made by stripping away the outer conductor from Amphenol RG 188/U coaxial cable, and pushing the inner conductor together with its insulation through a 1·8 mm ID thin-walled tube, so as to form a rigid coaxial line. At the end of the coaxial line, the centre conductor was folded into a loop, and soldered to the tube. The coaxial line could be coupled to the magnetic field of the cavity by introducing the loop into the region of strong magnetic field, as shown in Fig. 7. The degree of coupling to the cavity was adjusted by sliding the probes in and out of their mounting bushes; when the required position was found, the probes were fixed with solder.

As our radar transmitter operated at a fixed frequency, it was necessary to provide a means of tuning the cavity to the transmitter. Large-scale changes in frequency were made by turning away the metal of the cavity, and smaller changes could be made by inserting a small brass rod into the region of high magnetic field. The arrangement is shown in Fig. 7b; the tuning slug and the surrounding metal parts formed two coaxial lines of different impedances, each a quarter-wavelength long. The effect of this was to transform the rather poor contact at the screw thread into a much lower impedance at the point where the slug entered the cavity. In this way contact troubles were largely avoided. The position of resonance

was always located by finding a maximum in the signal coupled from one probe to the other by the cavity.

2.6 Cryogenics

In order to observe zero sound in liquid He^3, it is necessary to satisfy two conditions:

(a) one must satisfy $\omega\tau \gg 1$ where τ is the relaxation time of the liquid, in order to see zero sound and not ordinary sound;

(b) one must work at temperatures below about $0{\cdot}05^\circ - 0{\cdot}1^\circ K$ in order for Landau's theory to hold.

Working at 10 000 Mc/s, the condition $\omega\tau \gg 1$ implies that the temperature $T \ll 0{\cdot}3^\circ K$, so the second of these conditions is the more restrictive. Therefore we had to aim to perform our final experiments below $0{\cdot}1^\circ K$.

Temperatures below $0{\cdot}1^\circ K$ are obtained by the complex technique of adiabatic demagnetization, so that even simple experiments are very time-consuming. There was therefore a need for a simple apparatus operating in a more accessible temperature range, with which to test our quartz crystals and to perform preliminary experiments. In order to keep the absorption of sound in the quartz crystals to an acceptably low level, it was necessary to work in the $4^\circ - 2^\circ$ temperature range.

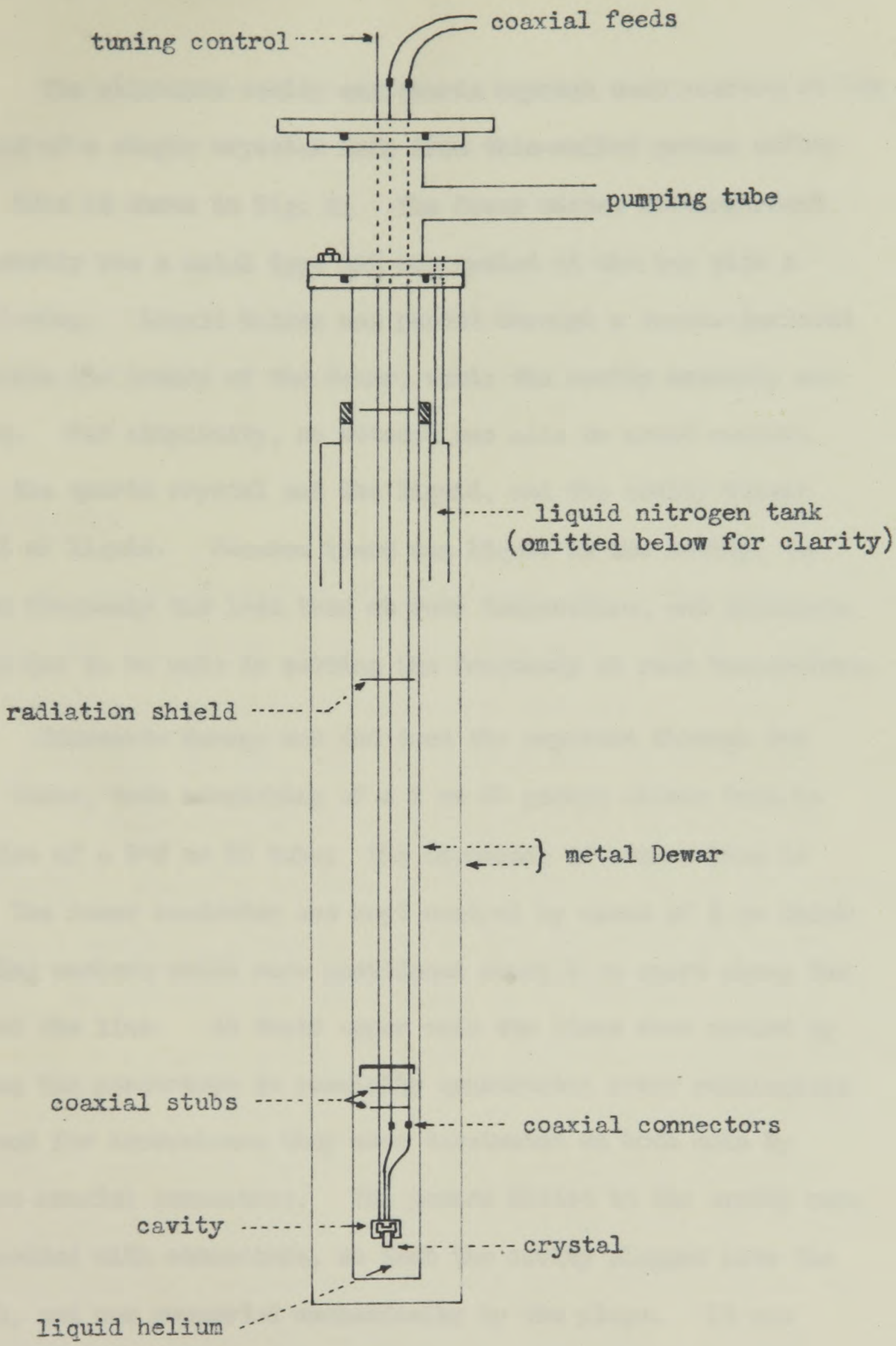

Fig. 8. Cryostat (diagrammatic)

The microwave cavity and quarts crystal were mounted at the lower end of a simple cryostat made from thin-walled german silver tubes; this is shown in Fig. 8. The Dewar vessel fitting round this assembly was a metal type and was sealed at the top with a rubber O-ring. Liquid helium was passed through a vacuum-jacketed siphon into the inside of the Dewar, until the cavity assembly was immersed. For simplicity, no attempt was made to avoid contact between the quarts crystal and the liquid, and the cavity itself was full of liquid. Because there was liquid in the cavity, the resonant frequency was less than at room temperature, and allowance for this had to be made in setting the frequency at room temperature.

Microwave energy was fed down the cryostat through two coaxial lines, each consisting of a 1 mm OD german silver tube in the centre of a 2·8 mm ID tube; the impedance of such a line is 68 Ω. The inner conductor was kept central by means of $\frac{1}{2}$ mm thick insulating washers which were positioned about 9 cm apart along the length of the line. At their upper ends the lines were sealed by soldering the conductors to coaxially constructed kovar metal-glass seals, and for convenience they were terminated at both ends by miniature coaxial connectors. The probes fitted to the cavity were also provided with connectors, so that the cavity plugged into the cryostat, and was supported mechanically by the plugs. It was therefore easy to remove the cavity when adjustments were required, or if the crystal was to be changed.

It was possible to tune the cavity in situ by means of a 3/32″ diameter stainless steel tube which passed through an o-ring seal at the upper end of the cryostat, and which was coupled at the lower end to the tuning slug. To avoid the necessity of accurately aligning the control mechanism and the tuning slug, a universal joint linkage was used to transfer the rotational movement.

2.7 Electronics

The radar set used in our experiment was a BTH Marine Radar, type RMS 1-A, loaned to us by the Admiralty. It was housed in a radar cabin intended to be fitted onto the deck of a ship; on account of its size the radar set was kept outside the laboratory (Fig. 9). To make connections to the experimental apparatus, it was necessary to remove a rotating scanner from the top of the radar cabin, and a length of waveguide was run from the radar set to the cryostat. As the radar set was designed to be controlled from a display unit at a remote point, it was not difficult to arrange for the transmitter to be turned on and off, and for the receiver to be tuned, from a convenient place near to the experimental apparatus. The only modifications which we had to make to the radar set consisted in removing from the receiver the automatic gain control circuit and the circuits which varied the receiver gain with time. A block diagram of the radar set is given in Fig. 10.

Fig. 9. Radar set RMS 1-A



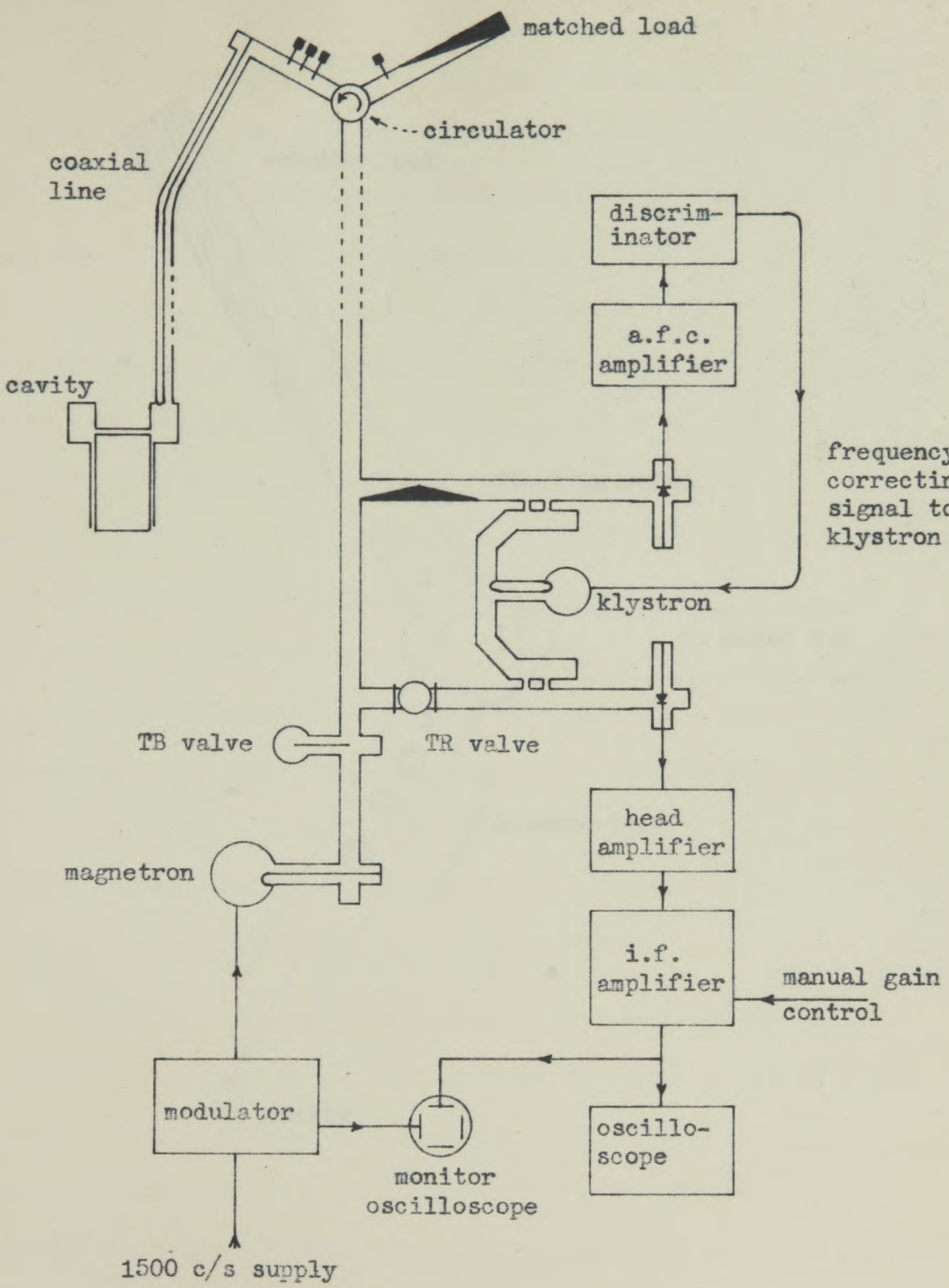

Fig. 10. Block Diagram of Electronics.

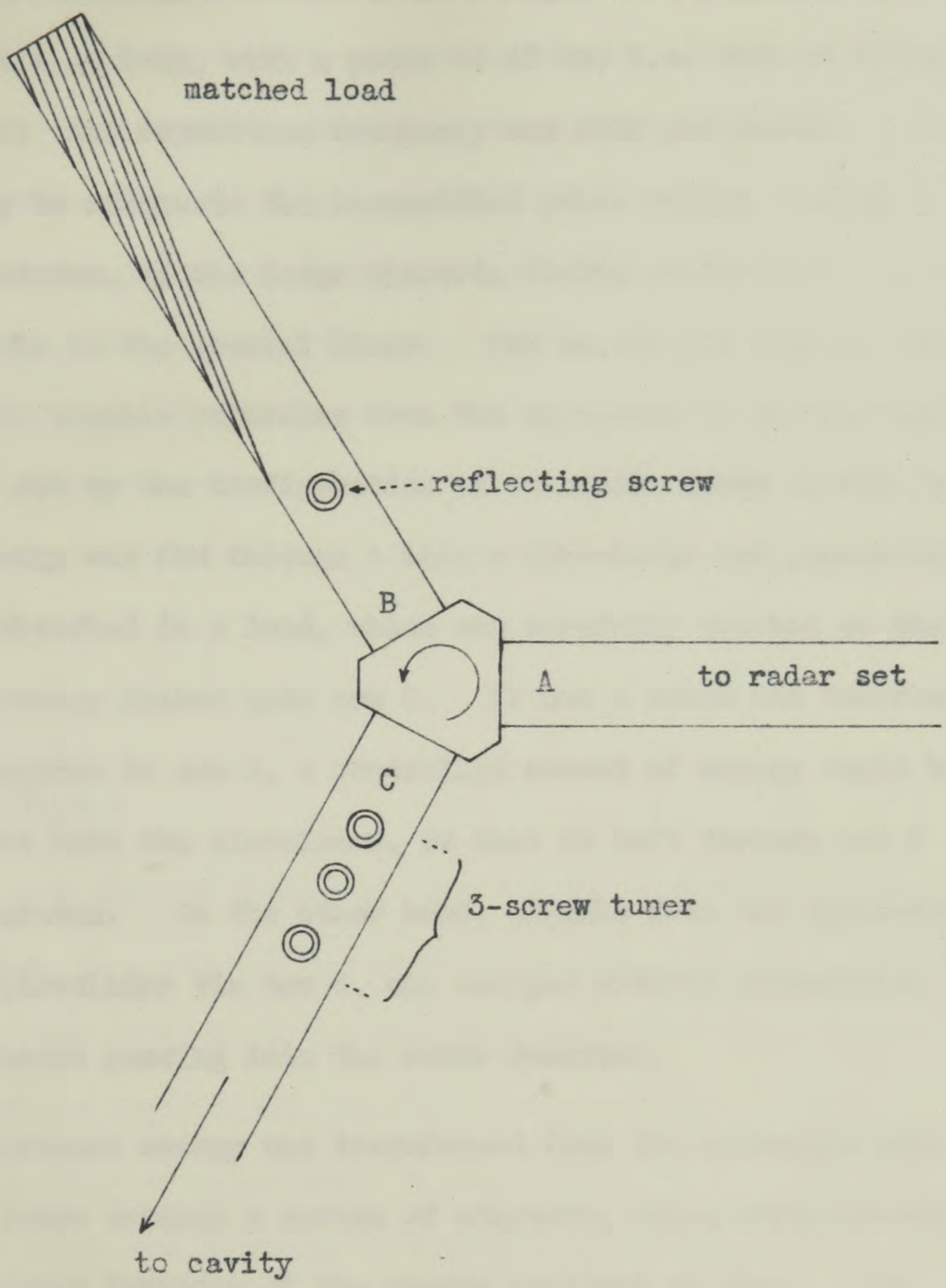

Fig. 11. The Circulator.

The transmitter of the radar set gave out pulses of microwave energy 1/4 μs long, with a power of 40 kw, i.e. with an energy of 10^{-2} joule; the repetition frequency was 1500 per second. It was necessary to attenuate the transmitted pulse before feeding it into the apparatus, as the large electric fields could give rise to a gas discharge in the coaxial lines. Yet we did not wish to attenuate the small signals returning from the apparatus to the receiver. We therefore set up the configuration of waveguide shown in Fig. 11. Microwave energy was fed through A into a circulator and passed into arm B to be absorbed in a load, which was carefully matched so that very little energy leaked into arm C. If now a screw was inserted into the waveguide in arm B, a controlled amount of energy could be reflected back into the circulator, so that it left through arm C into the apparatus. On the other hand, signals from the apparatus entered the circulator via arm C, and emerged without attenuation into arm A, hence passing into the radar receiver.

Microwave energy was transferred from the waveguide into the coaxial lines through a series of adaptors, which unfortunately reflected a large fraction of the energy incident on them. The system was therefore matched by means of a 3-screw tuner in the waveguide. The adjustment of these screws was carried out by connecting a klystron to arm B of the circulator, and adjusting until the signal reflected into arm A was a minimum. Preliminary tests established that this gave the same settings as a standing wave

ratio apparatus, provided that the circulator was used near its design frequency, and the method involving the use of the circulator was considerably the easier. Matching arrangements were also provided at the bottom of one of the coaxial lines, as it was found that the miniature connectors shown in Fig. 8 could also give rise to reflections. The coaxial line was therefore provided with a 2-stub tuner consisting of two short lengths of 3 mm coaxial line 3/8 of a wavelength apart. The stubs were shorted by movable plungers which made contact with the inner and outer conductors through tiny spring fingers.

2.8 Crystal Testing

We have already discussed in § 2.4 the various reasons why a sound wave in a crystal may show a non-exponential decay pattern. Of these, the most serious is the interference effect which occurs if the ends of the crystal are not plane and parallel. A good crystal should have faces polished to better than 60 Å. Now the best accuracy which can normally be achieved in polishing is of the order of 500 Å (1/10 of an optical wavelength). There was therefore only a small probability that any given crystal would give a perfect decay pattern, but we hoped to obtain a crystal which was better than average by selecting among a number of crystals. We therefore ordered several crystals from different manufacturers, and tested each in turn using the cavity assembly already described. For each

test it was necessary to cool the cavity and crystal with liquid helium. In all we performed 29 experiments at helium temperature, using 5 cavities, and testing 17 crystals, each of which required a separate crystal holder.

Our best crystal was a cylinder 6 mm diameter × 12 mm long, supplied by Messrs. Gooch and Housego; its decay pattern is shown in Fig. 12. In Fig. 12 a, the first echo is shown filling the screen of the oscilloscope; no other echo being large enough to be visible. Fig. 12 b shows the pattern with the amplification increased so that the second echo just fills the screen, while the first disappears out of the top of the picture; even here most of the echoes appear very small. With the amplification increased still further, picture 12 c was obtained. Here the sixth echo three-quarter fills the screen, and the pattern is shown at the largest usable amplification, as the thickness of the base-line in this picture is due to receiver noise. About 100 echoes are visible in the photograph. (The last echo observed visually on the oscilloscope was the 108th, but no echo after the 95th could be described, even optimistically, as measurable.)

The decay pattern of Fig. 12 is representative of the results obtained with most of our crystals. The most striking feature of the decay is the very rapid drop in signal amplitude over the first 5 or 6 echoes. In Fig. 12, the ratio of the amplitudes of the first and 5th echoes is of the order of 500. After this

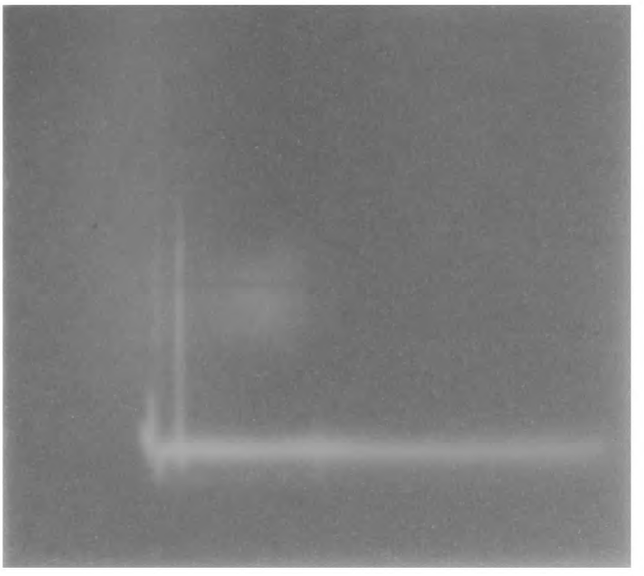

Fig. 12 a

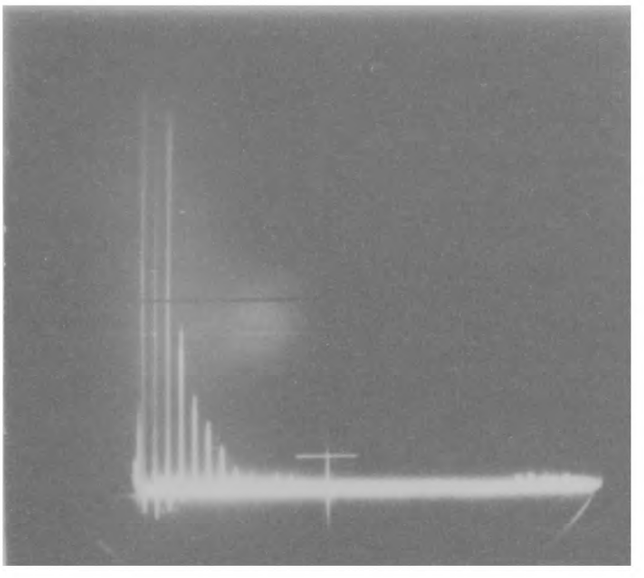

Fig. 12 b

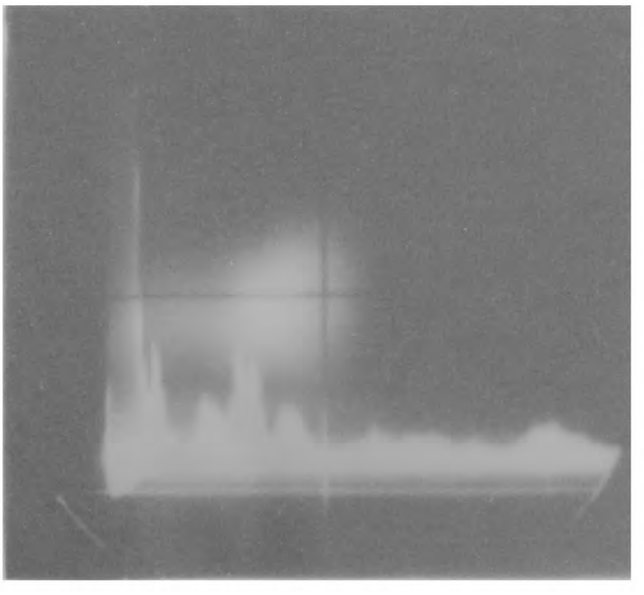

Fig. 12 c

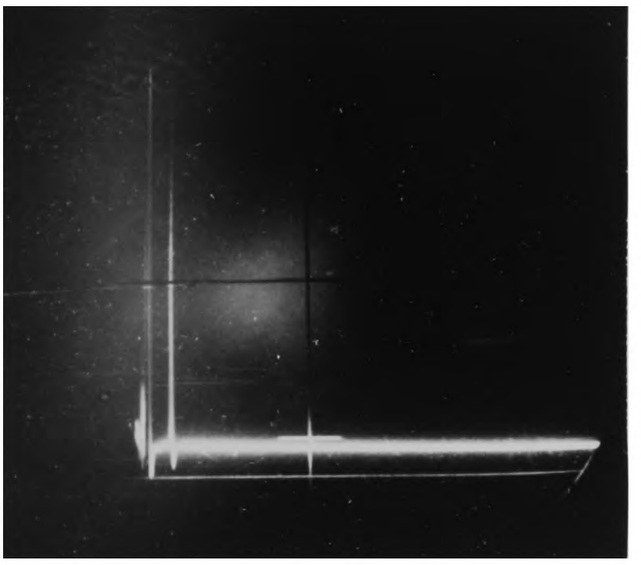

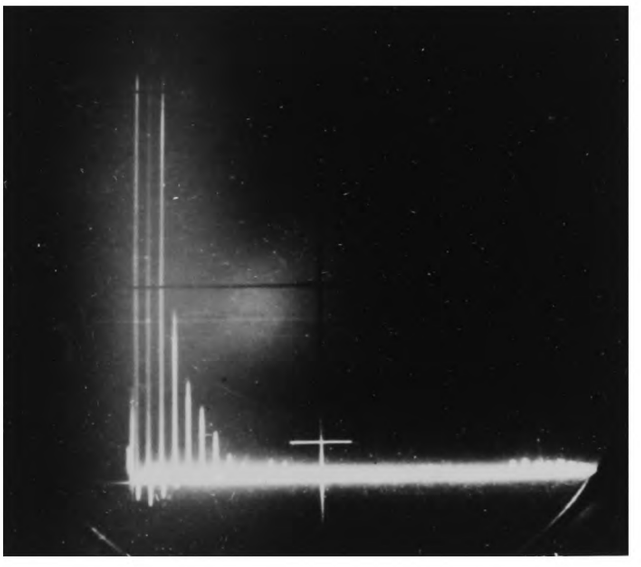

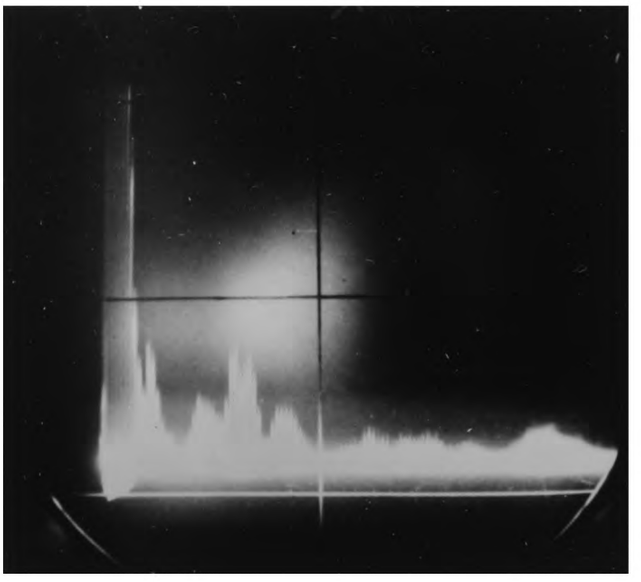

initial fall, the signals die away rather gradually, and with a decay which is obviously not exponential. The general shape of the decay pattern seemed to be roughly constant for any one crystal, as the pattern was not changed significantly either by turning the crystal upside down, or by changing to another cavity.

Before describing the measures taken to improve the number of echoes, we now show that the rapid decay in the signal cannot have been caused by the electronics, or by mounting losses. In Fig. 12, the first echo has a signal amplitude of the order of 15 000 × the noise level of the receiver. By estimating rough values for the power fed into the microwave cavity, and for the noise level of the receiver, we find the electro-acoustic conversion efficiency to be 4×10^{-4}. This is a little smaller than the efficiency of $1{\cdot}2 \times 10^{-3}$ calculated for a cavity with a Q_o of order 2000 (the value obtained from bandwidth measurements), but the difference may not be significant. Even accepting the larger figure, the amplitude of the sound wave in the crystal should not be reduced by a factor e until the 800th echo. There was therefore no likelihood that in our apparatus the rapid decay was due to removal of energy by the electrical system.

Apart from the electrical loss, the sound wave in the crystal was also attenuated by mounting losses, and in particular by the presence of liquid helium over the surface of the crystal. The rate of loss into the helium is easily estimated from the acoustic impedance of He^4, and it would cause the signal to fall to 1/e of its

original amplitude after 170 echoes. As in practice the signal fell by a factor of order 15 000 after 100 echoes, this loss should have been insignificant. Losses of acoustic energy into the metal crystal holder should also have been negligible, as the lower end of the crystal rested on a narrow ledge as indicated in Fig. 7, and under the weight of the crystal (0·9 gm) the microscopic area of contact should have been very small. The mounting arrangements used by Keen, Matthews, and Wilks (1963) in their 1000 Mc/s work were in any case very similar to ours, and their decay pattern contained 1000 - 1500 echoes, which implies that the mounting losses were very small. Care was always taken to ensure that the crystal was not held firmly as a result of thermal contraction as the apparatus was cooled. From the above considerations it seems that the observed decay of the sound wave was due to processes occurring in the crystal, and was probably due to a failure to polish the end faces to a sufficient degree of parallelism and flatness.

In order to perform our experiment we ideally needed about 250 echoes with an exponential decay. However, while the need for a large number of echoes was vital, an exponential decay pattern was less important. Keen, Matthews, and Wilks obtained a decay pattern approximating to the shape $e^{-\frac{\alpha n}{2}} |\sin (n/50)|$, and obtained the decay constant α by fitting an exponential curve to the peaks in the signal height. Even without so regular a decay, one could still hope to make a measurement of the acoustic impedance of liquid He^3 by

fitting an exponential curve to the change in signal height caused by introducing liquid round the crystal. Thus the irregular shape of the decay pattern was not a serious disadvantage.

Although the decay pattern shown in Fig. 12 was the best that could be obtained by selecting among the crystals available, it was not good enough for a measurement of the acoustic impedance of helium 3 because the echoes were too few. To achieve a larger number of echoes, it was necessary either to obtain a better crystal, or to improve the sensitivity of the electronics so that more echoes could be detected in the existing decay. As we had already tested 17 crystals, and had no guarantee that any crystals subsequently acquired would be much better, we now tried to improve the electronics.

2.9 Improving the Sensitivity

The microwave power which could be fed into the cavity to drive the crystal was limited by a tendency for sparking to occur in the coaxial lines due to the large electric fields set up during the passage of the driving pulse. The transmission lines were filled with helium gas at atmospheric pressure. While this limitation could have been removed by using larger transmission lines or by filling the lines with dielectric, these structures would have been hard to build into the demagnetization cryostat into which the apparatus had eventually to be fitted. We therefore decided not to

make any change to the coaxial lines. The insertion loss of each coaxial line was about 5·3 dB, which was considered acceptable, and the noise level of the radar receiver was of the same order as thermal noise, so the only opportunity for making a large improvement to the electronics lay in changing the design of the microwave cavity.

The first change which we made to the apparatus was to try using a superconducting lead cavity. Lead was chosen as it is one of the few readily available metals whose energy gap at $4^{\circ}K$ is large enough to prevent the absorption of photons of frequency 10^{10} c/s. The main cavity assembly and crystal holder were both made from copper, and were then electroplated with as thick a layer of lead as could be deposited evenly. The two components were then clamped together hard in the hope that slight extrusion of the lead would give a good electrical join. The intention in using a superconducting cavity was to increase the electro-acoustic conversion efficiency, so as to obtain larger signals. Equation (2.13) shows that a high conversion efficiency is only attained if the loading of the cavity by the coaxial lines is small, so both probes were set well out of the cavity, to give a high Q_E.

When the superconducting cavity was tried out at helium temperatures, it was found to have a loaded Q of over 10 000, most of the loading being due to the probes. A decay pattern obtained with a rather poor crystal is shown in Fig. 15; about 100 echoes are visible, and echoes up to the 80th are large enough to be measured.

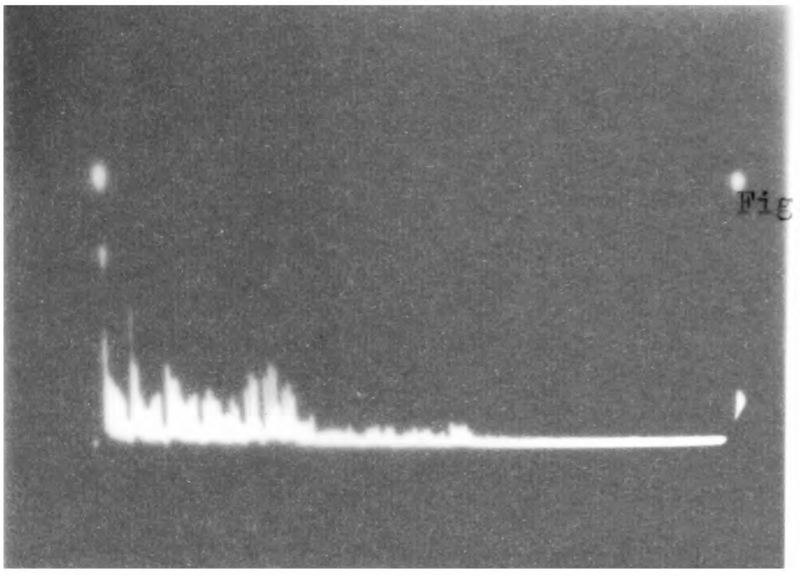

Fig. 13 a

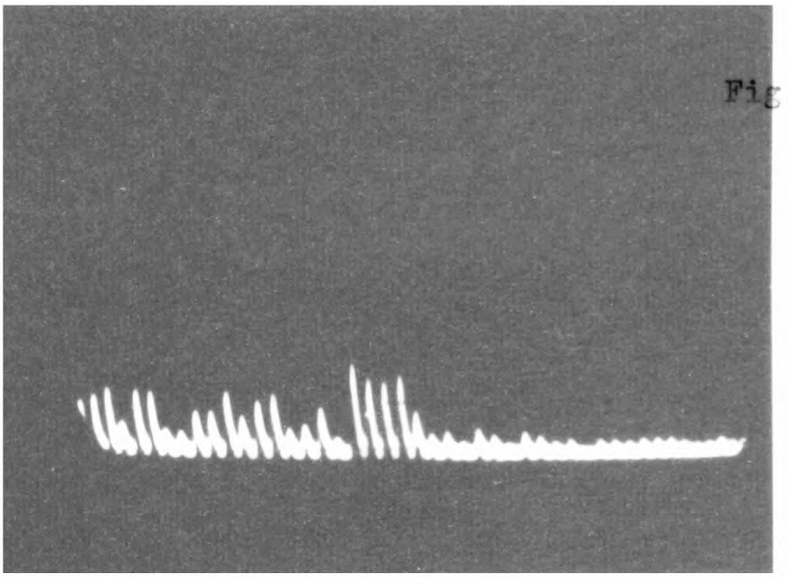

Fig. 13 b

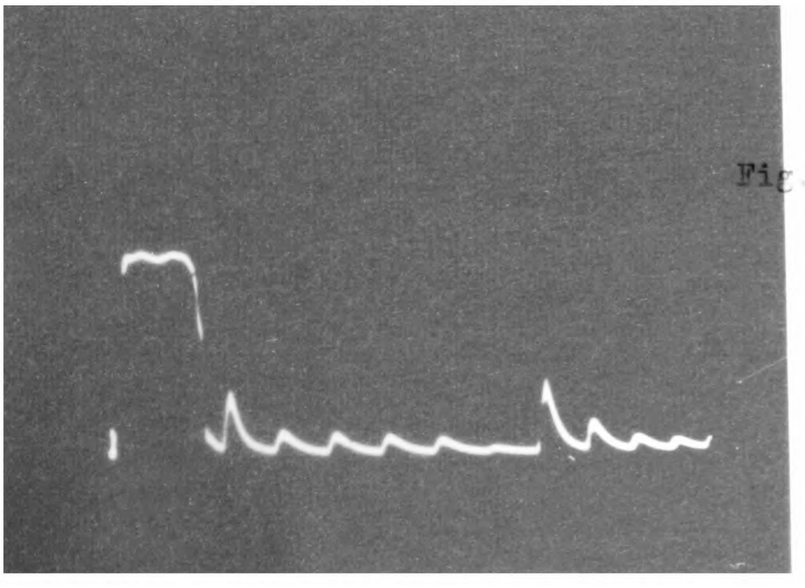

Fig. 13 c

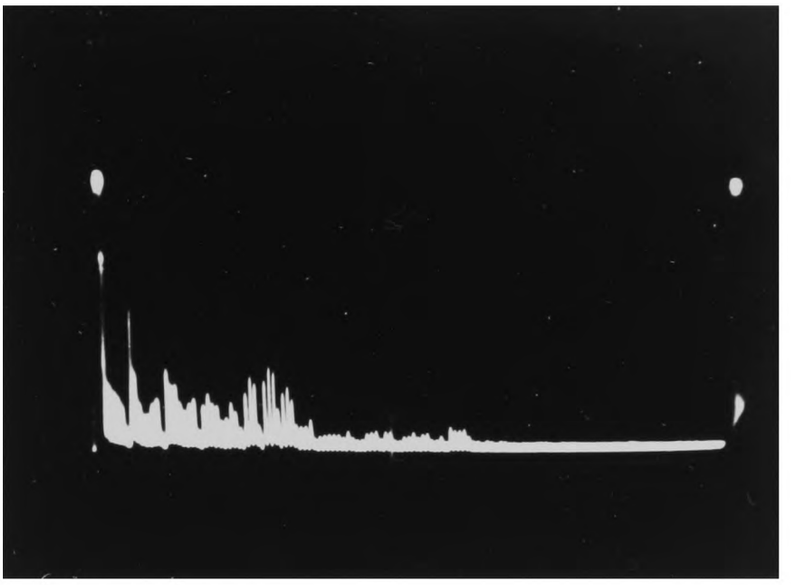

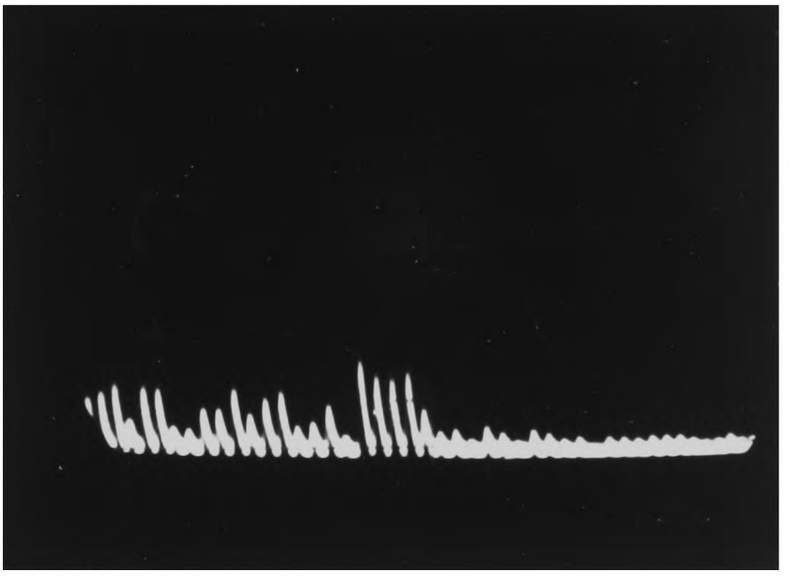

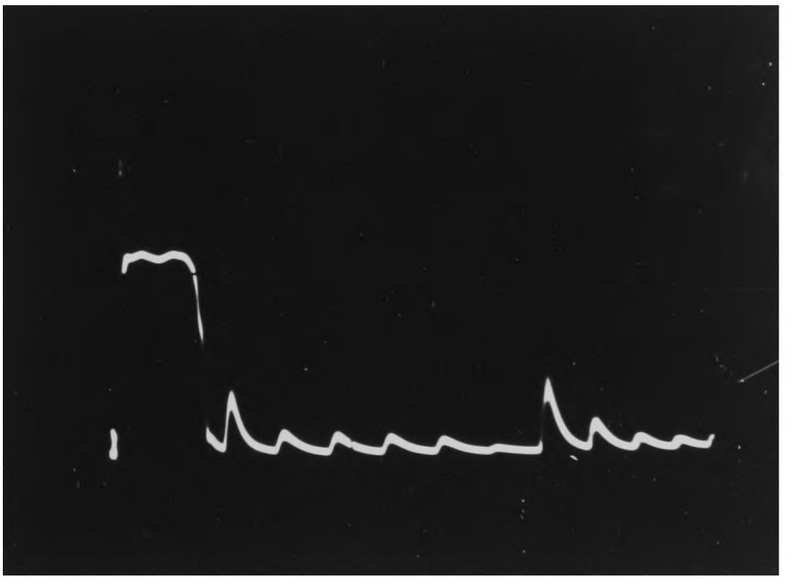

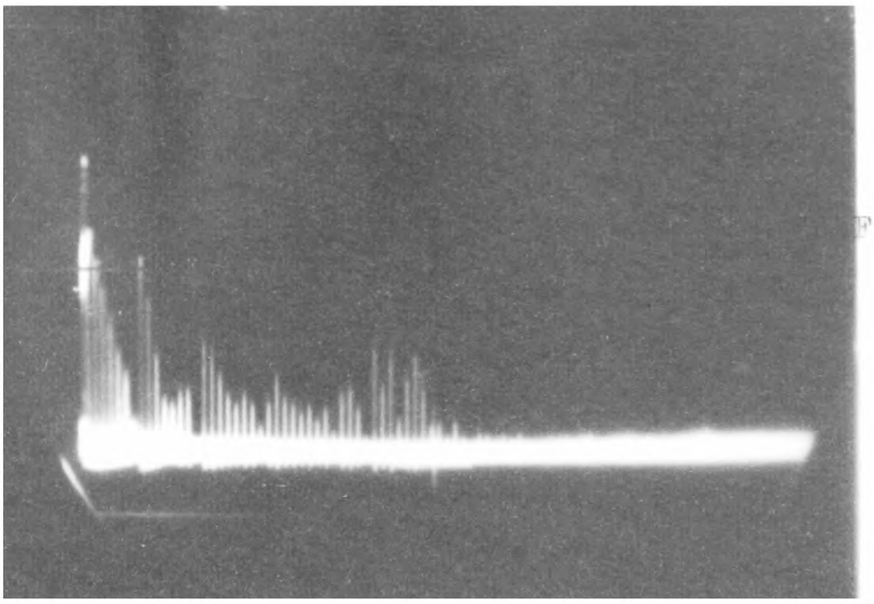

Fig. 14 a

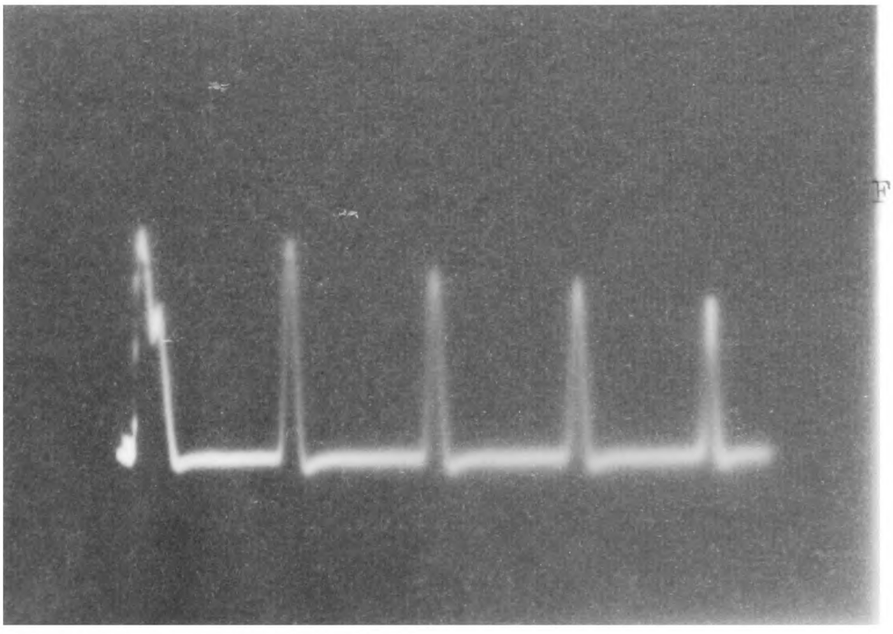

Fig. 14 b

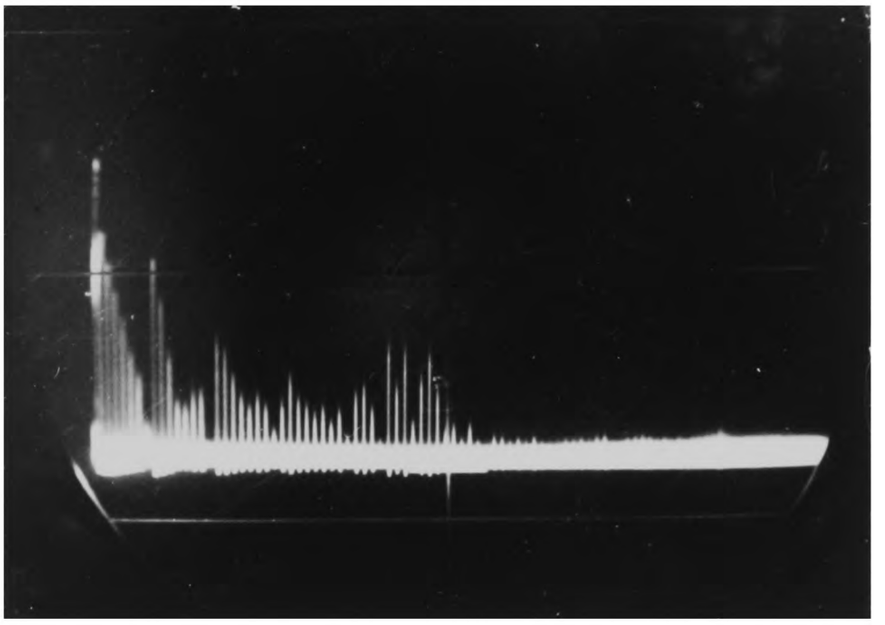

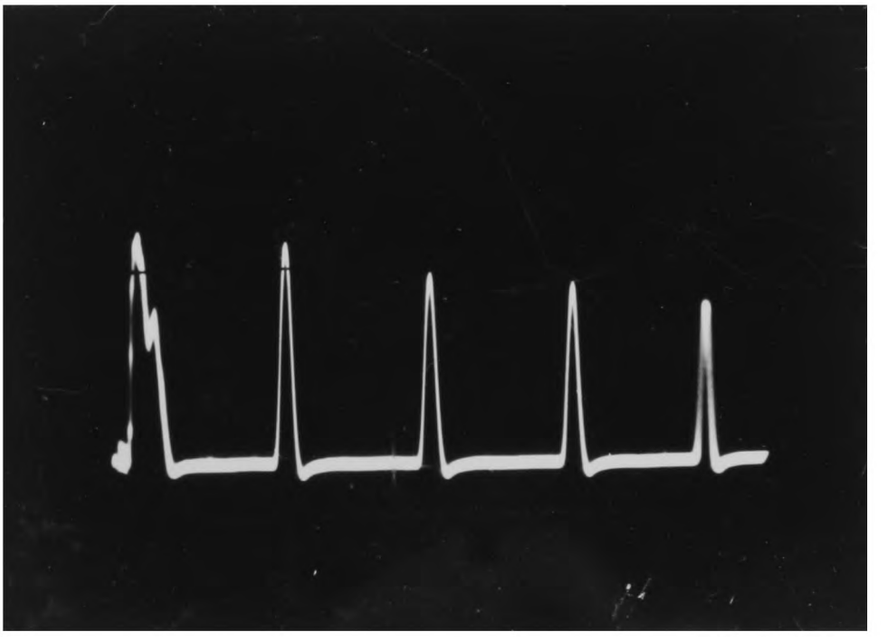

(Fig. 13b has the 81st echo in the centre.) For reference, the decay pattern of the same crystal in a copper cavity is shown in Fig. 14a. It is clear that the use of a superconducting cavity made a worthwhile improvement in the size of the signal received from the crystal.

In addition to the increase in signal size which was achieved by using a lead cavity, there was also a change in the shape of the pulses. This may be seen by comparing Fig. 13c, which was obtained with the superconducting cavity, and Fig. 14b, which was obtained with a copper cavity (not actually for the same crystal). The pulse shape given by the superconducting cavity shows an exponential tail which appears to be due to ringing of the cavity on account of its high Q. Estimating the Q from the ringing time gives $Q \sim 25\,000$, which is consistent with the rough value given by a bandwidth measurement.

The pulse shape shown in Fig. 15 is sufficiently distorted that no further increase in the Q of the cavity could be contemplated. Since by equation (2.15) the efficiency of electro-acoustic conversion is proportional to Q (i.e. to Q_E), a natural limit to the efficiency was reached. With the crystal chosen for this test, the number of echoes visible was increased from 80 to 120 by plating the cavity with lead. This increase was very useful, but not enough to make the experiment workable without some additional improvement in the performance of the apparatus.

As we had by now made all the improvements to the electronics which were not unduly inconvenient, it was necessary to consider whether the crystals themselves could be improved in any way. The decay pattern is sensitive to movements of 50 Å or less in the end faces of the crystal, so it should be possible to alter the decay by deforming the crystal. Our next step was therefore to try to produce an elastic deformation in a crystal while observing the decay pattern; this required that a controlled force should be applied to the crystal while it was at liquid helium temperature. As our final experiments necessitated the use of demagnetization techniques where the tolerable heat input to the specimen is very small, the use of rods or wires running from the crystal to the outside world at room temperature was out of the question. Magnetic forces were also excluded because they would have interfered with the demagnetization apparatus. This left electrical forces as the only remaining possibility. The possible ways of deforming a quartz rod electrically are:

(i) using the piezoelectric effect in the quartz itself;

(ii) using the force between condenser plates;

(iii) using the tendency of a dielectric to move into a non-uniform field.

Methods (i) and (ii) both require the use of potentials of 50 kv or more to produce any appreciable strain, but method (iii) would be just feasible if applied to a material with a dielectric constant of order 10^4. We therefore considered attaching a piece of ferroelectric

material to the quartz crystal and pulling this laterally with a non-uniform electric field. For this experiment, the crystal was clamped at one end in a small collet, and the ferroelectric, a ceramic containing barium titanate and made by Hunts' Capacitors Ltd., was attached to the free end.

When this arrangement was tried, only a few echoes were observed, and their pattern was quite different from that given by the free crystal. This change in decay pattern was apparently caused by clamping the crystal. The echoes obtained were too small and too few for an attempt at bending the crystal to be profitable.

At this stage, it was felt that the progress in the experimental work at 10 000 Mc/s was such that we could not be sure that it would give results within a reasonable time. We therefore decided to devote all our attention to some theoretical studies, which had been progressing in parallel with the experiments, and which seemed to offer a more encouraging prospect. The work at 1000 Mc/s by Keen, Matthews, and Wilks was by now complete, so there were some results available which could be compared with the theory. The theoretical work will be discussed in the next few chapters.

In concluding this discussion of the attempt to measure the acoustic impedance of liquid He^3 at a frequency of 10 000 Mc/s, we would emphasise that there is no fundamental reason why the experiment should not be possible. The major difficulty is simply the technical problem of obtaining a sufficiently good quartz crystal.

However it should be noted that even with a decay pattern containing say 300 echoes, one does not necessarily have sufficient means to perform an impedance measurement. If the amplitude of the nth echo is $y_o(n)$ with the crystal mounted in vacuo, and $y_1(n)$ with the crystal surrounded by helium, we must ensure that the extra decay produced by introducing the liquid is exponential, i.e.

$$y_1(n) = y_o(n)\, e^{-\frac{an}{2}},$$

and one must check also that a has the correct value for a case where the acoustic impedance of the liquid is known, e.g. for He^4 at any temperature, or for He^3 above 1^oK. While there is no obvious reason why these conditions should not be met, the physical situation within the quartz crystal is sufficiently complicated that this point requires experimental confirmation for any given crystal.

An alternative approach would be to use a double-quantum detector as discussed by Shiren (1961). As this measures acoustic energy rather than amplitude, it should avoid the untidy decay patterns obtained by piezoelectric detection. However, the detector used by Shiren was a MgO crystal doped with Fe^{++}, and one would have either to bond a quartz crystal to a MgO crystal, or to devise a means of doping the quartz itself with a suitable ion. Neither of these arrangements is particularly attractive for the present experiment.

CHAPTER 3

Theory of Sound Propagation in Liquid He^3

3.1 Landau's Theory

In this chapter we shall work through the calculations performed by Landau to find the velocity and attenuation of sound in liquid He^3. Up to § 3.3, the material is based on a review of Landau's theory given by Abrikosov and Khalatnikov (1959).

To describe the properties of liquid He^3, Landau assumes that there exists in the liquid an assembly of elementary excitations, which he calls quasi-particles. Each quasi-particle has a definite momentum. One may imagine the quasi-particles as being derived from the atoms of a perfect Fermi gas by slowly "turning on" the interaction between the atoms. It follows from the continuity of this transition that the number of quasi-particles is equal to the number of atoms, and that the quasi-particles are fermions with spin $\frac{1}{2}$. It is further assumed that the density of states in momentum space is the same for quasi-particles as for atoms in a gas, that is, the number of levels in an element of momentum space $dp_x\, dp_y\, dp_z$ is

$$\frac{1}{2}\, d\tau = \frac{dp_x\, dp_y\, dp_z}{(2\pi\hbar)^3}$$

for each spin orientation.

It is necessary to define carefully the energy $\varepsilon(\underline{p})$ of a quasi-particle since the quasi-particles are assumed to interact. If the occupation probability $n(\underline{p})$ of a quantum level identified by momentum $\underline{p}$ is changed by $\delta n(\underline{p})$, the energy E of the liquid as a whole will change by δE. Landau defines the energy of a particle in level $\underline{p}$ by

$$\delta E = \varepsilon(\underline{p})\ \delta n(\underline{p}) . \qquad (3.1)$$

Equation (3.1) is the equation which one obtains for the energy when using the self-consistent field method in the Hartree approximation. The total energy of the system is not equal to the sum of the energies of the quasi-particles, because the latter contains all the interaction energies counted twice over.

It is an obvious generalization of (3.1) to allow for particles to be moved in several quantum levels, so that

$$\delta E = \sum_{\text{levels}} \varepsilon_i\, \delta n_i = \int \varepsilon(\underline{p})\ \delta n(\underline{p})\ d\tau . \qquad (3.2)$$

If it is necessary to distinguish between the different spin orientations, as for example in a magnetic field, we have to include the spin-dependence explicitly:

$$\delta E = \tfrac{1}{2} S p_\sigma \int \varepsilon(\underline{p},\underline{\sigma})\ \delta n(\underline{p},\underline{\sigma})\ d\tau . \qquad (3.3)$$

In this thesis, we shall be concerned with sound waves, for which spin-dependent quantities do not arise; we shall therefore usually

ignore spin.

Because the quasi-particles interact, the energy $\varepsilon(\underline{p})$ of one quantum level $\underline{p}$ will change if the occupation number of any other level $\underline{p}'$ is changed. Landau defines an interaction function $f(\underline{p},\underline{p}')$ by the relation

$$\delta\varepsilon(\underline{p}) = \int f(\underline{p},\underline{p}')\ \delta n(\underline{p}')\ d\tau' . \tag{3.4}$$

The function $f(\underline{p},\underline{p}')$ is left undetermined, and its properties are found by experiment.

By minimizing the entropy

$$S = -k\int [\, n \ln n + (1-n)\ln(1-n)\,]\, d\tau ,$$

one can show that the particles of liquid He^3 obey a Fermi distribution

$$n = \frac{1}{e^{\frac{\varepsilon-\mu}{kT}} + 1} . \tag{3.5}$$

Now in calculating any property of liquid He^3, we use (3.3) or (3.4), in which it is necessary to know $\varepsilon(\underline{p})$ and $n(\underline{p})$. The energy of a given particle depends on the distribution of all the other particles through (3.4), and so (3.5) relates $n(\underline{p})$ to $\underline{p}$ only in a very indirect way.

When the liquid is in equilibrium and is not in a magnetic field, it is isotropic, so ε cannot depend on the direction of $\underline{p}$.

No assumption is made in Landau's theory about the details of the relation between ε and the magnitude of $\underline{p}$, but it is assumed that there is only one Fermi momentum. That is, $\varepsilon(p_F) = \mu$ defines an unique value of p_F. The Fermi momentum p_F is given by

$$N = \int n(p)\, d\tau$$

which gives

$$p_F = \hbar (3\pi^2 N)^{1/3} \tag{3.6}$$

as for a perfect Fermi gas.

Landau defines an effective mass m^* by

$$\frac{\partial \varepsilon}{\partial \underline{p}} = \frac{\underline{p}}{m^*}, \tag{3.7}$$

where $\frac{\partial \varepsilon}{\partial \underline{p}}$ is the vector $\left(\frac{\partial \varepsilon}{\partial p_x}, \frac{\partial \varepsilon}{\partial p_y}, \frac{\partial \varepsilon}{\partial p_z}\right)$, and is the velocity of a a quasi-particle. m^* is in general a function of p. Landau shows that

$$\frac{\partial \varepsilon}{\partial \underline{p}} = \frac{\underline{p}}{m} - \int n(p') \frac{\partial f(\underline{p}, \underline{p}')}{\partial \underline{p}'} d\tau' \tag{3.8}$$

$$= \frac{\underline{p}}{m} + \int f(\underline{p}, \underline{p}') \frac{\partial n'}{\partial \underline{p}'} d\tau' . \tag{3.9}$$

In evaluating the integral in (3.9), one uses the fact that $\frac{\partial n'}{\partial \underline{p}'}$ approximates to $-\frac{\underline{p}'}{p'} \delta(p' - p_F)$ at low temperatures. Then $f(\underline{p},\underline{p}')$ has only to be evaluated for the case $p = p' = p_F$, and so it reduces to a function of χ, the angle between $\underline{p}$ and $\underline{p}'$. Defining a dimen-

sionless function

$$F(\chi) = \left[\frac{\partial \tau}{\partial \varepsilon}\right]_{\varepsilon=\mu} f(\chi) , \qquad (3.10)$$

and expanding $F(\chi)$ as a series of Legendre polynomials,

$$F(\chi) = \sum_n F_n P_n(\cos\chi) , \qquad (3.11)$$

one obtains

$$\frac{m^*(p_F)}{m} = 1 + F_1/3 . \qquad (3.12)$$

Landau also calculates values for the specific heat and the velocity of sound in liquid He^3. As the details of these calculations are not of immediate concern to us, we shall quote the results. The thermal capacity per unit volume is

$$C = \frac{k^2 T}{3\hbar^3} p_F m_F^* = \frac{k^2 p_F m}{3\hbar^3} T (1+F_1/3) \qquad (3.13)$$

$$= C_{\text{perfect gas}} \times (1+F_1/3) .$$

The velocity of sound c is given by

$$c^2 = \frac{p_F^2}{3m^2} \frac{(1+F_0)}{(1+F_1/3)} . \qquad (3.14)$$

As the specific heat is just that of a Fermi gas multiplied by $(1 + F_1/3)$ (cf equation (1.4)), we can use (3.13) to evaluate F_1 from experimental measurements of the specific heat. Similarly, the velocity of sound is that of a Fermi gas multiplied by $\left[\frac{(1+F_0)}{(1+F_1/3)}\right]^{1/2}$

(of equation (1.6)), from which F_0 can be determined.

The specific heat of liquid He^3 has been measured at the vapour pressure by Anderson, Salinger, Steyert, and Wheatley (1961 a,b), by Strongin, Zimmerman, and Fairbank (1961), and by Brewer and Keyston (1961). From these measurements, one obtains the following values of m^*/m and F_1:

$m^*/m = 2{\cdot}82$	$F_1 = 5{\cdot}46$	(ASSW)
$2{\cdot}19$	$3{\cdot}57$	(SZF)
$2{\cdot}20$	$5{\cdot}60$	(BK)

The values given in this table do not agree very well among themselves, but the results of Anderson et al. were obtained at rather lower temperatures than the others, and so may be a little more reliable. The specific heat is proportional to T below $0{\cdot}04^\circ K$, so the above values may be used in the first instance only below this temperature. The velocity of sound has been measured by Laquer, Sydoriak, and Roberts (1959), and by Abel, Anderson, and Wheatley (1961). Of these measurements, the first appears to be more accurate, and so we use the value

$$c = 183{\cdot}4 \text{ m/s}$$

for the velocity of sound at the vapour pressure. c is almost independent of temperature below $0{\cdot}1^\circ K$, though it increases with pressure. The density of liquid He^3 has been measured by Sherman and Edeskuty (1960), and by Rives and Meyer (1961). The density

varies little with temperature below $0{\cdot}2^{\circ}K$, as the expansion coefficient never exceeds $-8{\cdot}4 \times 10^{-3}\ {}^{\circ}K^{-1}$ in this range (Anderson, Reese, and Wheatley (1963)). We accept the value

$$\rho = 0{\cdot}0817 \text{ gm cm}^{-3}$$

as an average over temperature for $T < 0{\cdot}2^{\circ}K$. From the above values, we can obtain the following table of F_0 and F_1, and of the Fermi velocity $v_F = p_F/m^*$, calculated for the liquid at $0{\cdot}1^{\circ}K$ and at the saturated vapour pressure.

	m^*/m	F_0	F_1	v_F (m/s)
ASSW	2·82	9·42	5·46	58·6
SZF	2·19	7·09	3·57	75·5
BK	2·20	7·13	3·60	75·1

3.2 Oscillations in He^3: General

After this brief introduction to Landau's theory, we go on to outline Landau's calculation of the properties of sound vibrations in liquid He^3. We start by writing the Boltzmann transport equation

$$\frac{\partial n}{\partial t} + \frac{\partial n}{\partial \underline{r}} \cdot \frac{\partial \varepsilon}{\partial \underline{p}} - \frac{\partial n}{\partial \underline{p}} \cdot \frac{\partial n}{\partial \underline{r}} = I(n) \qquad (3.15)$$

which describes how the distribution function n of the quasi-particles is affected by kinetic processes occurring in the liquid. It is

necessary to introduce a simplified expression for the collision integral I(n) in this equation, as the integral expression for I(n) is unmanageable; it is therefore natural to introduce a relaxation time τ so that

$$I(n) \sim - \frac{\delta n}{\tau} .$$

Unfortunately as it stands this definition of τ leads to inconsistencies, but it can be modified to give an acceptable form, and we now show how this is obtained. Let us describe the situation by means of spherical polar co-ordinates, with the Z-axis along the direction in which we try to propagate a wave motion (Fig. 20). Then I(n), which is a function of the momentum $\underline{p} = (p,\theta,\phi)$ of a quasi-particle, can be expanded in a series of spherical harmonics. Since momentum and energy are conserved in collisions, it is necessary that

$$\int \underline{p}\ I(n)\, d\tau = 0 \qquad \text{and} \qquad \int \varepsilon\ I(n)\, d\tau = 0 .$$

This implies that the coefficients of $P_0(\cos\theta)$, $P_1^0(\cos\theta)$ and $P_1^1(\cos\theta)$ in the expansion of I(n) must all be zero. The simplest way of defining a relaxation time compatible with these requirements is to subtract out the coefficients of the appropriate terms in the expansion of $\delta n(p)$:

$$I(n) = - \frac{\left[\delta n - (\delta n)_0 - (\delta n)_1^0 \cos\theta - (\delta n)_1^1 \sin\theta \cos\phi \right]}{\tau} . \qquad (3.16)$$

If we try to propagate a disturbance $\delta n \sim e^{i(kz - \omega t)}$ (where k, the propagation constant, is to be determined), equation (3.15) reduces to

$$-i\omega\,\delta n + ik\,v_F\left(\delta n - \frac{\partial n_o}{\partial \varepsilon_o}\,\delta\varepsilon\right)\cos\theta = I(n) \qquad (3.17)$$

where $\frac{\partial n_o}{\partial \varepsilon_o}$ is the derivative of the equilibrium Fermi distribution taken at the relevant value of p. As $\delta\varepsilon(\underline{p})$ only varies slowly with $\underline{p}$ in the neighbourhood of the Fermi surface, $\delta n(\underline{p})$ varies with $\underline{p}$ roughly as $\frac{\partial n_o}{\partial \varepsilon_o}$. In order to use only well-behaved functions of $\underline{p}$, Landau defines a quantity ν by

$$\delta n(\underline{p}) = \frac{\partial n_o}{\partial \varepsilon_o}\,\nu(\underline{p}). \qquad (3.18)$$

In order to calculate the properties of sound propagation in liquid He^3 it will be sufficient to solve the kinetic equation for the special value $p = p_F$ only. With this simplification, we expand $\nu(\underline{p}) = \nu(p_F, \theta, \phi)$ as a series of spherical harmonics

$$\nu(\theta,\phi) = \sum_n \sum_{m=o}^{n} \nu_n^m\, P_n^m(\cos\theta)\cos m\phi. \qquad (3.19)$$

Then
$$\delta\varepsilon(\theta,\phi) = -\sum_n \sum_{m=o}^{n} \frac{F_n}{2n+1}\,\nu_n^m\, P_n^m(\cos\theta)\cos m\phi. \qquad (3.20)$$

The kinetic equation (3.17) now reduces to

$$(\cos\theta - \xi)\,\nu(\theta,\phi) = \frac{\nu_o + \nu_1^o\cos\theta + \nu_1'\sin\theta\cos\phi}{\sigma} - \cos\theta \sum_n \sum_{s=o}^{n} \frac{F_n}{2n+1}\,\nu_n^s\, P_n^s(\cos\theta)\cos s\phi$$

(3.21)

where we have defined $\xi = \frac{i\omega\tau - 1}{ik\tau v_F}$ and $\sigma = ik\tau v_F$. Multiplying through by $\frac{P_r^m(\cos\theta)\cos m\phi}{\cos\theta - \xi}$ and integrating, we can reduce equation (3.21) to the form

$$\sum_{n \geq m} \frac{\nu_n^m}{2n+1} A_{rn}^m = 0 \qquad (3.22)$$

where $A_{rn}^m = F_n \Omega_{rn}^m + \delta_{rn} - [(\delta_{no} + \delta_{n1})\delta_{mo} + \delta_{n1}\delta_{m1}] \frac{\Phi_{rn}^m}{\sigma}$

$$\Omega_{rn}^m = \frac{(r-m)!}{(r+m)!} \int \frac{\cos\theta}{\cos\theta - \xi} P_r^m(\cos\theta) P_n^m(\cos\theta) \frac{\sin\theta\, d\theta}{2}$$

$$\Phi_{rn}^m = (2n+1)\frac{(r-m)!}{(r+m)!} \int \frac{1}{\cos\theta - \xi} P_r^m(\cos\theta) P_n^m(\cos\theta) \frac{\sin\theta\, d\theta}{2}.$$

The notation here is very condensed, so we shall pause to discuss the interpretation of equation (3.22). For each value of m and $r \geq m$, there exists an equation of the form (3.22). We can collect the equations into separate groups dealing with different m's, for no equation occurs connecting ν_n^m's with different m-values. This means that motions of the liquid which are characterized by different values of m propagate independently.

To obtain some insight into the significance of the different m's, we use (3.18), and see that a motion with a given m has $\delta n = \frac{\partial n_o}{\partial \varepsilon_o} \nu$ where $\nu \sim \cos m\phi\, e^{i(kz - \omega t)}$.

Therefore $\delta n \sim e^{i(kz - \omega t + m\phi)} + e^{i(kz - \omega t - m\phi)}$.

Thus the distribution of the quasi-particles is disturbed by two

circularly polarized waves which rotate with opposite senses. It is physically obvious that in an isotropic medium the wave vectors k of these circularly polarized oscillations must be equal. In fact in the calculation given by Abrikosov and Khalatnikov (1958) on which the present discussion is based, the identity of the two propagation constants is explicitly established.

For definiteness, let us suppose that the series (3.11) for $F(\chi)$ terminates at the term containing F_t. Then for any $m \leqslant t$, (3.22) gives us a set of $(t - m + 1)$ equations, each of which contains $\nu_m^m \ldots . \nu_t^m$. As these equations are homogeneous in the unknown quantities $\dfrac{\nu_n^m}{2n + 1}$, they can only have non-trivial solutions if the determinant of the coefficients vanishes, i.e.

$$\| A_{rn}^m \| = 0 . \qquad (3.23)$$

There is an equation of the form (3.23) for each value of m. To find ξ, and hence the propagation constant k for the mth circularly polarized wave, we have to solve the mth equation (3.23). Once (3.23) is solved, (3.22) gives all the ν_n^m to within a multiplicative constant.

Certain general conclusions can be drawn concerning the solutions of equations (3.22) at this stage, without our actually solving the equations. The momentum flux tensor π'_{ik} is shown by Landau to be equal to

$$\Pi'_{ik} = \int n p_i \frac{\partial \varepsilon}{\partial p_k} d\tau + \delta_{ik} \left[\int n \varepsilon \, d\tau - E \right] . \qquad (3.24)$$

For our problem, we want the periodically fluctuating part of Π'_{ik} which is

$$\Pi_{ik} = \int p_i \frac{\partial \varepsilon}{\partial p_k} \frac{\partial n_o}{\partial \varepsilon_o} (\nu - \delta\varepsilon) \, d\tau . \qquad (3.25)$$

One can show that the spherical harmonics of $\psi = \nu - \delta\varepsilon$ are connected with those of ν by the relation

$$\psi_n^m = \left(1 + \frac{F_n}{2n+1} \right) \nu_n^m .$$

Therefore if $\nu(\theta,\phi)$ varies as $\cos m\phi$, $\psi(\theta,\phi)$ also varies as $\cos m\phi$. In the case of a plane wave propagated in the Z-direction, one can readily show from the angular integration of (3.25) that the only components of the stress tensor which can be non-zero are

$$\Pi_{33} = - N \left(\psi_o + \tfrac{2}{5} \psi_2^o \right)$$

$$\Pi_{13} = - \frac{3}{5} N \psi_2'$$

where ψ_o, ψ_2^o, ψ_2' are evaluated at the Fermi surface ($p = p_F$). It follows that an $m = 0$ wave contributes only to the pressure stress Π_{33} while an $m = 1$ wave contributes only to the shear stress Π_{13}. From this, we might expect to be able to identify $m = 0$ waves with sound, and $m = 1$ waves with viscous waves - at least in the limit $\omega\tau \to 0$. This identification is confirmed by calculation of the wave vectors for these waves (see equation (3.35) for the

$m = 0$ case). Waves with $m \geq 2$ do not contribute to a momentum transfer, or a mass flow, or to any other quantity which is detectable by means of acoustical apparatus. They are therefore not waves which can be detected by mechanical means (and therefore they cannot be set up mechanically), so we shall not consider them further.

3.3 Dispersion of Sound

We now set up the equation which describes the dispersion of sound ($m = 0$) waves in liquid helium 3. Abrikosov and Khalatnikov (1958) perform this analysis with the assumption that the series (3.11) for $F(\chi)$ terminates at its second term. We shall later need to use the equations which result from retaining the third term in this series, so as the analysis does not become unduly complicated, we shall include the third term at this stage by assuming

$$F(\chi) = F_0 + F_1 \cos\chi + F_2 P_2(\cos\chi) \quad \text{(only)}. \tag{3.26}$$

Equation (3.21) now becomes

$$(\cos\theta - \xi)\,\nu(\theta) = \frac{\nu_0 + \nu_1 \cos\theta}{\sigma} - \cos\theta \left[F_0\nu_0 + \frac{F_1}{3}\nu_1 \cos\theta + \frac{F_2}{5} P_2(\cos\theta) \right] \tag{3.27}$$

where we have omitted all terms which do not have $m = 0$, since these do not contribute to the description of sound waves.

By including F's up to F_2, we make it necessary to keep ν's up to ν_2 in (3.21). To obtain the determinant (3.25) for this case

we have to obtain three relations between ν_0 , ν_1 , and ν_2 . Any relations which are not redundant will do, so we may use the simplest ones that we can find. Integrating (3.27) gives us

$$\nu_0 \, . \, 3\xi(1+\alpha) \; - \; \nu_1 (1 + F_1/3) \; = 0 \, , \tag{3.28}$$

where $\alpha = (i\omega\tau - 1)^{-1}$, i.e. $(1 + \alpha)^{-1} = 1 + i/\omega\tau$.

Equation (3.28) is in fact the equation of continuity $\frac{\partial \rho}{\partial t} + div(\rho \underline{v}) = 0$ in an unfamiliar form. Multiplying (3.27) by $\cos\theta$ and integrating gives

$$\nu_0 (1 + F_0) \; - \; \nu_1 \, . \, \xi (1+\alpha) \; + \; \frac{2}{5} \nu_2 (1 + F_2/5) \; = 0. \tag{3.29}$$

This is equivalent to the equation of motion $\frac{\partial P_i}{\partial t} + \frac{\partial \Pi_{ik}}{\partial x_k} = 0$.

To obtain the third relation between ν_0 , ν_1 , and ν_2 , we divide (3.27) by $(\cos\theta \; - \xi)$ and integrate. This gives

$$\nu_0 \left[(1+\alpha) \; + \omega(\alpha - F_0) \right] \; + \nu_1 \omega \xi (\alpha - F_1/3) \; + \nu_2 \, \frac{F_2}{10} \, Z \; = 0 \tag{3.30}$$

where
$$\omega(\xi) = \frac{\xi}{2} \ln\left(\frac{\xi + 1}{\xi - 1}\right) - 1 \tag{3.31}$$

and
$$Z(\xi) = (1 - 3\xi^2)\omega \; + 1 \, . \tag{3.32}$$

The equations (3.28), (3.29), and (3.30) for ν_0, ν_1 , ν_2 are consistent only if the determinant of the coefficients is zero, so we have

$$\begin{vmatrix} (1+\alpha)+\omega(\alpha-F_0) & \omega\xi(\alpha-F_1/3) & \frac{F_2}{10}Z \\ 3\xi(1+\alpha) & -(1+F_1/3) & 0 \\ (1+F_0) & -\xi(1+\alpha) & \frac{2}{5}(1+F_2/5) \end{vmatrix} = 0 .$$

Defining
$$a = \frac{F_2/4}{1+F_2/5} , \tag{3.33}$$

this may be reduced to

$$\xi^2 = \frac{(1+F_0)(1+F_1/3)}{3(1+\alpha)^2} - \frac{(1+F_1/3)}{3(1+\alpha)} \frac{Z}{aZ+\omega} . \tag{3.34}$$

Equation (3.34) is an implicit equation which determines ξ, and hence the propagation constant for sound waves.

There is one point of definition which must be mentioned at this stage. As ξ is in general a complex number, $\ln\left(\frac{\xi+1}{\xi-1}\right)$ is determined only to within an additive multiple of $2\pi i$. Now this quantity enters the analysis as $\int_{-1}^{1} \frac{dx}{\xi-x}$ where x is real. If we make the reasonable requirement that $\int_a^b \frac{dx}{\xi-x} \to 0$ when $a \to b$, $\int_{-1}^{1} \frac{dx}{\xi-x} = \ln\left(\frac{\xi+1}{\xi-1}\right)$ must have an imaginary part which is restricted to lie between $-\pi$ and π.

When $\omega\tau \to 0$, equation (3.34) reduces to

$$\left(\frac{\omega}{k v_F}\right)^2 = \xi^2(1+\alpha)^2 = \frac{(1+F_0)(1+F_1/3)}{3} - \frac{4}{15}(1+F_1/3)(1+F_2/5)\, i\omega\tau . \tag{3.35}$$

To the zeroth order in $\omega\tau$ this gives

$$\left(\frac{\omega}{k}\right)^2 = v_F^2 \frac{(1+F_0)(1+F_1/3)}{3} = \frac{p_F^2}{3m^2} \frac{(1+F_0)}{(1+F_1/3)}$$

which is identical with equation (3.14). This enables us to make a positive identification of the $m = 0$ wave with ordinary sound in the limit $\omega\tau \to 0$.

By using the small term in (3.35), one can calculate the absorption of sound, which comes to

$$\mathrm{Im}\, k = \frac{2}{15} \frac{v_F^2}{c^3} (1+F_1/3)(1+F_2/5)\, \omega^2\tau \,.$$

Identifying this with the classical expression

$$\mathrm{Im}\, k = \frac{\omega^2}{2\rho c^3} \cdot \frac{4\eta}{3}$$

results in

$$\tau = \frac{5\eta}{\rho v_F^2} \frac{1}{(1+F_1/3)(1+F_2/5)} \,. \qquad (3.36)$$

We shall use this relation later to obtain a rough estimate of F_2.

For values of $\omega\tau$ which are not very small, equation (3.34) has to be solved numerically. The values of the phase velocity $\omega/\mathrm{Re}\, k$ and attenuation $\mathrm{Im}\, k$ which are obtained for the parameters given on page 53 are shown in Figs. 15 and 16. In order to correspond with the circumstances of actual experiments, the velocity and attenuation are plotted against temperature, assuming a constant frequency $\omega/2\pi = 1000$ Mc/s. It may be seen that there is a smooth transition between the case of ordinary sound ($\omega\tau \ll 1$, high temperatures), and of zero sound ($\omega\tau \gg 1$, low temperatures).

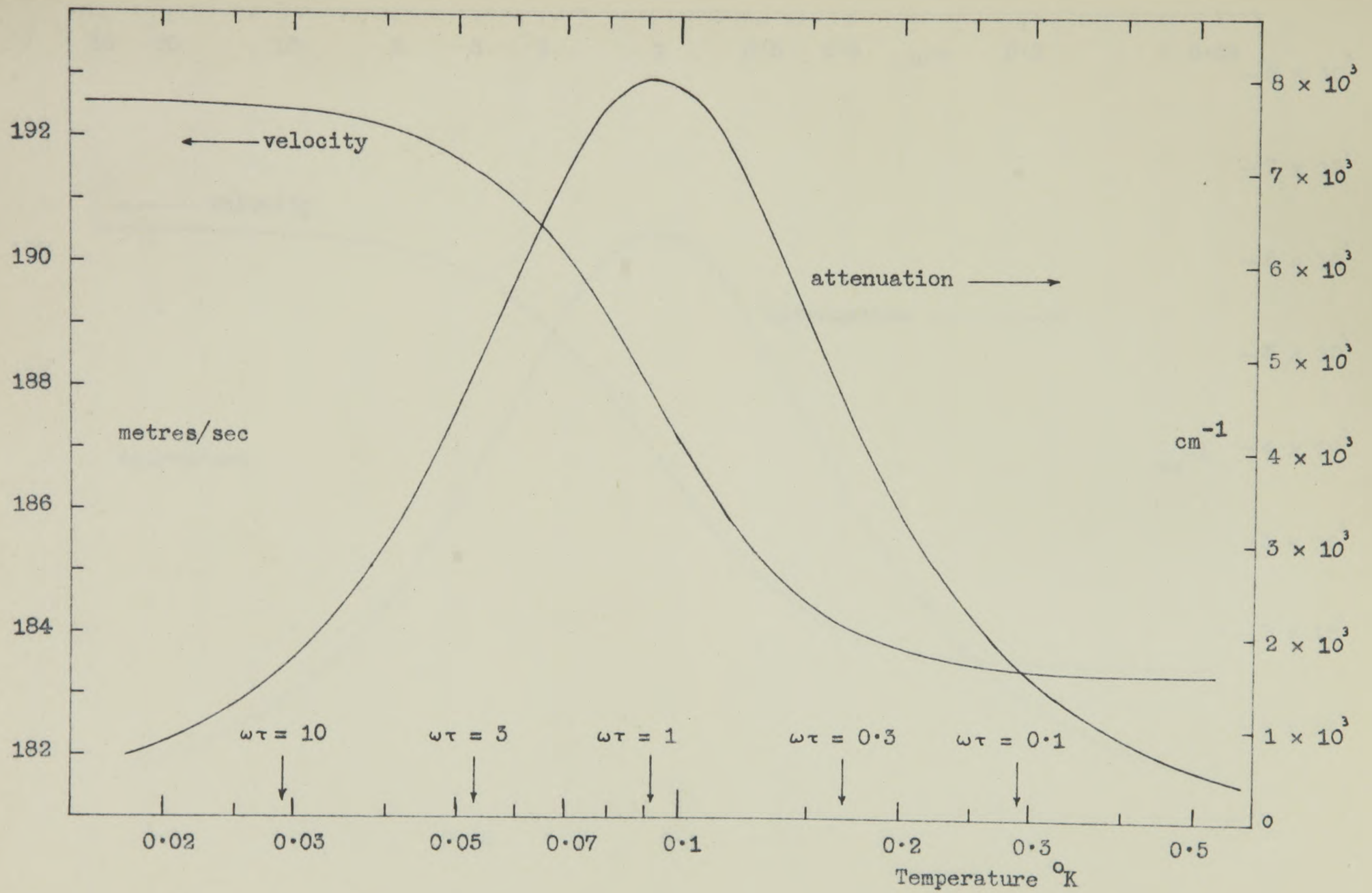

Fig. 15. Velocity and Attenuation at 1000 Mc/s. ($F_0 = 7{\cdot}1320$; $F_1 = 3{\cdot}6$; $F_2 = 0$)

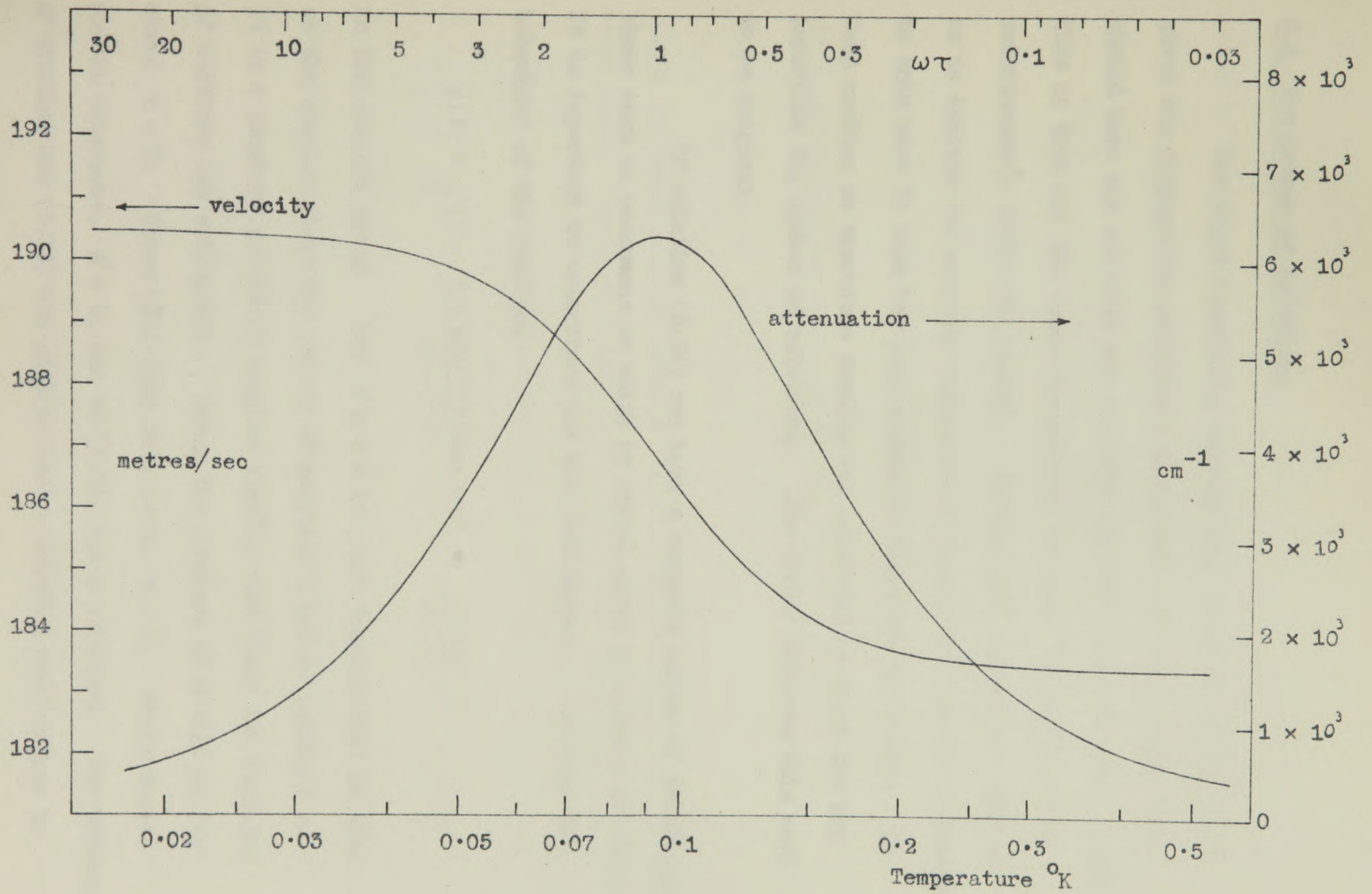

Fig. 16. Velocity and Attenuation at 1000 Mc/s. ($F_0 = 9{\cdot}4237$; $F_1 = 5{\cdot}46$; $F_2 = 0$)

3.4 The Number of Solutions

One might reasonably suppose that equation (3.34) which gives the propagation constant k for sound (and zero sound) waves should have one and only one solution for all values of $\omega\tau$. While this is true for the cases illustrated in Figs. 15 and 16, it is unfortunately untrue in general. In the next chapter we shall go on to discuss the acoustic impedance of liquid He^3, and it is necessary in this work to know how many solutions there are to (3.34). In this section we therefore develop the equations by which one may ascertain the number of solutions. The writer believes this work to be original.

If equation (3.34) can have a variable number of solutions, there must be occasions on which it either gains or loses a solution. It is important to understand how this can happen. Consider the behaviour of the function

$$\phi(\xi) = \left(\xi^2 - \frac{(1+F_0)(1+F_1/3)}{3(1+\alpha)^2} \right)(aZ + \omega) + \frac{(1+F_1/3)}{3(1+\alpha)} Z$$

in the complex plane. Let $\phi = u + iv$, and imagine that we draw on the complex plane the curves of constant u and of constant v. It is a standard result of complex algebra that these two families of contours are orthogonal. Among the contours of u will be the curve $u = 0$. There will also be a curve $v = 0$. Where these curves intersect, $\phi = 0$, and so (3.34) has a solution. Our problem of finding how (3.34) can gain or lose a solution now reduces to

asking how it is that the curves $u = 0$, $v = 0$ can gain or lose a point of intersection.

Using Fig. 17a, we find that

$$\ln\left(\frac{\xi+1}{\xi-1}\right) = \ln(\xi+1) - \ln(\xi-1)$$

$$= \left[\ln|\xi+1| + iA\right] - \left[\ln|\xi-1| + iB\right]$$

$$= \ln\left|\frac{\xi+1}{\xi-1}\right| + i(A-B).$$

If ξ approaches the real axis in the range $-1 < \mathrm{Re}\,\xi < 1$,

$$\ln\left(\frac{\xi+1}{\xi-1}\right) \to \ln\left|\frac{\xi+1}{\xi-1}\right| \mp i\pi$$

where the upper sign is taken if $\mathrm{Im}\,\xi \to 0$ from positive values, and vice versa. As we restrict $\mathrm{Im}\ln\left(\frac{\xi+1}{\xi-1}\right)$ to lie between $-\pi$ and π, $\ln\left(\frac{\xi+1}{\xi-1}\right)$ has a discontinuity on the real axis. $\phi(\xi)$ contains $\ln\left(\frac{\xi+1}{\xi-1}\right)$ so it too is discontinuous on the real axis between -1 and 1. This means that the contours $u = 0$ and $v = 0$ just stop at the real axis in this range, and therefore these curves can lose a point of intersection by the mechanism shown in Fig. 17 b. Thus we see that if a solution of (3.34) (which is an intersection point of the contours $u = 0$, $v = 0$) meets the real axis between -1 and 1, it can disappear. This is the only mechanism by which the number of solutions possessed by (3.34) can change.

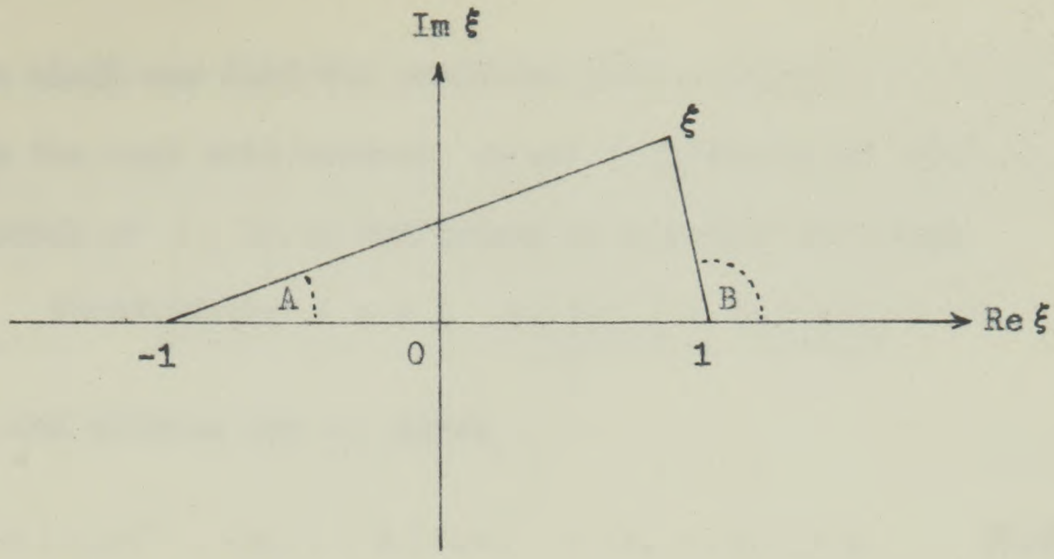

Fig. 17a.

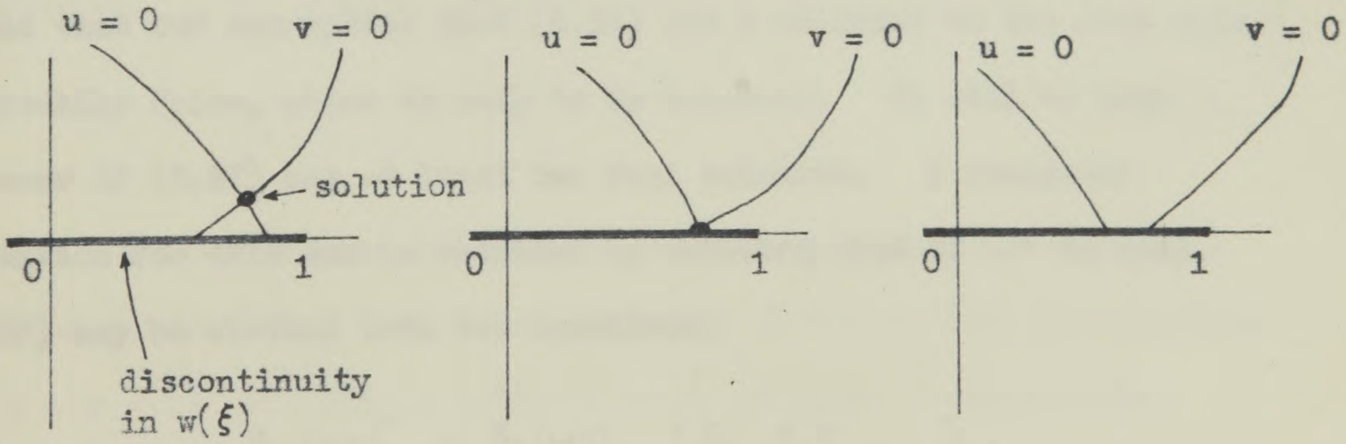

Fig. 17b. Disappearance of a Solution.

We shall now find the condition that a solution of (3.34) shall lie on the real axis between -1 and 1 (actually as $\phi(\xi)$ is an even function of ξ, it is sufficient to consider the range $0 \leq \xi \leq 1$). Substituting $\xi = x$, $\ln\left(\frac{\xi+1}{\xi-1}\right) = \ln\left(\frac{1+x}{1-x}\right) \mp i\pi$ into (3.34) and solving for $\omega\tau$ gives

$$(A_o + iA_1)(\omega\tau)^2 + (B_o + iB_1)(\omega\tau) + (C_o + iC_1) = 0 \qquad (3.37)$$

where

$$\left.\begin{aligned}
(A_o + iA_1) &= (aZ+\omega)\left[x^2 - \tfrac{1}{3}(1+F_o)(1+F_1/3)\right] + Z\cdot\tfrac{1}{3}(1+F_1/3) \\
(B_o + iB_1) &= -2i(aZ+\omega)\cdot\tfrac{1}{3}(1+F_o)(1+F_1/3) + iZ\cdot\tfrac{1}{3}(1+F_1/3) \\
(C_o + iC_1) &= (aZ+\omega)\cdot\tfrac{1}{3}(1+F_o)(1+F_1/3).
\end{aligned}\right\} \qquad (3.38)$$

Now $\omega\tau$ is of course a real number, and in general, the solution of the quadratic equation (3.37) is complex. This simply means that our assumption that (3.34) has a solution on the real axis is usually false, which is only to be expected. It will be true however if (3.37) has at least one real solution. A necessary condition for this can be obtained by noticing that if $\omega\tau$ is real, (3.37) may be divided into two equations:

$$\left.\begin{aligned}
A_o(\omega\tau)^2 + B_o(\omega\tau) + C_o &= 0 \\
A_1(\omega\tau)^2 + B_1(\omega\tau) + C_1 &= 0.
\end{aligned}\right\} \qquad (3.39)$$

These have a common solution if

$$(A_0 B_1 - A_1 B_0)(B_0 C_1 - B_1 C_0) = (C_0 A_1 - C_1 A_0)^2. \qquad (3.40)$$

It is possible to show from the properties (3.38) of the coefficients that (3.40) is also a sufficient condition that (3.39) shall have one common root. Substituting (3.38) into (3.40) gives

$$f(x) = XY - \frac{(1+F_0)(1+F_1/3)}{3}\,\frac{\pi^2 x^2}{4} = 0, \qquad (3.41)$$

where

$$\left.\begin{aligned} X(x) &= 2(1+F_0)(X_1^2 + Y_1^2) - (X_0 X_1 + Y_0 Y_1) \\ Y(x) &= \tfrac{1}{3}(1+F_1/3)(X_0^2 + Y_0^2) + \left[x^2 - (1+F_0)(1+F_1/3)\right](X_0 X_1 + Y_0 Y_1) \\ &\quad - \left[x^2 - \tfrac{1}{3}(1+F_0)(1+F_1/3)\right] 2(1+F_0)(X_1^2 + Y_1^2) \end{aligned}\right\} \qquad (3.42)$$

and $(X_0 + iY_0) = Z(x)$, $(X_1 + iY_1) = \alpha Z + \omega$.

Eliminating $(\omega\tau)^2$ between equations (3.39) also gives us

$$\omega\tau = \frac{\frac{1}{3}(1+F_0)(1+F_1/3)\,\frac{\pi x}{2}}{Y} = \frac{X}{\pi x/2}. \qquad (3.43)$$

To find the details of the occasions on which (3.34) gains or loses a solution one has first to solve (3.41) to find the position x $(0 < x < 1)$ at which a solution comes or goes. Substituting this x into (3.43) then gives the critical value of $\omega\tau$. One can find whether increase of $\omega\tau$ through the critical value causes the solution to appear from or disappear into the real axis by considering

the sign of $\frac{\partial \mathrm{Im}\,\xi}{\partial(\omega\tau)}$. Differentiating (5.34),

$$\left[\frac{\partial \xi}{\partial \omega\tau}\right]_{\mathrm{Im}\,\xi=0} = -\tfrac{1}{3}i(1+F_1/3)\left[\frac{2(1+F_0)(1+\tfrac{i}{\omega\tau})(aZ+\omega) - Z}{[x^2 - \tfrac{1}{3}(1+F_0)(1+F_1/3)(1+\tfrac{i}{\omega\tau})^2](aZ'+\omega') + 2x(aZ+\omega) + \tfrac{1}{3}(1+F_1/3)(1+\tfrac{i}{\omega\tau})Z'}\right]. \quad (3.44)$$

Here $\omega' = \frac{d\omega}{d\xi}$ and $Z' = \frac{dZ}{d\xi}$. It can be shown, though we shall not do so here, that solutions of (5.34) can only enter the real axis from above, so an extra solution appears if $\mathrm{Im}\left[\frac{\partial \xi}{\partial(\omega\tau)}\right]_{\mathrm{Im}\,\xi=0} > 0$.

A detailed analysis of (5.41) leads to the following results, which for lack of space we shall not prove here:

(i) There is one solution to (5.34) in the limit $\omega\tau \to 0$ if $F_2 < 10/3$; there are two solutions in this limit if $F_2 > 10/3$.

(ii) When $(F_2 - 10/3)$ is small and positive, $(2a - 1)$ is small positive, and the extra solution lies just above the real axis ($\mathrm{Re}\,\xi > 1$) when $\omega\tau$ is small. With increase of $\omega\tau$ it moves round and enters the upper side of the axis again, this time at a point $x < 1$ given by

$$\frac{x}{2}\ln\left(\frac{1+x}{1-x}\right) - 1 \simeq \frac{1}{2(2a-1)}.$$

The critical $\omega\tau$ at which this solution disappears is given by

$$(\omega\tau)_{crit} = \frac{\pi}{2}(1+F_0)(2a-1)^2.$$

This second solution may reappear for a larger $\omega\tau$. For

large F_2 (e.g. > 6), the extra solution may exist for all $\omega\tau$.

(iii) $(\omega\tau)_{crit}$ can take very large values, and when it does, increase of $\omega\tau$ through the critical value causes (3.34) to gain a solution. This may be a reappearance of the sound wave solution which has previously disappeared ($F_2 < 10/3$ only), or a reappearance of the second solution ($F_2 > 10/3$ only).

(iv) When there are two solutions, the second one always lies very close to $\xi = 1$, so that to an accuracy of 1% or so, the second wave solution has a velocity v_F and an attenuation distance of τv_F.

It is necessary to give an account of what happens physically when equation (3.34) gains or loses a solution. Superficially, it looks as though the mathematical treatment of disturbances in liquid He^3 is predicting a discontinuity in the properties of liquid He^3 when a solution comes or goes. But this is not so. In any experiment where one excites a sample of liquid He^3, one sets up not only the $e^{i(kz - \omega t)}$ disturbances discussed in this chapter, but also another type of disturbance, which we shall give attention to later, where particles in the liquid are individually excited. These particles travel through a free path and then give up their ordered motion in collisions with other particles. When the total disturbance of the liquid from all these causes is considered, the physical situation is not discontinuous, although the separate contributions

to the disturbance may be.

It may also seem surprising that (3.34) can have two solutions in the limit $\omega\tau \to 0$, since one would expect the liquid to support only sound then. The physical situation is saved by the fact that the extra solution has an attenuation distance very closely equal to a mean free path. This means that it would be very hard to distinguish physically between this motion and the single-particle motion referred to above, and it is difficult to see how one could observe this extra wave solution experimentally. However we shall be discussing the acoustic impedance of liquid He^3 later in this thesis, and if we are to calculate consistently what Landau's theory predicts, we must include both solutions where relevant.

As an example of the disappearance of a solution to (3.34), let us consider the case of a perfect Fermi gas. Any property of a perfect Fermi gas can be obtained formally from Landau's theory by setting $F(\chi) = 0$. Thus we obtain the dispersion curve for sound in a Fermi gas by solving (3.34) with $F_0 = F_1 = F_2 = a = 0$. The velocity and attenuation of sound are shown in Fig. 18. Both curves stop when $\omega\tau = 4{\cdot}545$, because at this point, the solution to (3.34) enters the real ξ-axis and ceases to exist. The solution does not reappear for any higher $\omega\tau$. When the solution is about to disappear, the wave motion's attenuation distance is 0·879 mean free paths, which means that it is actually attenuated slightly more rapidly than some of the single quasi-particles which are also excited

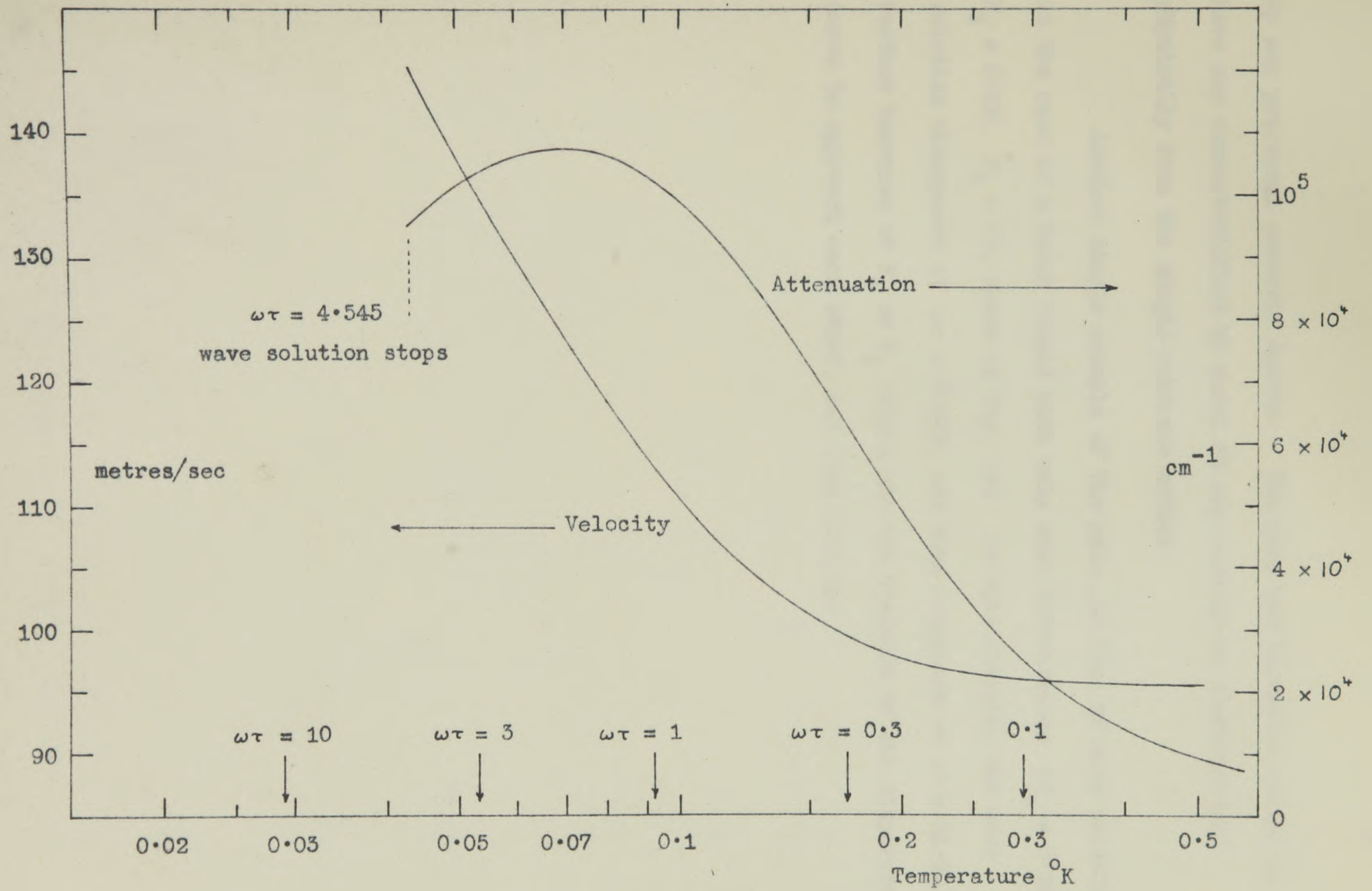

Fig. 18. Velocity and Attenuation in a Fermi gas at 1000 Mc/s.

by any practical acoustic source. The wave has therefore ceased to have any characteristics by which it may readily be distinguished physically from the single-particle motion.

Another simple example of the gain and loss of wave solutions is the case of a Fermi liquid with only weak interactions ($F_0 = 0{\cdot}14$, $F_1 = 0{\cdot}15$, $F_2 = 0$), shown in Fig. 19. In this example, the wave solution disappears at $\omega\tau = 8{\cdot}805$, and then reappears at $\omega\tau = 21{\cdot}90$. Further increase of F_0 or F_1 causes the two branches of the dispersion curve to approach each other, and then join up.

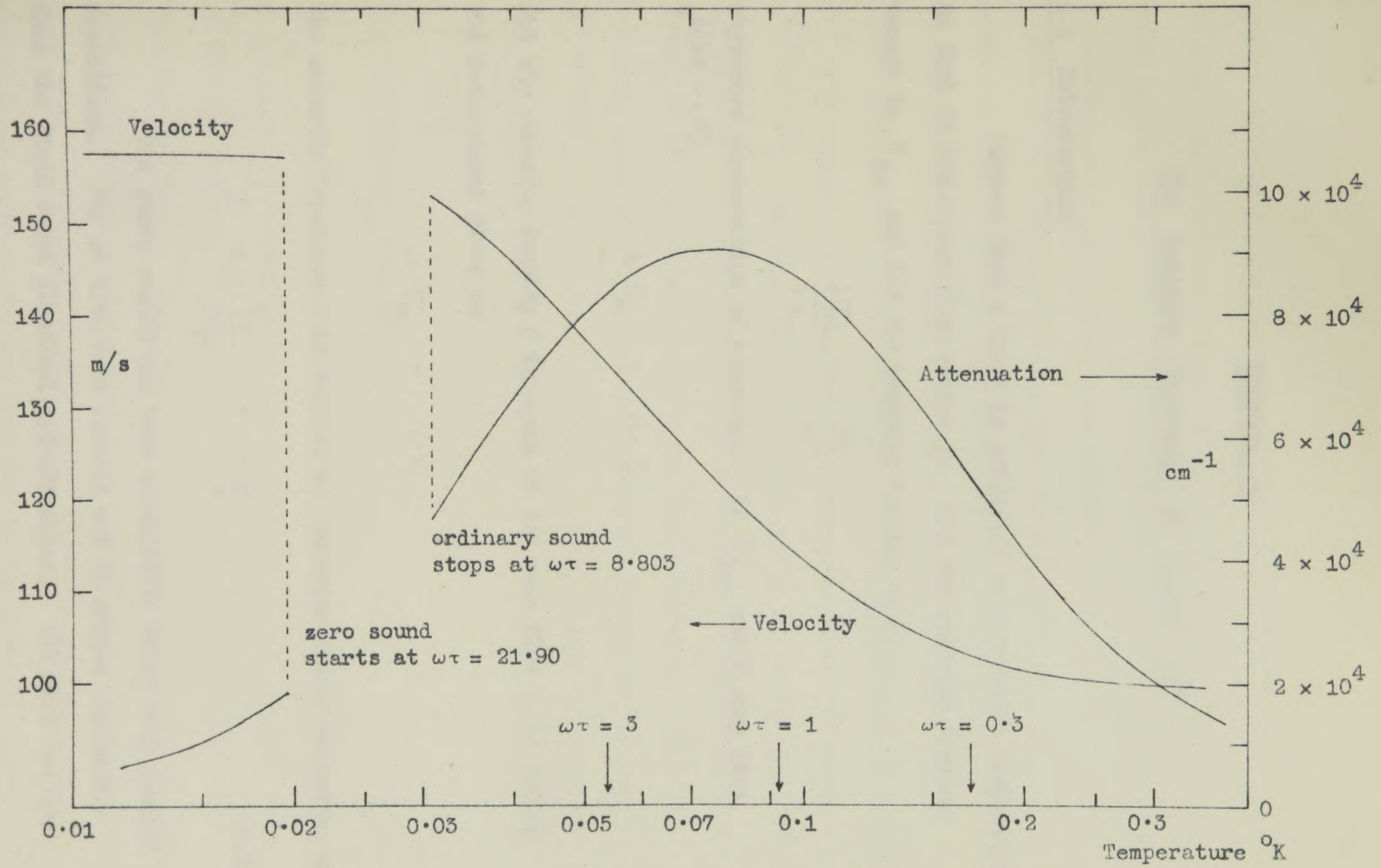

Fig. 19. Velocity and Attenuation in a weakly-interacting Fermi liquid.
($F_0 = 0{\cdot}1397$; $F_1 = 0{\cdot}15$; $F_2 = 0$; $v_F = 157{\cdot}36$ m/s)

CHAPTER 4

The Acoustic Impedance of Liquid He^3

4.1 Introduction

Suppose that a fluid is subjected to a periodic disturbance so that it has a mass flow vector $\underline{j}$. Let the momentum transfer tensor be Π_{lm} and let the momentum density be $\underline{P}$.

$$\frac{\partial \Pi_{lm}}{\partial x_m} + \frac{\partial P_l}{\partial t} = 0$$

expresses conservation of momentum. If Π_{lm} and $\underline{P}$ vary like $e^{i(kz - \omega t)}$,

$$ik\,\Pi_{l3} = i\omega\,P_l .$$

But the momentum density $\underline{P}$ is equal to the mass flow $\underline{j}$, so taking the Z-component gives us

$$ik\,\Pi_{33} = i\omega\,j_3 .$$

The acoustic impedance Z is defined as momentum flow / velocity, so

$$Z = \frac{\Pi_{33}}{j_3/\rho} = \rho\,\frac{\omega}{k} . \qquad (4.1)$$

The above result has been established under very general conditions. For we have been careful not to assume explicitly that the fluid obeys classical hydrodynamics. All that has been

assumed is that a disturbance propagates like $e^{i(kz - \omega t)}$. Now we have seen in chapter 3 that there can be motions in liquid He^3 which behave like $e^{i(kz - \omega t)}$, but we have also seen that there can be circumstances where these wave motions are impossible. Yet if liquid He^3 is disturbed by a moving boundary, particles which are scattered off the surface must carry away information about the disturbance for a distance of at least a mean free path. These ideas suggest that a complete description of disturbances in liquid He^3 must contain more complicated motions than waves varying as $e^{i(kz - \omega t)}$. In this chapter we shall set up the description given by Bekarevich and Khalatnikov (1961), and show that it leads to a satisfactory understanding of the physical situation. As a disturbance propagated in liquid He^3 is not in general of the form $e^{i(kz - \omega t)}$, equation (4.1) does not apply to liquid He^3 (except for the limiting case $\omega\tau \to 0$).

4.2 The Kinetic Equation

Before we start the calculation of the acoustic impedance, a few words on notation are appropriate here. The notation used so far has been kept fairly close to that used by Abrikosov and Khalatnikov (1959). The paper by Bekarevich and Khalatnikov (1961) differs in several respects from this, notably by a different definition of F_1. We shall continue to use the Abrikosov-Khalatnikov notation for consistency, but this will necessitate our writing

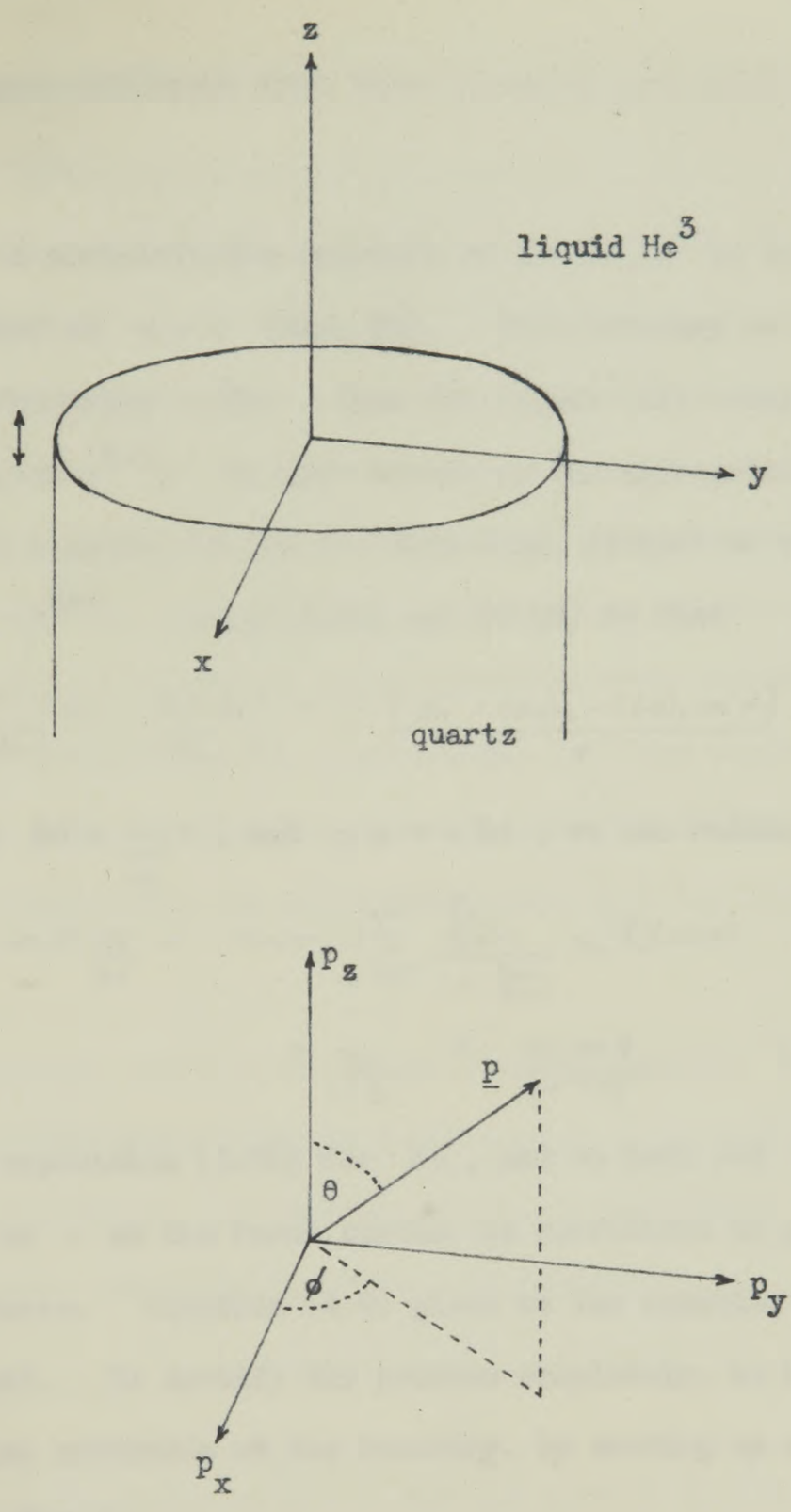

Fig. 20. Co-ordinates describing sound propagation.

equations which appear different from those given by Bekarevich and Khalatnikov.

Consider a semi-infinite specimen of liquid He^3 in contact with a solid boundary at $z = 0$ (Fig. 20). This boundary is made to oscillate with frequency $\omega/2\pi$. Then the liquid will carry a disturbance varying as $e^{-i\omega t}$. We have to set up the appropriate form of the kinetic equation (3.15) for this case, without of course assuming that $\delta n \sim e^{ikz}$. Using (3.15) and (3.16) we find

$$-i\omega\,\delta n + v_F \cos\theta \frac{\partial}{\partial z}\left(\delta n - \frac{\partial n_0}{\partial \varepsilon_0}\delta\varepsilon\right) = -\frac{\left[\delta n - (\delta n)_0 - (\delta n)_1 \cos\theta\right]}{\tau}.$$

Defining $\nu(\theta)$ by $\delta n = \frac{\partial n_0}{\partial \varepsilon_0}\nu$, and $\psi = \nu - \delta\varepsilon$, we can reduce this to

$$-(i\omega\tau - 1)\psi + \tau v_F \cos\theta \frac{\partial \psi}{\partial z} = -(i\omega\tau - 1)\sum_n \frac{\frac{F_n}{2n+1}}{1 + \frac{F_n}{2n+1}} \psi_n P_n(\cos\theta) + \frac{\psi_0}{1+F_0} + \frac{\psi_1 \cos\theta}{1 + F_1/3}. \qquad (4.2)$$

Here we have used expression (3.20) for $\delta\varepsilon$, and we have put $p = p_F$ since a solution for ψ at the Fermi surface is sufficient to give the acoustic impedance. Equation (4.2) gives us the equation of motion of the liquid. To specify the problem completely, we have also to describe the situation at the boundary, by setting up a boundary condition for ψ.

4.3 Boundary Condition

Consider what happens when quasi-particles collide with a solid boundary. They will in general be scattered in a manner which is neither perfectly diffuse, nor perfectly specular. However, we are concerned only with those particles which lie close to the Fermi surface, and these have a wavelength of about 8 Å; while even an optically polished surface can be expected to have irregularities of a hundred Angstroms or so. Therefore it should be a good approximation to regard the scattering of quasi-particles from a polished quartz surface (the surface used in experiments) as being perfectly diffuse. We shall only consider the case of perfectly diffuse scattering, though Bekarevich and Khalatnikov deal with the specular case as well.

To an observer moving with an oscillating boundary surface, particles scattered diffusely from the surface seem to be distributed equally over all directions, and to have a Fermi distribution. Thus to this observer, the particles have a distribution

$$n(\underline{p}) = \left[e^{\frac{\varepsilon(\underline{p}) - \mu}{kT}} + 1 \right]^{-1} . \qquad (4.5)$$

Since the particles which are scattered off the surface interact with all the other particles in the vicinity, $\varepsilon(\underline{p})$ is the actual energy of the particles (as seen in the moving frame of reference) and not the equilibrium energy $\varepsilon_o(\underline{p})$. Now the Fermi energy μ in (4.5) is essentially a normalizing constant which ensures that the

number of particles which leave the surface after scattering is the same as the number which arrived. The number of particles which arrives at the boundary will be a periodically fluctuating quantity, so μ will vary periodically. Let us write

$$\mu = \mu_0 + p_F u_z \gamma$$

where μ_0 is the Fermi energy of the undisturbed liquid, u_z is the velocity of the surface ($u_z \sim e^{-i\omega t}$), and γ is a number to be found. Then particles leaving the boundary ($\theta < \pi/2$) have the distribution (in the laboratory frame)

$$n(\underline{p}) = \left[e^{\frac{\varepsilon(\underline{p}) - p u_z \cos\theta - p_F u_z \gamma - \mu_0}{kT}} + 1 \right]^{-1}. \qquad (4.4)$$

Defining $$n_0(p) = \left[e^{\frac{\varepsilon_0 - \mu_0}{kT}} + 1 \right]^{-1},$$

we can write (4.4) as

$$n(\theta) = n_0 + \frac{\partial n_0}{\partial \varepsilon_0} \left[\delta\varepsilon - p_F u_z (\cos\theta + \gamma) \right]$$

where we have also put $p = p_F$. Comparing this with the definition of ν,

$$n = n_0 + \frac{\partial n_0}{\partial \varepsilon_0} \nu$$

we have $$\nu = \delta\varepsilon - p_F u_z (\cos\theta + \gamma)$$

or $$\psi = \nu - \delta\varepsilon = - p_F u_z (\cos\theta + \gamma) \qquad (\cos\theta > 0 \text{ only}).$$

We shall introduce the notation $\Psi = \psi_{z=0}$, so that the distribution

(4.4) becomes

$$\Psi(\theta) = -p_F u_z (\cos\theta + \gamma) \qquad \text{for } \cos\theta > 0. \quad (4.5)$$

Equation (4.5) gives a part of the boundary condition on ψ. In addition, γ is determined by the condition that the number of particles which leave the boundary after collision must be the same as the number that arrived. This leads to

$$\Psi_1 = -p_F u_z \qquad (4.6)$$

where $\Psi_1 = 3\int_0^{\pi} \Psi(\theta)\cos\theta \frac{\sin\theta\, d\theta}{2}$ is the usual spherical component of Ψ.

We can obtain the boundary conditions (4.5) and (4.6) in another form which is needed in later work by taking the Laplace transform of equation (4.2). If

$$\psi(s,\mu) = \int_0^{\infty} \psi(\zeta,\mu)\, e^{-s\zeta}\, d\zeta$$

where $\zeta = z/\tau v_F$, $\mu = \cos\theta$

equation (4.2) now becomes

$$(i\omega\tau - 1 - \mu s)\psi + \mu\Psi = (i\omega\tau - 1)\sum_n \frac{\frac{F_n}{2n+1}}{1+\frac{F_n}{2n+1}} \psi_n P_n(\mu) - \frac{\psi_0}{1+F_0} - \frac{\psi_1 \mu}{1+F_1/3}. \qquad (4.7)$$

Here ψ now stands for $\psi(s,\mu)$, but Ψ still means $[\psi(\zeta,\mu)]_{\zeta=0}$. Integrating (4.7) gives

$$\psi_1(s) = \left[\frac{3\, i\omega\tau}{1+F_0}\psi_0 + \Psi_1\right]\frac{1}{s}. \qquad (4.8)$$

This is the Laplace transform of (3.28), and represents the equation of continuity. If $\psi_1(s)$ varies like $1/s$ at the origin, the disturbance $\psi_1(\zeta)$ contains a component which is periodic in time but which is uniform over the whole sample of helium. Such a motion implies that a disturbance can be propagated with an infinite velocity, which is physically unreasonable. Therefore $\psi_1(s)$ may not have a pole at the origin. It follows that

$$\frac{3\, i\omega\tau}{1+F_0}\,\psi_0(0) = -\Psi_1 = p_F u_z \qquad (4.9)$$

using (4.6). In the same way, we can multiply (4.7) by μ and integrate to obtain

$$(\psi_0 + \tfrac{2}{5}\psi_2) = \left[\frac{i\omega\tau}{1+F_1/3}\,\psi_1 + (\Psi_0 + \tfrac{2}{5}\Psi_2)\right]\frac{1}{s} \qquad (4.10)$$

which implies

$$(\Psi_0 + \tfrac{2}{5}\Psi_2) = -\frac{i\omega\tau}{1+F_1/3}\,\psi_1(0) = \frac{3(\omega\tau)^2}{(1+F_0)(1+F_1/3)}\left[\frac{\partial\psi_0}{\partial s}\right]_{s=0}. \qquad (4.11)$$

4.4 Solution of the Kinetic Equation

By setting up the kinetic equation (4.7) and the boundary condition (4.5), (4.9), (4.10), we have put into mathematical form all the physical information available on the excitation of liquid He^3 by a moving boundary. Obtaining a solution from now onwards is therefore entirely a mathematical problem. We shall return to a

discussion of the physics again in § 4.5.

Because the equations obtained are very complicated, we shall not at this stage include F_2 in the expansion of $F(\chi)$; in this respect we follow the treatment of Bekarevich and Khalatnikov. The kinetic equation (4.7) reduces to

$$(i\omega\tau - 1 - \mu s)\psi + \mu\Psi = (i\omega\tau - 1)\left[\frac{F_0}{1+F_0}\psi_0 + \frac{F_1/3}{1+F_1/3}\psi_1\mu\right] - \frac{\psi_0}{1+F_0} - \frac{\psi_1\mu}{1+F_1/3}$$

$$= \frac{(F_0 - \alpha)}{(1+F_0)}\frac{\psi_0}{\alpha} + \frac{(F_1/3 - \alpha)}{(1+F_1/3)}\frac{\psi_1\mu}{\alpha} \qquad (4.12)$$

where $\alpha = (i\omega\tau - 1)^{-1}$ as usual.

Dividing (4.12) by $(i\omega\tau - 1 - \mu s)$ and integrating gives

$$\psi_0\left[\frac{(F_0 - \alpha)}{(1+F_0)}(\omega + 1) - 1\right] + \psi_1\frac{(F_1/3 - \alpha)}{(1+F_1/3)}\frac{\omega}{\alpha s} = \int_{-1}^{1}\frac{\mu\Psi(\mu)}{i\omega\tau - 1 - \mu s}\frac{d\mu}{2} \qquad (4.13)$$

where $$\omega(s) = \frac{i\omega\tau - 1}{2s}\ln\left(\frac{i\omega\tau - 1 + s}{i\omega\tau - 1 - s}\right) - 1. \qquad (4.14)$$

Equations (4.13) and (4.8) give two linear relations for ψ_0 and ψ_1; solving for ψ_0 leads to

$$\psi_0\,\Delta(s) = -\int_{-1}^{1}\frac{\mu\Psi(\mu)}{i\omega\tau - 1 - \mu s}\frac{d\mu}{2} - \frac{p_F u_z}{\alpha s^2}\frac{(F_1/3 - \alpha)}{(1+F_1/3)}\omega \qquad (4.15)$$

where $$\Delta(s) = \frac{3(1+\alpha)^2}{(1+F_0)(1+F_1/3)}\left\{\left(\frac{1}{\alpha^2 s^2} - \frac{(1+F_0)(1+F_1/3)}{3(1+\alpha)^2}\right)\omega + \frac{(1+F_1/3)}{3(1+\alpha)}Z\right\} \qquad (4.16)$$

and $$Z = \omega\left(1 - \frac{3}{\alpha^2 s^2}\right) + 1.$$

Using the known form (4.5) for $\Psi(\mu)$ when $\mu > 0$, equation (4.15) can be reduced to

$$\psi_0 \, \Delta(s) = Q(s) + \frac{(F_0 - \alpha)}{(1 + F_0)} \frac{\omega}{s^2} F(s) \qquad (4.17)$$

where $$Q(s) = - \int_{-1}^{+} \mu \frac{[\Psi(\mu) + p_s u_z (\nu + \mu)]}{i\omega\tau - 1 - \mu s} \frac{d\mu}{2} \qquad (4.18)$$

and $$F(s) = p_s u_z \frac{(1 + F_0)}{(F_0 - \alpha)} \left(\frac{i\omega\tau}{1 + F_1/3} + \nu s \right) . \qquad (4.19)$$

The function $\Delta(s)$ will be an important one in the analysis which follows, so we pause here to mention one of its more significant properties. Consider the equation $\Delta(s) = 0$; it can be rearranged as

$$\frac{1}{\alpha^2 s^2} = \frac{(1 + F_0)(1 + F_1/3)}{3(1+\alpha)^2} - \frac{(1 + F_1/3)}{3(1+\alpha)} \frac{Z}{\omega}$$

which is identical with (3.54) if we put $1/\alpha s = - \xi$. Suppose that (3.54) has solutions $\xi = \pm y_0$ (since (3.54) defines ξ by means of an even function, all solutions occur in pairs). Then the equation $\Delta(s) = 0$ has solutions which we call $s = \pm s_0$. We fix the signs of y_0 and s_0 by making $\mathrm{Re}\, y_0 > 0$, $\mathrm{Re}\, s_0 > 0$, so that

$$s_0 = - \frac{1}{\alpha y_0} . \qquad (4.20)$$

Equation (4.17) shows that unless the right-hand side of (4.17) is zero at $s = \pm s_0$, $\psi_0(s)$ must have poles at $s = \pm s_0$. Actually, $\psi_0(s)$ cannot have a pole at $s = + s_0$, because then $\psi_0(\zeta)$ would be an exponentially increasing function of ζ, but a pole at $s = - s_0$ implies that $\psi_0(\zeta)$ contains a term like $e^{-s_0 \zeta}$. Remembering that y_0 is a solution of (3.54), so that $y_0 = \frac{i\omega\tau - 1}{ik\tau v_s}$, we find that this

pole contributes a term of the form e^{ikz} to $\psi_o(\zeta)$. Here k is the propagation constant of sound or zero sound, so we see that a pole at $s = -s_o$ is closely related to the propagation of a wave motion in liquid helium 3.

Equation (4.17) is an integral equation, since $Q(s)$ is an integral containing the unknown function $\Psi(\mu)$ which is related to the $\psi(s)$ occurring elsewhere in the equation. Bekarevich and Khalatnikov solve (4.17) by putting it into the form

$$L(s) = R(s) \qquad (4.21)$$

where $L(s)$ is a regular function of s for $\mathrm{Re}\, s < 0$, and $R(s)$ is regular for $\mathrm{Re}\, s > 0$, and the two sides are equal for a range of Re s. Once this has been done, one can define a function $\Phi(s)$ which is regular in the entire complex plane by defining it as

$$\left.\begin{aligned} \Phi(s) &= L(s) \quad \text{for} \quad \mathrm{Re}\, s < 0 \\ \Phi(s) &= R(s) \quad \text{for} \quad \mathrm{Re}\, s > 0 . \end{aligned}\right\}$$

The most general function which can be regular over the entire complex plane is a polynomial in s i.e. $\Phi(s) = a_o + a_1 s + a_2 s^2 + \ldots$. We shall always arrange that $L(s)$ and $R(s)$ vary as $1/s$ as $s \to \infty$, so the polynomial reduces to a single, constant, term with the value zero. Therefore if we can arrange (4.17) into the form (4.21), we can at once deduce that $L(s) = 0$ for $\mathrm{Re}\, s < 0$, and $R(s) = 0$ for $\mathrm{Re}\, s > 0$. These equations enable us to solve the problem.

The method described here was first used by Wiener and Hopf (1931).

Before we can construct the regular functions L(s) and R(s), we have to know what are the singularities in the terms of (4.17) in order to eliminate them. Let us look first at $\Delta(s)$. $\Delta(s)$ has the following properties:

(i) it is zero at $s = \pm s_0$;

(ii) it is infinite logarithmically at $s = \pm (i\omega\tau - 1)$;

(iii) it is discontinuous on the lines $s = \pm \dfrac{(i\omega\tau - 1)}{x}$

where x is real and $\leqslant 1$;

(iv) it is regular elsewhere, and behaves like $1 + O(1/s)$ as $s \to \infty$.

The discontinuities in $\Delta(s)$ come from w(s) which is discontinuous when $1/\alpha s$ is real and lies between -1 and 1 (cf the function $w(\xi)$ discussed in chapter 3). The lines of discontinuity are illustrated in Fig. 21, and they will be referred to as cuts in the complex plane. On the cuts,

$$w(s) = \frac{x}{2}\left[\ln\left(\frac{1+x}{1-x}\right) \pm i\pi \right] - 1$$

where $x = |1/\alpha s|$ is a real number $\leqslant 1$. The positive sign is taken on the upper side of the right-hand cut, and on the lower side of the left-hand cut.

As $\Delta(s)$ has discontinuities in both halves of the complex plane, we need to define from it new functions each of which is

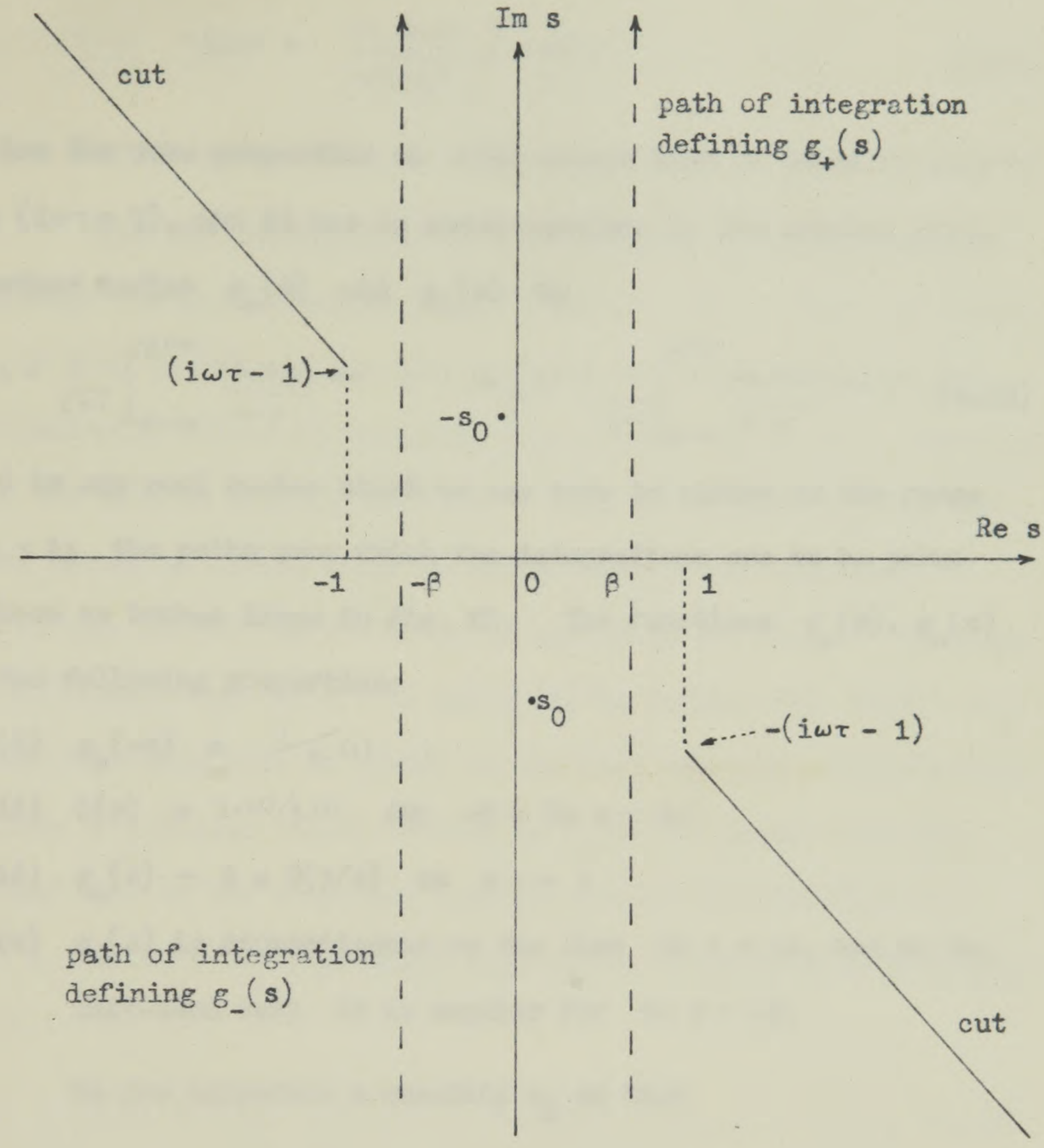

Fig. 21. Geometry of the complex plane.

regular in a half of the complex plane. To do this we first define

$$G(s) = \frac{s^2 - (i\omega\tau - 1)^2}{s^2 - s_0^2}\,\Delta(s) \,. \qquad (4.22)$$

G(s) has the same properties as $\Delta(s)$ except that it tends to zero at $s = \pm(i\omega\tau - 1)$, and it has no zeros anywhere in the complex plane. We further define $g_+(s)$ and $g_-(s)$ by

$$g_-(s) = \frac{1}{2\pi i}\int_{-\beta-i\infty}^{-\beta+i\infty} \frac{\ln G(u)}{u-s}\,du \quad ; \quad \ln g_+(s) = \frac{1}{2\pi i}\int_{\beta-i\infty}^{\beta+i\infty} \frac{\ln G(u)}{u-s}\,du \,. \qquad (4.23)$$

Here β is any real number which we may care to choose in the range $0 < \beta < 1$; the paths over which the integrations are to be taken are shown as broken lines in Fig. 21. The functions $g_+(s)$, $g_-(s)$ have the following properties:

(i) $g_+(-s) = \dfrac{1}{g_-(s)}$;

(ii) $G(s) = g_+(s)/g_-(s)$ for $-\beta < \mathrm{Re}\ s < \beta$;

(iii) $g_-(s) \to 1 + O(1/s)$ as $s \to \infty$;

(iv) $g_-(s)$ is discontinuous on the line $\mathrm{Re}\ s = -\beta$, and on the left-hand cut; it is regular for $\mathrm{Re}\ s > -\beta$.

We now introduce a quantity s_1 so that

$$\Delta(s) = \frac{1}{1+F_0}\left\{(\alpha - F_0) + \frac{(s^2 - s_1^2)}{s^2} + (1+\alpha)\right\} \qquad (4.24)$$

which implies that

$$s_1^2 = -\frac{(1+\alpha)(3\alpha - F_1)}{\alpha^2(\alpha - F_0)(1 + F_1/3)} \,. \qquad (4.25)$$

We also add the condition $\mathrm{Re}\ s_1 > 0$ so that s_1 is completely defined.

Using (4.22) to eliminate w and Δ from (4.17) we find

$$\left(Q(s) + \frac{(1+\alpha)}{(1+F_0)} \frac{F(s)}{s^2-s_1^2} \right) = \frac{s^2-s_0^2}{s^2-(i\omega\tau-1)^2} \frac{g_+(s)}{g_-(s)} \left(\psi_0(s) + \frac{F(s)}{s^2-s_1^2} \right). \qquad (4.26)$$

Equation (4.26) is true for $-\beta < \text{Re } s < \beta$ only.

With the introduction of the functions g_+ and g_-, we can now arrange the last equation into the form (4.21). From the definition of Q(s) (4.18), we see that Q(s) may be badly-behaved on the right-hand cut, but it is certainly regular for Re s < 0. Therefore we put the term in Q(s) on the left. F(s) is regular over all the complex plane, so it may occur on either side of the equation. $\psi_0(s)$ is regular for Re s > 0, so it may go on the right. Finally, $g_+(s)$ is regular for Re s < β, and $g_-(s)$ is regular for Re s > $-\beta$, so these functions must be placed on the left and right respectively. Therefore by dividing (4.26) through by $g_+(s)$, we ensure that the left-hand side of the resulting equation has no discontinuity for Re s < 0, and that the right-hand side has no discontinuous behaviour for Re s > 0:

$$\frac{(s+i\omega\tau-1)}{(s-s_0)\,g_+(s)} \left[Q(s) + \frac{(1+\alpha)}{(1+F_0)} \frac{F(s)}{s^2-s_1^2} \right] = \frac{(s+s_0)}{(s-i\omega\tau+1)\,g_-(s)} \left(\psi_0(s) + \frac{F(s)}{s^2-s_1^2} \right). \qquad (4.27)$$

We have still not succeeded in obtaining a regular left-hand side, for there is a pole at $s = -s_1$. The right-hand side also has a pole at $s = +s_1$. We can remove these poles by adding to both sides of (4.27) the expression

$$\frac{1}{2s_1}\,\frac{\alpha s_0}{g_-(0)}\left(-A\,\frac{F(s_1)}{s-s_1}+B\,\frac{F(-s_1)}{s+s_1}\right)$$

where
$$\left.\begin{aligned} A &= \frac{g_-(0)}{\alpha s_0}\,\frac{(s_0+s_1)}{(s_1-i\omega\tau+1)\,g_-(s_1)} \\ B &= \frac{g_-(0)}{\alpha s_0}\left(\frac{1+\alpha}{1+F_0}\right)\frac{(s_1-i\omega\tau+1)}{(s_0+s_1)\,g_+(-s_1)}\,. \end{aligned}\right\} \qquad (4.28)$$

Thus finally we have

$$\frac{(s+i\omega\tau-1)}{(s-s_0)\,g_+(s)}\left(Q(s)+\frac{(1+\alpha)}{(1+F_0)}\,\frac{F(s)}{s^2-s_1^2}\right)+\frac{\alpha s_0}{2s_1\,g_-(0)}\left(B\,\frac{F(-s_1)}{s+s_1}-A\,\frac{F(s_1)}{s-s_1}\right)$$

$$=\frac{(s+s_0)}{(s-i\omega\tau+1)\,g_-(s)}\left(\psi_0(s)+\frac{F(s)}{s^2-s_1^2}\right)+\frac{\alpha s_0}{2s_1\,g_-(0)}\left(B\,\frac{F(-s_1)}{s+s_1}-A\,\frac{F(s_1)}{s-s_1}\right). \qquad (4.29)$$

Equation (4.29) is now of the required form (4.21) in that both sides are regular in their respective half-planes, both tend to zero like $1/s$ as $s\to\infty$, and the two sides are equal for $-\beta<\mathrm{Re}\ s<\beta$. Therefore both sides of (4.29) are zero, from which we derive

$$\psi_0(s)=-\frac{F(s)}{s^2-s_1^2}+\frac{\alpha}{2}\,\frac{(s-i\omega\tau+1)}{(s+s_0)}\,\frac{g_-(s)}{g_-(0)}\,\frac{s_0}{s_1}\left(A\,\frac{F(s_1)}{s-s_1}-B\,\frac{F(-s_1)}{s+s_1}\right), \qquad (4.30)$$

$$Q(s)=-\frac{(1+\alpha)}{(1+F_0)}\,\frac{F(s)}{s^2-s_1^2}+\frac{\alpha}{2}\,\frac{(s-s_0)}{(s+i\omega\tau-1)}\,\frac{g_+(s)}{g_-(0)}\,\frac{s_0}{s_1}\left(\frac{A\,F(s_1)}{s-s_1}-\frac{B\,F(-s_1)}{s+s_1}\right). \qquad (4.31)$$

Equation (4.30) holds for $\mathrm{Re}\ s>-\beta$ only, while (4.31) holds for $\mathrm{Re}\ s<\beta$ only.

Having obtained a closed expression for $\psi_0(s)$, we now have to find the acoustic impedance and the constant γ. Substituting (4.30) into the boundary condition (4.11) gives the expression for

the acoustic impedance Z

$$\frac{Z}{\rho} = \frac{v_s (1+F_1/3)(1+\alpha)}{\alpha - F_1/3}\left[\gamma + 1 + \frac{1}{\alpha s_0} - \frac{1}{\alpha}\frac{g_-'(0)}{g_-(0)} + \frac{1}{2s_1}\left(\frac{(A-B)\, i\omega\tau}{1+F_1/3} + (A+B)\gamma s_1\right)\right]. \quad (4.32)$$

In this expression we still have to find γ. Substituting (4.30) into the boundary condition (4.9) gives

$$(A+B)\frac{i\omega\tau}{1+F_1/3} + \gamma s_1 (A-B) = -\frac{2}{\alpha} \quad (4.33)$$

from which γ may be found.

In order to put (4.32) into a form which can be evaluated numerically, it remains only to find a convenient expression for $g_-(s)$. By a contour integration which we shall not reproduce, Bekarevich and Khalatnikov reduce (4.25) to an equation which is equivalent to

$$g_-(s) = \frac{e^{-\phi(y)}}{\sqrt{G(s)}} \qquad (\mathrm{Re}\ s > -\beta \text{ only}) \quad (4.34)$$

where

$$\phi(y) = \frac{y}{2\pi i}\int_0^1 \ln\left[\frac{\left[x^2 + \frac{(\alpha - F_0)(1+F_1/3)}{(1+\alpha)(3\alpha - F_1)}\right]\left[\frac{x}{2}\ln\left(\frac{1+x}{1-x}\right) + \frac{i\pi x}{2} - 1\right] + \frac{(1+F_1/3)}{(3\alpha - F_1)}}{\left[x^2 + \frac{(\alpha - F_0)(1+F_1/3)}{(1+\alpha)(3\alpha - F_1)}\right]\left[\frac{x}{2}\ln\left(\frac{1+x}{1-x}\right) - \frac{i\pi x}{2} - 1\right] + \frac{(1+F_1/3)}{(3\alpha - F_1)}}\right]\frac{dx}{y^2 - x^2} \quad (4.35)$$

and $y = (i\omega\tau - 1)/s$.

(These substitutions differ slightly from those used by Bekarevich and Khalatnikov, as our form is a little more convenient for numerical work.) Substituting (4.34) into the definition (4.28) of A and B

gives

$$A = \pm\sqrt{\frac{(1+F_1/3)}{(1+\alpha)}\cdot\frac{(y_1-y_0)}{(y_1+y_0)}\frac{(y_1+1)}{(y_1-1)}}\; e^{\phi(y_1)} = \frac{\sqrt{G(s_1)}}{\sqrt{G(0)}}\frac{(y_1-y_0)}{(y_1-1)}\, e^{\phi(y_1)} \qquad (4.36)$$

$$B = \pm\sqrt{\frac{(1+F_1/3)}{(1+\alpha)}\cdot\frac{(y_1+y_0)}{(y_1-y_0)}\frac{(y_1-1)}{(y_1+1)}}\; e^{-\phi(y_1)} = \frac{(1+F_1/3)}{(1+\alpha)}\frac{1}{A} \qquad (4.37)$$

where $y_0 = -1/\alpha s_0$, $y_1 = 1/\alpha s_1$.

Substituting (4.34) into (4.32) we obtain the required expression for the acoustic impedance

$$\frac{Z}{\rho} = v_F\frac{(1+F_1/3)(1+\alpha)}{(F_1/3-\alpha)}\left[(y_0-1)-\gamma+\Phi(0) - \frac{1}{2}\left(\frac{(A-B)}{1+F_1/3}\frac{(1+\alpha)}{}y_1+(A+B)\gamma\right)\right] \qquad (4.38)$$

where $\Phi(0) = -\lim_{y\to\infty} y\,\phi(y)$.

At this stage, we have completed the calculation of the acoustic impedance of liquid He^3, as given by Bekarevich and Khalatnikov. It has been explicitly assumed that the equation $\Delta(s) = 0$ has only one pair of solutions $s = \pm s_0$, although we have seen in chapter 3 that this equation (in the form (3.34)) may have one pair of solutions, or it may have none (in the case $F_2 = 0$ which we are discussing there cannot be two). The calculation for the case in which $\Delta(s)$ has no solutions leads to the following changes in the results derived above:

$$A = \pm\sqrt{\frac{(1+F_1/3)}{(1+\alpha)}}\; e^{\phi(y_1)} = \frac{\sqrt{\Delta(s_1)}}{\sqrt{\Delta(0)}}\, e^{\phi(y_1)} \quad ; \qquad (4.39)$$

$$B = \pm\sqrt{\frac{(1+F_1/3)}{(1+\alpha)}}\; e^{-\phi(y_1)} = \frac{(1+F_1/3)}{(1+\alpha)}\frac{1}{A} \quad ; \qquad (4.40)$$

$\phi(y)$ is unaltered;

equation (4.33), which gives γ is unaltered;

$$\frac{Z}{\rho} = v_E \frac{(1+F_1/3)(1+\alpha)}{(F_1/3-\alpha)} \left[-\gamma + \Phi(0) - \frac{1}{2}\left((A-B)\frac{(1+\alpha)}{(1+F_1/3)} y_1 + (A+B)\gamma \right) \right]. \quad (4.41)$$

There is one important precaution to be noted when the expressions given here are evaluated. In the definitions of $\ln g_-(s)$ and $\ln g_+(s)$ there occurs the quantity $\ln G(s)$. This is undetermined within an added multiple of $2\pi i$. But it is a necessary part of the algebraic analysis that $\ln G(s) \to 0$ as $s \to \infty$, and that $\ln G(s)$ shall be regular except on the two cuts. Therefore we must specify the imaginary part of $\ln G(s)$ by requiring it to be zero when $s \to \infty$, and to be a continuous function of s elsewhere (except on the cuts). This requirement carried through the calculation leads to our requiring that $\sqrt{G(s)}$ shall be so defined that it is continuous between $s = 0$ and $s = s_1$. The second expression given for A in (4.36) and (4.39) determines the sign of A under this convention. Also the complex logarithm under the integral in (4.33) is required to be zero when $x = 0$ and a continuous function of x thereafter.

4.5 Physical Interpretation

At the beginning of this chapter, we established the result that the acoustic impedance of a medium is necessarily $\rho\omega/k$ if a moving boundary sets up a disturbance which is purely of the form $e^{i(kz - \omega t)}$. As equation (4.38) does not reduce to $Z/\rho = \omega/k$, we are led to suppose that there is some other disturbance present, and to ask what it means physically. We can obtain an expression for the disturbance $\psi_0(\xi)$ by combining (4.31) and (4.17) to obtain

$$\psi_0(s) = -\frac{F(s)}{s^2 - s_1^2} + \frac{\alpha}{2}\frac{(s - i\omega\tau + 1)}{(s + s_0)}\frac{s_0}{s_1}\frac{g_+(s)}{G(s)\,g_-(0)}\left(\frac{A\,F(s_1)}{s - s_1} - \frac{B\,F(-s_1)}{s + s_1}\right). \qquad (4.42)$$

This equation holds for Re $s < \beta$, and may be compared with (4.30) which holds for Re $s > -\beta$.

Having obtained an expression for $\psi_0(s)$ which is valid in the left half-plane, we can now perform the converse Laplace transformation to find the real disturbance $\psi_0(\xi)$.

$$\psi_0(\xi) = \frac{1}{2\pi i}\int e^{s\xi}\,\psi_0(s)\,ds$$

where the integration is taken up the imaginary axis. We can evaluate this integral by closing the contour shown in Fig. 22, and evaluating $\oint e^{s\xi}\psi_0(s)\,ds$ round the whole contour. It is easy to show that the contributions from the small circle round the point $(i\omega\tau - 1)$ and from the infinite semicircle are zero. Let the integral taken round the cut in the sense indicated be $-J(\xi)$; then the integral

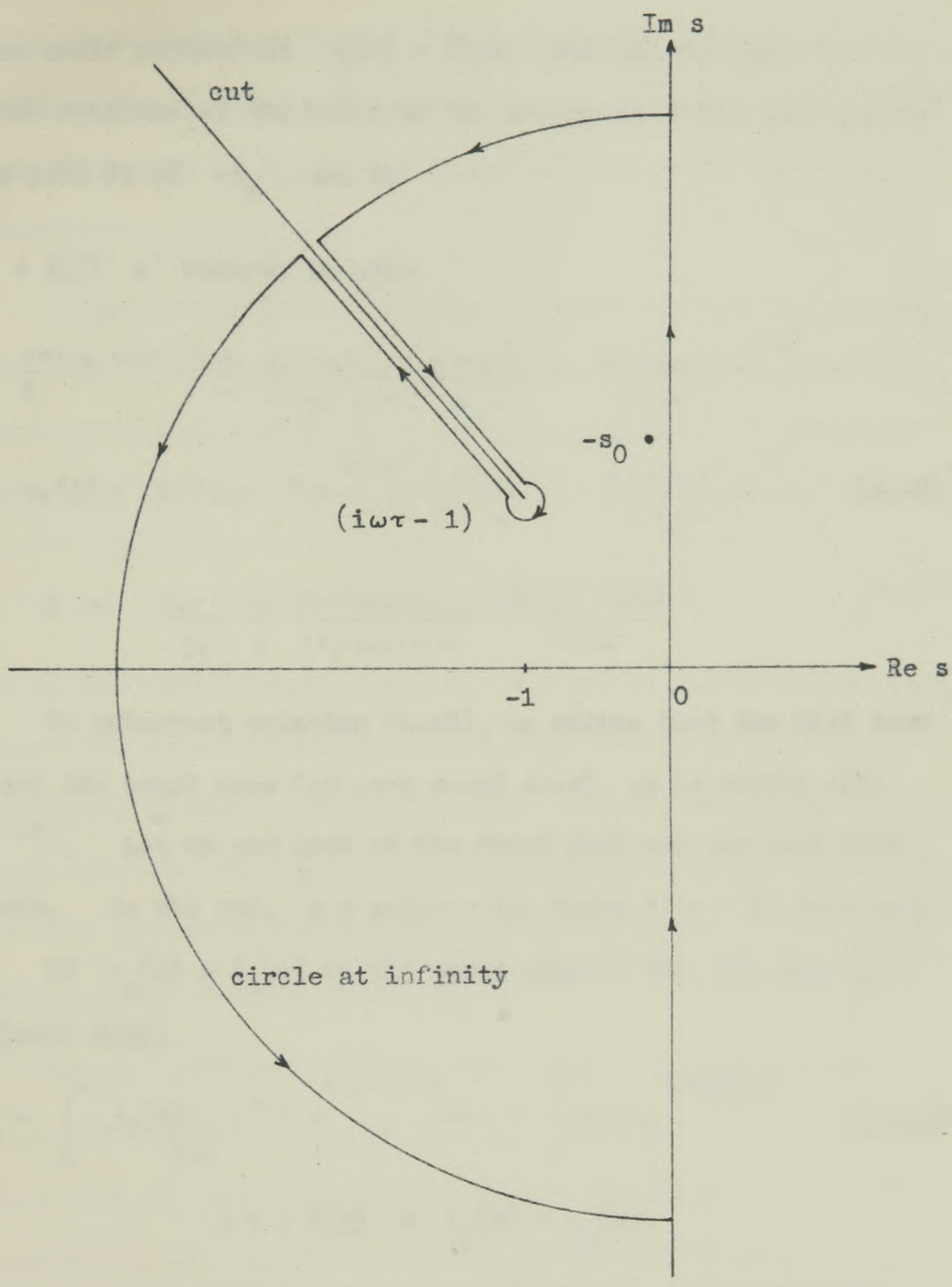

Fig. 22. Contour for evaluating $\psi_0(\zeta)$.

round the whole contour is $\psi_0(\zeta) - J(\zeta)$, and this is equal to the sum of the residues at the poles of the integrand within the contour. The only pole is at $-s_0$, and so

$$\psi_0(\zeta) - J(\zeta) = \text{residue at pole}$$

$$= \frac{\alpha}{2}(-s_0 - i\omega\tau + 1)\frac{s_0}{s_1}\frac{g_+(-s_0)}{G(-s_0)\,g_-(0)}\left(\frac{A\,F(s_1)}{-s_0 - s_1} - \frac{B\,F(-s_1)}{-s_0 + s_1}\right) e^{-s_0\zeta}.$$

Hence
$$\psi_0(\zeta) = J(\zeta) + \Lambda e^{-\phi(y_0)}\left(\frac{-A\,F(s_1)}{y_1 - y_0} + \frac{B\,F(-s_1)}{y_1 + y_0}\right) e^{ikz} \qquad (4.43)$$

where
$$\Lambda = \frac{y_0 - 1}{y_0}\,\frac{\alpha}{2}\,\frac{(1 + F_1/3)(F_0 - \alpha)}{(F_1 - 3\alpha)(1 + \alpha)}\,\frac{\sqrt{G(s_0)}\,\sqrt{G(0)}}{G(s_0)}.$$

To interpret equation (4.43), we notice that the last term represents the sound wave (or zero sound wave), as it varies like $e^{i(kz - \omega t)}$. Let us now look at the first term and see what that represents. On the cut, $s = x(i\omega\tau - 1)$, where x $(x > 1)$ is a real number. If $\psi_0(s) = I_1(x)$ on the upper edge of the cut, and $I_2(x)$ on the lower edge,

$$J(\zeta) = \int_1^\infty \frac{I_2(x) - I_1(x)}{2\pi i}\, e^{(i\omega\tau - 1)x\zeta}\, dx = \int_1^\infty K(x)\, e^{\frac{(i\omega\tau - 1)xz}{\tau v_F}} \qquad (4.44)$$

where
$$2\pi i\, K(x) = I_2(x) - I_1(x).$$

The precise form of $K(x)$ is of no great interest, as the physical interpretation of $J(\zeta)$ can be obtained from what we have written. We notice that each component of the integral $J(\zeta)$ has a velocity v_F/x and an attenuation coefficient $x/\tau v_F$ $(x > 1)$, so every component

of $J(\zeta)$ is attenuated by a factor e in a distance less than τv_F. On the other hand, the attenuation distance of sound is large compared with τv_F; therefore at large distances from the source the wave motion dominates.

It is not possible to interpret (4.44) further by arguments referring only to the calculation given here. But the calculation of the acoustic impedance in the case where particles are scattered specularly from the boundary gives rise to expressions of the form

$$\int_0^{\pi/2} K'(\theta) \exp\left(\frac{(i\omega\tau - 1)\, z}{\tau v_F \cos\theta}\right) \cdot 2\pi \sin\theta \, d\theta \qquad (4.45)$$

which is of the same form as (4.44) if $x = \sec\theta$. Expression (4.45) is readily interpreted in terms of particles travelling away from the boundary at an angle θ to the normal. The particle velocity in the normal direction is $v_F \cos\theta$, and the particles move for a distance of a mean free path (τv_F) before colliding, i.e. the excitation has an attenuation distance $\tau v_F \cos\theta$.

We can now give a physical description of what happens when we excite a sample of liquid He^3 by oscillating a solid boundary in contact with the liquid. Quasi-particles collide with the wall, and afterwards carry away information about how the wall is moving. After travelling for a distance of about τv_F, these particles collide with others. The information passed on in the collisions is out of date by a time τ. If τ is much less than the period of oscillation ($\omega\tau \ll 1$) the information passed on is coherent, and leads to the

generation of a sound wave. But if τ is of the same order as the period of oscillation the information passed on in the collisions is incoherent and cannot lead to a hydrodynamic wave. If the particles interact, information may also be passed on through the interaction even before any collisions have taken place; this information is coherent because it is passed on instantaneously, so it can lead to a wave motion, which we identify with zero sound. What the calculation has told us is that in an experiment conducted in the range $\omega\tau \gtrsim 1$, one always sets up a mixture of the incoherent particle motion together with zero sound.

In the case of a perfect Fermi gas, the wave motion ceases to exist when $\omega\tau = 4{\cdot}545$. In terms of Fig. 22, the pole at $-s_0$ has moved until it has met the cut. When the pole is very close to the cut, the attenuation of the wave motion (which is measured by the distance between the pole and the imaginary s-axis) is greater than that for some of the particle contribution. There is therefore little physical distinction between the two motions in this case. When the pole enters the cut and disappears, the motion $J(\zeta)$ remains. The fact that $J(\zeta)$ represents a motion which can exist in a perfect gas where no sound propagates confirms our interpretation of it as describing the excitation of single quasi-particles.

It is possible to show that when a pole enters the cut, the contribution $J(\zeta)$ to the disturbance changes discontinuously in just such a way that $\psi_0(\zeta)$ remains a continuous function of $\omega\tau$.

Therefore all physically observable quantities, including the acoustic impedance, vary continuously, in spite of the apparent discontinuity caused by the disappearance of the pole. This is an important result, because it makes the disappearance and reappearance of poles in $\psi_0(s)$ (solutions of (3.34)) physically reasonable, which at first sight it appears not to be.

CHAPTER 5

Extending the Theory

5.1

After the long algebraic analysis given in the last chapter, we give some numerical results obtained from the theory. Details of the numerical procedures used will not be given here, as the expressions programmed were not the same as those given in the last section, though they were equivalent. A discussion will be given later (§ 5.4) when the final expressions have been derived.

Fig. 23 shows the acoustic impedance of a Fermi gas, with the velocity of sound shown for comparison on the same graph. It will be noted that the acoustic impedance is a completely smooth function of $\omega\tau$, even though the propagation of sound is discontinuous. This agrees with the discussion given in the last chapter (§ 4.5). For comparison we also give in Fig. 24 the acoustic impedance of the weakly-interacting Fermi liquid which we discussed on page 70. As the Fermi gas model was shown in chapter 1 to be unsatisfactory for describing liquid He^3, the results obtained from the gas model are mainly of academic interest.

The curves of practical importance are illustrated in Fig. 25, where we use the values of F_0 and F_1 labelled ASSW (lower curve) and BK (upper curve) in the table on page 55. The experi-

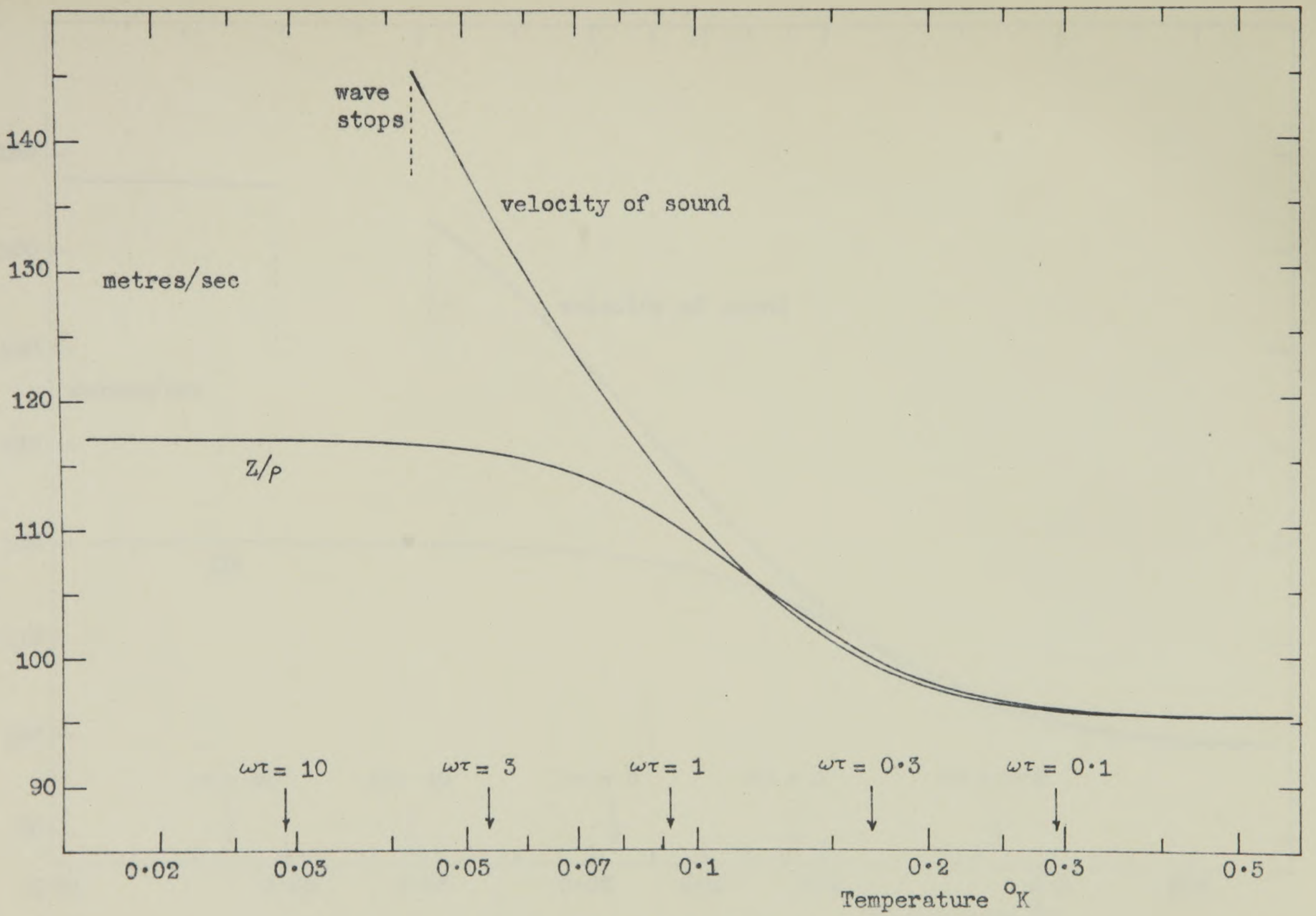

Fig. 23. Acoustic Impedance of a Fermi gas at 1000 Mc/s.

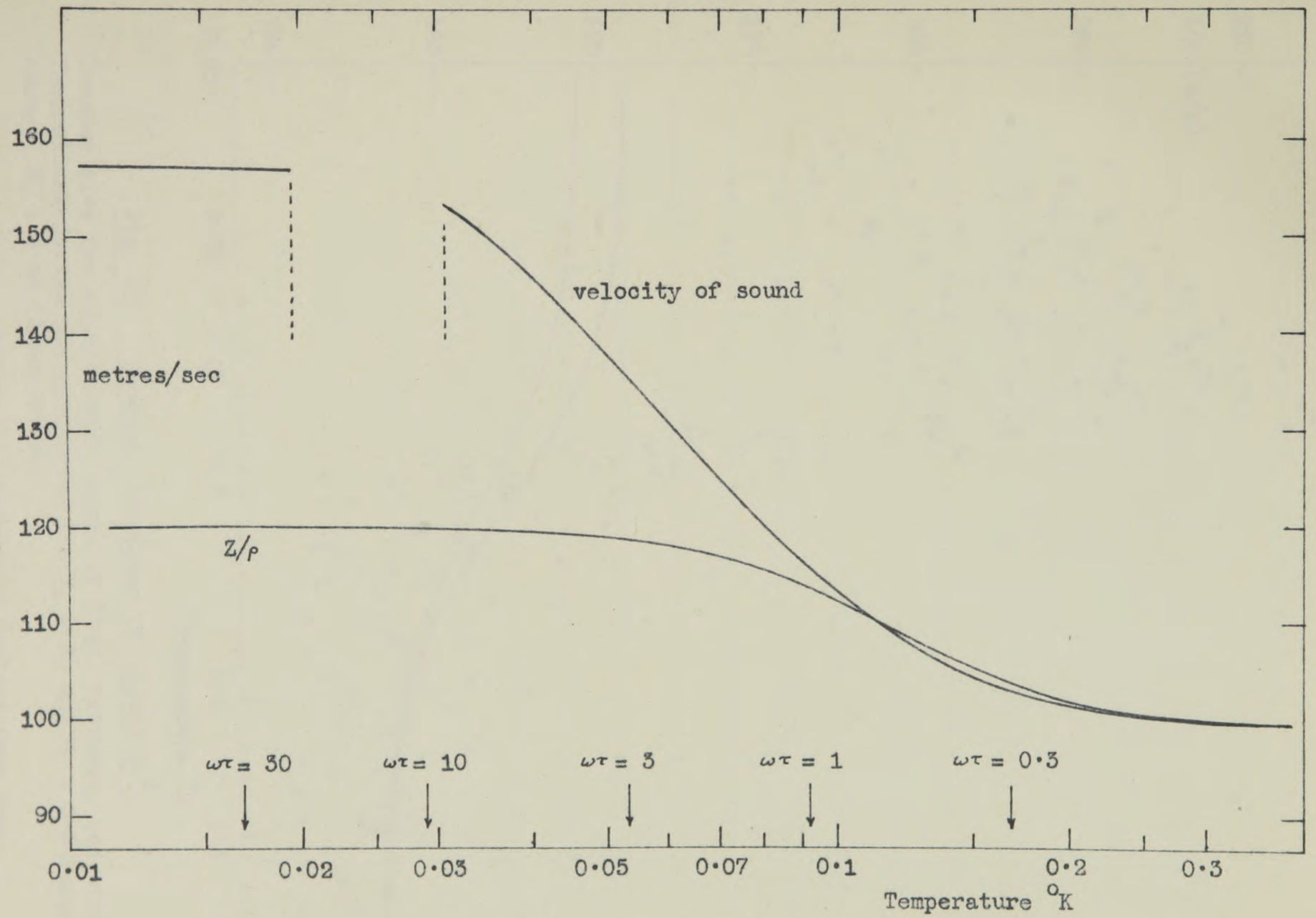

Fig. 24. Acoustic Impedance of a Weakly-interacting Fermi liquid.

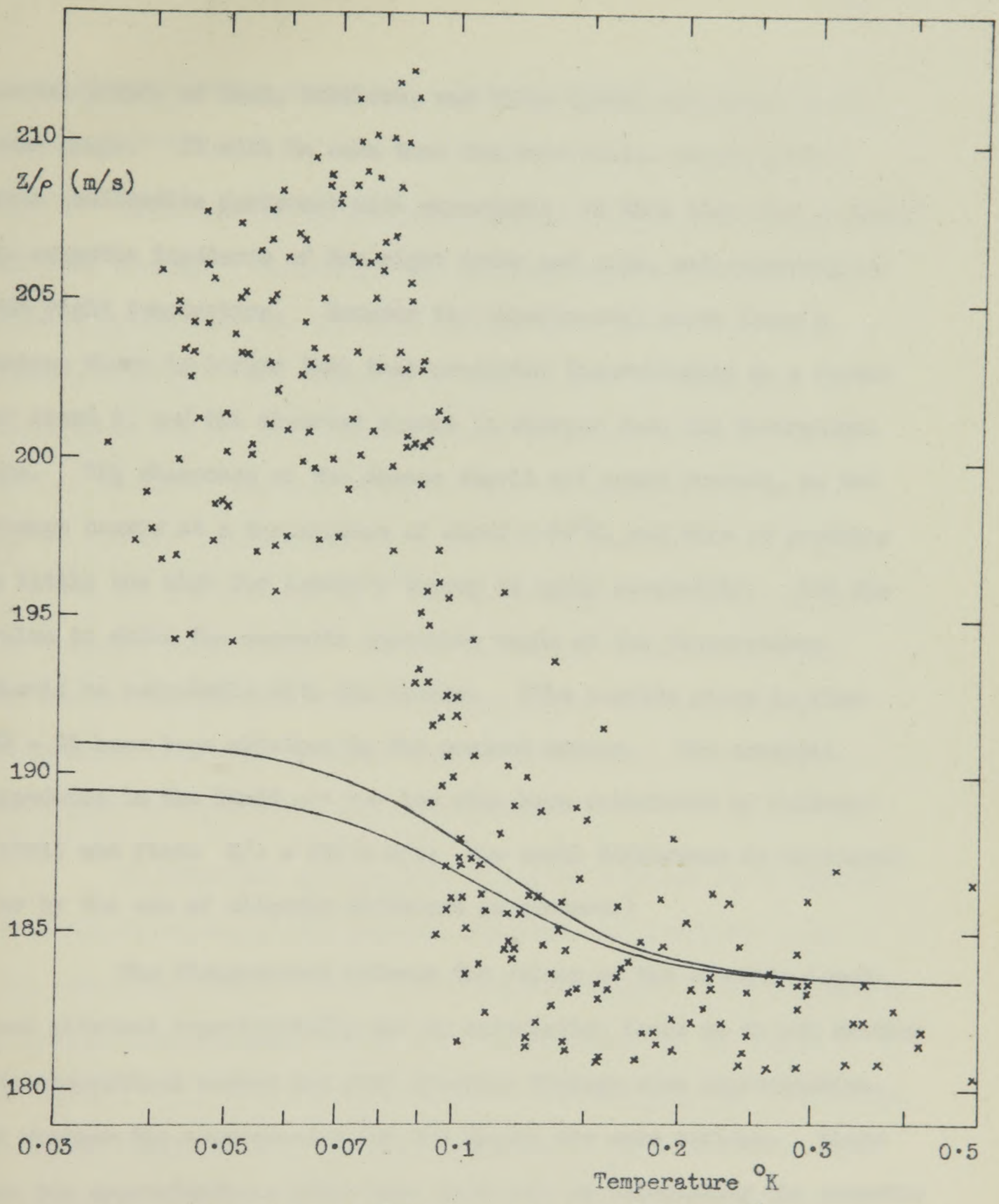

Fig. 25. Acoustic Impedance of liquid He^3.

Crosses give the experimental values of Keen, Matthews, and Wilks. Theoretical curves are calculated for $F_2 = 0$, and $F_1 = 3{\cdot}6$ (upper curve), $F_1 = 5{\cdot}46$ (lower curve).

In order to use no adjustable parameters derived from the experiment, τT^2 has been given the value $1{\cdot}7 \times 10^{-12}$ sec $°K^2$ (Abel et al. (1961)).

mental points of Keen, Matthews, and Wilks (1963) are shown on the same graph. It will be seen that the theoretical curves show a good qualitative agreement with experiment, in that they show a change in acoustic impedance of the right order and sign, and occurring at the right temperature. However the experimental curve shows a change which is larger than that predicted theoretically by a factor of about 2, and the observed change is sharper than the theoretical one. The sharpness of the change should not cause concern, as the change occurs at a temperature of about $0{\cdot}09^{\circ}K$, and this is probably a little too high for Landau's theory to apply accurately. But the value to which the acoustic impedance tends at low temperatures should be comparable with the theory. (The results given in Figs. 23 - 25 have been obtained by the present writer. The acoustic impedance in the limit $\omega\tau \to \infty$ has also been calculated by Salinger (1961) who finds $Z/\rho = 187{\cdot}4$ m/s; the small difference is accounted for by the use of slightly different parameters.)

The disagreement between the values of the acoustic impedance obtained experimentally and by calculation leads us to ask whether the theoretical answer has lost accuracy through some approximation, or whether the consequences for the theory are more serious. There are two approximations which have been made in calculating the acoustic impedance:

(i) we have assumed that quasi-particles are scattered diffusely at the solid boundary;

(ii) we have terminated the series (3.11) for $F(\chi)$ at its second term.

The first of these approximations (diffuse scattering) is not very serious. Bekarevich and Khalatnikov (1961) obtain very similar results for Z/ρ for both diffuse and specular scattering of quasi-particles. The values of F_0 and F_1 used by Bekarevich and Khalatnikov are not very close to those currently accepted, but a similar agreement has been obtained with the accepted parameters (Sykes (1964)) (Sykes finds Z/ρ = 190 m/s in the limit $\omega\tau \to \infty$ when F_1 = 5·4 and 192 m/s when F_1 = 5·3, these figures being calculated for specular scattering). As the two extreme assumptions about the scattering law give almost the same values for the acoustic impedance, it is very unlikely that an intermediate scattering law would give an appreciably different result.

It therefore appears that if Landau's theory is to explain the measured values of the acoustic impedance of liquid He^3, one must extend the series (3.11) beyond the second term. It is possible to make a rough estimate of the order of magnitude of the next coefficient F_2 by methods which we shall describe shortly, but nothing at all is known about F_3 and the higher F's. Therefore if we were to introduce F_3 into the calculations we should have to treat it as an adjustable parameter. Such a procedure would be an exercise in curve fitting, with no physical usefulness. The same observation applies to the inclusion of all higher parameters. It follows that

if any physically meaningful results are to be obtained by extending the series for $F(\chi)$ beyond its second term, it is necessary that the extra terms should be limited to one only.

5.2 Estimates of F_2

The experiment of Keen, Matthews, and Wilks (1963), with an acoustic frequency of 1000 Mc/s, can be taken as showing that the acoustic impedance of liquid He^3 reaches a value half-way between its two limits when the temperature is $0{\cdot}092^{\circ}K$. As the theoretical curves of Fig. 25 reach the same condition when $\omega\tau = 1$, we can use this to obtain a value of τ, which is

$$\tau = 1{\cdot}35 \times 10^{-12}\, T^{-2} \text{ sec.}$$

Now equation (3.36) is equivalent to

$$\tau = \left(\frac{5m^2}{\rho p_F^2}\right)\frac{(1 + F_1/3)}{(1 + F_2/5)}\,\eta \quad , \tag{5.1}$$

so we can estimate $(1 + F_2/5)$ from the known values of τ and the viscosity η. (It should be mentioned that (5.1) has been derived here by retaining only the first three terms in the series for $F(\chi)$, but it has been shown to be exact (Sykes (1964)).)

Abel, Anderson, and Wheatley (1961) measured the attenuation of sound in liquid He^3 at a frequency of 5·15 Mc/s. Below $0{\cdot}06^{\circ}K$, they found that the absorption was $5{\cdot}47 \times 10^{-3}\, T^{-2}\ cm^{-1}$,

which implies a viscosity $\eta = 2{\cdot}68 \times 10^{-6}\ T^{-2}$ poises. A direct measurement of the viscosity (Betts and Wilks (1964)) gives the value $\eta = 4{\cdot}25 \times 10^{-6}\ T^{-2}$ poises. Combining these figures with the above estimate of τ and the values of $(1 + F_1/5)$ given on page 55, we obtain

	F_1	$1 + F_2/5$	F_2
$\eta = 2{\cdot}68\ T^{-2}\ \mu p$	5·6	0·98	-0·1
	5·46	1·26	1·3
$\tau = 4{\cdot}25\ T^{-2}\ \mu p$	5·6	1·56	2·8
	5·46	1·99	5·0

The wide range of values for F_2 given here is a consequence of the rather indirect evaluation. From the table, it may be seen that a value of F_2 between 0 and 5 would not be at variance with the available data.

The estimates just made of F_2 include values sufficiently large that they might well affect the acoustic impedance. It therefore becomes necessary to recalculate the acoustic impedance with F_2 included, to see if theory and experiment can thereby be reconciled.

5.3 Calculation of the Acoustic Impedance: including F_2

The calculation of Z/ρ in the present case does not differ in principle from the calculation given in § 4.4, so we shall not repeat the explanations in detail, but just give the more important equations which are found.

The kinetic equation for the present case is

$$(i\omega\tau - 1 - \mu s)\psi + \mu\Psi = \frac{(F_0 - \alpha)}{(1+F_0)}\frac{\psi_0}{\alpha} + \frac{(F_1/3 - \alpha)}{(1+F_1/3)}\frac{\psi_1}{\alpha}\mu + \frac{4a}{5}\frac{\psi_2}{\alpha}P_2(\mu)$$

where $$\alpha = \frac{F_2/4}{1+F_2/5}.$$

Hence, dividing by $(i\omega\tau - 1 - \mu s)$ and integrating,

$$\psi_0\left[\frac{(F_0-\alpha)}{(1+F_0)}(\omega+1) - 1\right] + \psi_1\frac{(F_1/3-\alpha)}{(1+F_1/3)}\frac{\omega}{\alpha s} - \frac{2a}{5}\left[\omega\left(1 - \frac{3}{\alpha^2 s^2}\right) + 1\right]\psi_2 = \int_{-1}^{1}\frac{\mu\Psi(\mu)}{i\omega\tau - 1 - \mu s}\frac{d\mu}{2}.$$

This is a linear equation relating ψ_0, ψ_1, and ψ_2. Two other relations between these quantities are (4.8) and (4.10); solving between these gives

$$\psi_0\,\Delta(s) = Q(s) - E\,\frac{H(s)}{s^4}\,\omega(s) + \frac{\alpha^2}{3}E\,\frac{H(0)}{s^2} + \frac{\alpha^2}{3}E\,\frac{H'(0)}{s} \qquad (5.2)$$

where $$Q(s) = -\int_{-1}^{0}\mu\,\frac{[\Psi(\mu) + p_F u_z(\gamma+\mu)]}{i\omega\tau - 1 - \mu s}\frac{d\mu}{2} \qquad \text{(as before)},$$

$$\Delta(s) = \frac{3(1+\alpha)^2}{(1+F_0)(1+F_1/3)}\left\{(aZ+\omega)\left(\frac{1}{\alpha^2 s^2} - \frac{(1+F_0)(1+F_1/3)}{3(1+\alpha)^2}\right) + \frac{(1+F_1/3)}{3(1+\alpha)}Z\right\} \qquad (5.3)$$

$$E\,H(s) = -\frac{s^2}{\alpha}p_F u_z\left\{\frac{(1+\alpha)}{(1+F_1/3)}\left[a\left(1 - \frac{3}{\alpha^2 s^2}\right) + 1\right] + \gamma\alpha s\right\} + (\Psi_0 + \tfrac{2}{5}\Psi_2)s^3 a\left(1 - \frac{3}{\alpha^2 s^2}\right) \qquad (5.4)$$

$$E = \frac{\alpha - F_0}{1 + F_0} - a \tag{5.5}$$

$$H'(0) = \left[\frac{dH}{ds}\right]_{s=0} = -3a\frac{(\Psi_0 + \frac{2}{5}\Psi_2)}{\alpha^2 E}$$

and $$Z(s) = \left(1 - \frac{3}{\alpha^2 s^2}\right)\omega + 1.$$

Since in § 4.4 we simplified $\Delta(s)$ to the form (4.24) by defining s_1, we now write

$$\Delta(s) = E\left(1 - \frac{s_2^2}{s^2}\right)\left(1 - \frac{s_3^2}{s^2}\right)\omega + (1+E)\left(1 - \frac{s_4^2}{s^2}\right) \tag{5.6}$$

where

$$\frac{1}{\alpha^2 s_4^2} = \frac{(1+F_0)(1+F_1/3)}{3(1+\alpha)^2} - \frac{(1+F_1/3)}{3a(1+\alpha)} \tag{5.7}$$

and s_2^2 and s_3^2 are the roots of the quadratic equation

$$\frac{1}{\alpha^4 s^4} - \frac{1}{\alpha^2 s^2}\left(\frac{(1+F_0)(1+F_1/3)}{3(1+\alpha)^2} - \frac{(1+F_1/3)}{3a(1+\alpha)} + \frac{(1+a)}{3a}\right) + \left(\frac{(1+F_0)(1+F_1/3)(1+a)}{9a(1+\alpha)^2} - \frac{(1+F_1/3)}{9a(1+\alpha)}\right) = 0. \tag{5.8}$$

To complete the definitions of s_2, s_3, and s_4, we require all these quantities to have positive real parts.

To solve equation (5.2) by the Wiener-Hopf method, it is necessary to define functions

$$G(s) = \frac{s^2 - (i\omega\tau - 1)^2}{s^2 - s_0^2}\,\Delta(s),$$

$$\ln q_-(s) = \frac{1}{2\pi i}\int_{-\beta-i\infty}^{-\beta+i\infty} \frac{\ln G(u)}{u-s}\,du, \qquad \ln q_+(s) = \frac{1}{2\pi i}\int_{\beta-i\infty}^{\beta+i\infty} \frac{\ln G(u)}{u-s}\,du$$

in exactly the same way as before.

Performing the solution is straightforward, though the expressions are cumbersome. The result is

$$\psi_0(s) = \frac{-H(s)}{(s^2-s_2^2)(s^2-s_3^2)}$$

$$\frac{-\alpha s_0\sqrt{1+F_2/5}}{2g_-(0)(s_2^2-s_3^2)}\ \frac{(s-i\omega\tau+1)}{(s+s_0)}\ g_-(s)\left[\frac{-A\,H(s_2)}{s_2(s-s_2)}+\frac{B\,H(-s_2)}{s_2(s+s_2)}+\frac{C\,H(s_3)}{s_3(s-s_3)}-\frac{D\,H(-s_3)}{s_3(s+s_3)}\right]. \quad (5.9)$$

Here

$$\left.\begin{aligned} A &= \frac{(s_2+s_0)}{(s_2-i\omega\tau+1)}\ \frac{g_-(0)}{g_-(s_2)}\ \frac{1}{\alpha s_0\sqrt{1+F_2/5}} \\ B &= (1+E)\frac{(s_2^2-s_4^2)}{s_2^2}\ \frac{(s_2-i\omega\tau+1)}{(s_2+s_0)}\ \frac{g_-(0)}{g_+(-s_2)}\ \frac{1}{\alpha s_0\sqrt{1+F_2/5}} \\ C &= \frac{(s_3+s_0)}{(s_3-i\omega\tau+1)}\ \frac{g_-(0)}{g_-(s_3)}\ \frac{1}{\alpha s_0\sqrt{1+F_2/5}} \\ D &= (1+E)\frac{(s_3^2-s_4^2)}{s_3^2}\ \frac{(s_3-i\omega\tau+1)}{(s_3+s_0)}\ \frac{g_-(0)}{g_+(-s_3)}\ \frac{1}{\alpha s_0\sqrt{1+F_2/5}}\ . \end{aligned}\right\} \quad (5.10)$$

Substituting into the boundary conditions (4.9), (4.11) gives

$$\left.\begin{aligned} \frac{A\,H(s_2)+B\,H(-s_2)}{s_2^2}-\frac{C\,H(s_3)+D\,H(-s_3)}{s_3^2} &= 0 \\ \frac{A\,H(s_2)-B\,H(-s_2)}{s_2^3}-\frac{C\,H(s_3)-D\,H(-s_3)}{s_3^3} &= 0\ . \end{aligned}\right\} \quad (5.11)$$

The expressions resulting from (5.11) can be very complicated, so we simplify the notation by defining

$$y_2 = \frac{1}{\alpha s_2}\ ,\quad y_3 = \frac{1}{\alpha s_3}\ ,\quad y_4 = \frac{1}{\alpha s_4}\ ,\quad y_0 = -\frac{1}{\alpha s_0}\ ,$$

$$U = a(1-3y_2^2)+1 \quad , \qquad V = a(1-3y_3^2)+1 \ .$$

Using the definition of H(s), one can expand (5.11) into a pair of equations linear in the unknown quantities γ and $(\Psi_0 + \frac{2}{5}\Psi_2)/p_F u_z$. Eliminating γ gives an expression for $\frac{(\Psi_0+\frac{2}{5}\Psi_2)}{p_F u_z}$ and hence Z/ρ:

$$\frac{Z}{\rho} = -(1+F_1/3)\,v_F\,\frac{(\Psi_0+\frac{2}{5}\Psi_2)}{p_F u_z}$$

$$= v_F\left[\frac{8(1+F_1/3)y_2y_3 + (1+a)\left[(A-B)(C-D)(Uy_2^2+Vy_3^2) - (A+B)(C+D)(U+V)y_2y_3\right]}{-3a(y_2^2-y_3^2)\left[(A-B)(C+D)y_3 - (A+B)(C-D)y_2\right]}\right]. \qquad (5.12)$$

To evaluate A, B, C, and D one has to find an analytic form for $g_-(s)$. This is obtained by a contour integration in the same way as before, with the result

$$g_-(s) = \frac{e^{-\phi(y)}}{\sqrt{G(s)}}$$

where $y = \frac{1}{\alpha s}$ and

$$\phi(y) = \frac{y}{2\pi i}\int_0^1 \ln\left[\frac{\left[x^4 - x^2(y_2^2+y_3^2)+y_2^2y_3^2\right]\left[\frac{x}{2}\ln\left(\frac{1+x}{1-x}\right) - 1 + \frac{i\pi x}{2}\right] - \frac{x^2}{3} + \frac{y_4^2}{3}}{\left[x^4 - x^2(y_2^2+y_3^2)+y_2^2y_3^2\right]\left[\frac{x}{2}\ln\left(\frac{1+x}{1-x}\right) - 1 - \frac{i\pi x}{2}\right] - \frac{x^2}{3} + \frac{y_4^2}{3}}\right]\frac{dx}{y^2-x^2}. \qquad (5.13)$$

Then we find

$$\left.\begin{aligned}
A &= \pm\sqrt{V\frac{(y_2-y_0)}{(y_2+y_0)}\frac{(y_2+1)}{(y_2-1)}}\,e^{\phi(y_2)} = -\frac{(y_2-y_0)}{(y_2-1)}\frac{\sqrt{G(s_2)}}{\sqrt{G(0)}}\frac{e^{\phi(y_2)}}{\sqrt{1+F_2/5}} \\
B &= \pm\sqrt{V\frac{(y_2+y_0)}{(y_2-y_0)}\frac{(y_2-1)}{(y_2+1)}}\,e^{-\phi(y_2)} = \frac{V}{A} \\
C &= \pm\sqrt{U\frac{(y_3-y_0)}{(y_3+y_0)}\frac{(y_3+1)}{(y_3-1)}}\,e^{\phi(y_3)} = -\frac{(y_3-y_0)}{(y_3-1)}\frac{\sqrt{G(s_3)}}{\sqrt{G(0)}}\frac{e^{\phi(y_3)}}{\sqrt{1+F_2/5}}
\end{aligned}\right\} \qquad (5.14)$$

$$D = \pm\sqrt{U\,\frac{(y_3+y_o)}{(y_3-y_o)}\,\frac{(y_3-1)}{(y_3+1)}}\;e^{-\phi(y_3)} = \frac{U}{C}. \qquad (5.14)$$

The second expression in each of these equations is used for checking the sign of the first, as explained on page 87.

This completes the analysis for the case where $\Delta(s)$ has one pair of solutions $\pm s_o$. But we have learned in chapter 5 that there may be 0, 1, or 2 pairs of solutions. It is therefore necessary to repeat the analysis by writing

$$G(s) = \Delta(s)\prod_i \frac{s^2-(i\omega\tau-1)^2}{s^2-s_{oi}^2},$$

where the product contains terms for every solution of $\Delta(s)$. Here s_{oi} is the value of s_o for the ith solution. The product of factors is conventionally regarded as being equal to 1 in the case where there are no solutions.

The results of this analysis are as follows:

$$\left.\begin{aligned}
A &= \pm\sqrt{V\prod_i\left(\frac{(y_2-y_{oi})}{(y_2+y_{oi})}\,\frac{(y_2+1)}{(y_2-1)}\right)}\;e^{\phi(y_2)} = -\frac{e^{\phi(y_2)}}{\sqrt{1+F_2/5}}\,\frac{\sqrt{G(s_2)}}{\sqrt{G(0)}}\prod_i\frac{(y_2-y_{oi})}{(y_2-1)}\\
B &= \pm\sqrt{V\prod_i\left(\frac{(y_2+y_{oi})}{(y_2-y_{oi})}\,\frac{(y_2-1)}{(y_2+1)}\right)}\;e^{-\phi(y_2)} = \frac{V}{A}\\
C &= \pm\sqrt{U\prod_i\left(\frac{(y_3-y_{oi})}{(y_3+y_{oi})}\,\frac{(y_3+1)}{(y_3-1)}\right)}\;e^{\phi(y_3)} = -\frac{e^{\phi(y_3)}}{\sqrt{1+F_2/5}}\,\frac{\sqrt{G(s_2)}}{\sqrt{G(0)}}\prod_i\frac{(y_2-y_{oi})}{(y_2-1)}\\
D &= \pm\sqrt{U\prod_i\left(\frac{(y_3+y_{oi})}{(y_3-y_{oi})}\,\frac{(y_3-1)}{(y_3+1)}\right)}\;e^{-\phi(y_3)} = \frac{U}{C}.
\end{aligned}\right\} \qquad (5.15)$$

Equation (5.13), which defines $\phi(y)$, and equation (5.12), which gives the acoustic impedance, are true for any number of solutions.

As in § 4.5, it is possible to evaluate the physical disturbance to the distribution of the quasi-particles, $\nu_0(\xi)$, by performing the converse Laplace transformation. The physical interpretation of the expression obtained is exactly the same as we found before. The most useful result which we can derive from this analysis is the ratio

$$f = \frac{\text{contribution to the fluid velocity from wave (at the boundary)}}{\text{total fluid velocity } (u_z) \text{ at the boundary}}.$$

We can show that

$$f_j = \frac{\Lambda_j \; e^{-\phi(y_{oj})}}{6a(y_2^2 - y_3^2)} \left\{ U\left[(A'+B')\lambda_2 + (A'-B')\right] + V\left[(C'+D')\lambda_3 + (C'-D')\right] \right\} \qquad (5.16)$$

where
$$\lambda_2 = \frac{4y_3V - (A+B)(C+D)y_3 + (A-B)(C-D)y_2}{(A-B)(C+D)y_3 - (A+B)(C-D)y_2}$$

$$\lambda_3 = \frac{-4y_2U + (A+B)(C+D)y_2 - (A-B)(C-D)y_3}{(A-B)(C+D)y_3 - (A+B)(C-D)y_2}$$

$$A' = \frac{A}{y_2 - y_{oj}}, \quad B' = \frac{B}{y_2 + y_{oj}}, \quad C' = \frac{C}{y_3 - y_{oj}}, \quad D' = \frac{D}{y_3 + y_{oj}}$$

$$\left.\begin{aligned} \Lambda_j &= \pm \sqrt{\frac{2y_{oj}}{-9a\,f'(y_{oj})} \prod_i \frac{(y_{oj}-1)}{(y_{oj}+1)} \cdot \prod_{i\neq j} \frac{(y_{oj}+y_{oi})}{(y_{oj}-y_{oi})}} \\ &= \sqrt{1+F_2/5}\; \frac{\sqrt{G(0)}\,\sqrt{G(s_0)}}{G(s_0)} \; \frac{\prod_i (y_{oj}-1)}{\prod_{i\neq j}(y_{oj}-y_{oi})} \end{aligned}\right\} \qquad (5.17)$$

$$\frac{f'(y)}{2y} = (y^2 - y_2^2)(y^2 - y_3^2)\frac{w'}{2y} - w\left[2y^2 - (y_2^2 + y_3^2)\right] - \frac{1}{3}$$

$$\frac{w'}{2y} = \frac{1}{4y}\ln\left(\frac{y+1}{y-1}\right) - \frac{1/2}{y^2-1}$$

$$G(s_{oj}) = \frac{(1+\alpha)^2 \prod_i y_{oi}^2}{(1+F_0)(1+F_1/3)(1+F_2/5)} \cdot \frac{-9F_2}{4} \frac{f'(y_{oj})}{2y_{oj}} \frac{\prod_i (y_{oj}^2 - 1)}{\prod_{i\neq j} (y_{oj}^2 - y_{oi}^2)} .$$

In the above equations, f_j is the ratio f in the case where the jth wave motion is considered. Two expressions are given for Λ_j, so that the first determines its magnitude, and the second its sign.

5.4 Numerical Analysis

In order to evaluate the expressions given here, it was necessary to make use of an electronic computer. The machine used was a Ferranti Mercury, in the Oxford University Computing Laboratory. The Ferranti Mercury is neither very large nor very fast by the standard of the latest machines, and precautions had to be taken to ensure that excessive time was not spent by the machine. Only 852 machine instructions can be put into the fast store of the computer at any one time (the rest being kept on a magnetic drum), so a programme written for Mercury has to be divided up into blocks, called chapters, each of which contains less than 852 instructions. The maximum number of chapters which Mercury can hold is 22, but 17 is regarded as being a practical maximum. Our programme contained 13 chapters.

It was necessary at several stages of the calculation to take precautions to ensure that the accuracy was adequate, as the reliability of the answers depended critically on the maintenance of accuracy at each step. We shall now give a brief description of the steps in the calculation, together with the numerical methods used and the precautions observed.

(a) Preliminary Setting up

The first step in the calculation was to read into the computer certain numerical properties of He^3 which were taken as input data. These were the density ρ, the velocity of sound c, the parameters F_1, F_2, and the product τT^2, together with the frequency of measurement $\omega/2\pi$. From these, the Fermi momentum was calculated viz

$$\frac{p_F}{m} = \frac{\hbar}{m}\left(3\pi^2 \frac{\rho}{m}\right)^{1/3} . \qquad (3.6)$$

The Fermi velocity v_F was next found from

$$v_F = \frac{p_F}{m} \frac{1}{1 + F_1/3}$$

and the parameter F_0 from

$$(1 + F_0) = \frac{3c^2}{(p_F/m)^2} (1 + F_1/3) . \qquad \text{cf (3.14)}$$

Next the computer was instructed to find the critical values of $\omega\tau$ at which solutions to the wave equation appear or disappear.

This necessitated finding all the solutions in the range $0 \leq x \leq 1$ of

$$f(x) = X(x)\,Y(x) - \frac{(1+F_0)(1+F_1/3)}{3}\,\frac{\pi^2 x^2}{4} = 0. \qquad (5.41)$$

In order to find the zeros of $f(x)$, the computer tabulated the function $f(x)$ at a sequence of values of x. $f(x)$ is a smooth function of $(1 - x)$ for $(1 - x) \gtrsim 0{\cdot}01$, and a smooth function of $\ln\left(\frac{1+x}{1-x}\right)$ for $(1 - x) \lesssim 0{\cdot}01$; so in order to cover the whole range uniformly, the tabulation points were chosen to have a logarithmic distribution near $x = 1$. As each value of $f(x)$ was calculated, a check was made to see if $f(x)$ had changed sign in the last step; if it had, there was a root of $f(x)$ within that step. By this means a list of the zeros of $f(x)$ was constructed. Special arrangements were made to identify any root very close to $x = 1$, and also to ensure that a pair of roots close together was not missed if both lay within one step of the tabulation. Once the approximate positions of all the zeros of $f(x)$ were known, the roots were found accurately by an interpolation method, the independent variable being $(1 - x)$ or $\ln\left(\frac{2}{1-x}\right)$ according to the value of $(1 - x)$.

The values of $(1 - x)$ just obtained represented the positions at which solutions to (5.34) disappeared into the real ξ-axis, or appeared from it. The critical $\omega\tau$ at which this occurred was next calculated for each x from the expressions

$$(\omega\tau)_{crit} = \frac{\frac{1}{3}(1+F_0)(1+F_1/3)\,\frac{\pi x}{2}}{Y} = \frac{X}{\pi x/2}\,. \qquad (5.43)$$

Substitution into (3.44) to obtain $\partial\xi/\partial(\omega\tau)$ was then straightforward. Once these results were found for all the roots of (3.41), they were arranged as a table with the $(\omega\tau)_{crit}$'s in ascending order. The table for the case $F_0 = 0{\cdot}14$, $F_1 = 0{\cdot}15$, $F_2 = 0$ is given below for illustration (see Fig. 19 for the dispersion curve).

$(\omega\tau)_{crit}$	$(1 - x)$	$\partial\xi/\partial(\omega\tau)$ real part	$\partial\xi/\partial(\omega\tau)$ imaginary	δn
8·8031	$2{\cdot}6765 \times 10^{-2}$	$7{\cdot}24 \times 10^{-3}$	$-2{\cdot}52 \times 10^{-3}$	-1
21·899	$1{\cdot}8587 \times 10^{-3}$	$2{\cdot}40 \times 10^{-4}$	$9{\cdot}88 \times 10^{-5}$	+1

Here δn is the number of solutions gained by equation (3.34) when $\omega\tau$ is increased through $(\omega\tau)_{crit}$. This table contains all the information needed for the computer to find how many solutions are possessed by (3.34) for any given value of $\omega\tau$.

(b) Calculation of y_2, y_3, etc.

A value of the temperature T was now read into the computer, and from it the appropriate value of $\omega\tau$ was found. Knowing $\omega\tau$ made it possible to find the quantities y_2^2 and y_3^2 which are defined to be the solutions of the quadratic equation (cf equation (5.8))

$$y^4 - y^2\left(\frac{(1+F_0)(1+F_1/3)}{3(1+\alpha)^2} - \frac{(1+F_1/3)}{3a(1+\alpha)} + \frac{(1+a)}{3a}\right) + \left(\frac{(1+F_0)(1+F_1/3)(1+a)}{9a(1+\alpha)^2} - \frac{(1+F_1/3)}{9a(1+\alpha)}\right) = 0. \qquad (5.18)$$

y_3^2 was arbitrarily chosen to be the larger solution. In principle, the signs of y_2 and y_3 should be determined by making Re s_2 and

Re s_3 positive; however the expressions for Z/ρ and f_j are not affected if different signs are taken, so we chose for convenience to make Re $y_2 > 0$ and Re $(y_3/y_0) > 0$ (where y_0 is the largest solution of (5.34)).

Apart from y_2 and y_3 themselves, it was necessary to find $(y_2 \pm 1)$ and $(y_3 \pm 1)$ (see equation (5.15)). Usually $(y_2 - 1)$ could not be found to sufficient accuracy by applying the standard formula to (5.18), so a series method of solution was used. By a careful grouping of terms, an accurate value of $(y_2^2 - 1)$ was obtained, so that $(y_2 - 1)$ could be found as

$$y_2 - 1 = \frac{y_2^2 - 1}{y_2 + 1} .$$

At the same time, an accurate value was found for $y_2^2 - \frac{1+a}{3a}$ so that $U = -3a\left(y_2^2 - \frac{1+a}{3a}\right)$ could be found.

$y_3^2 - \frac{(1+F_0)(1+F_1/3)}{3(1+\kappa)^2}$ was also evaluated carefully for use later.

(c) Solution of Equation (5.34)

Before solving equation (5.34), it was first necessary to find how many solutions there were to be found. The number of solutions in the limit $\omega\tau \to 0$ was known to be 1 (for $F_2 < 10/3$) or 2 (for $F_2 > 10/3$). The number at the value of $\omega\tau$ under investigation was then found by reference to the table set up under section (a).

To find the solutions y_o of equation (3.34) three methods of solution were available. For $|y_o| > 2$, a rough value of ξ^2 was used to evaluate the right-hand side of

$$\xi^2 = \frac{(1+F_o)(1+F_1/3)}{3(1+\alpha)^2} - \frac{(1+F_1/3)}{3a(1+\alpha)} \frac{Z}{aZ+w} . \qquad (3.34)$$

This determined an improved value of ξ^2, and the process was repeated until a consistent result was obtained (y_o^2 being the consistent value of ξ^2). Since w and Z both tend to zero when ξ is large, they were evaluated by a power series in $1/\xi^2$. In the special case $|y_o - 1| < 10^{-10}$, the approximate relation

$$\ln\left(\frac{2}{y_o-1}\right) = 3 - \left(\frac{(1+F_o)(1+F_1/3)}{3(1+\alpha)^2} - 1\right)\left[\left(\frac{(1+F_o)(1+F_1/3)}{3(1+\alpha)^2} - 1\right)(1-2a) + \frac{2}{3}\frac{(1+F_1/3)}{(1+\alpha)}\right]^{-1}$$

was used. For all other values of y_o, Newton's approximation was applied to the function

$$f(\xi) = w\left\{\left[\xi^2 - \left(\frac{(1+F_o)(1+F_1/3)}{3(1+\alpha)^2} - \frac{(1+F_1/3)}{3a(1+\alpha)} + \frac{(1-2a)}{3a}\right)\right](\xi^2-1) + \frac{1}{3a}\left[\left(\frac{(1+F_o)(1+F_1/3)}{3(1+\alpha)^2} - 1\right)(1-2a) + \frac{2}{3}\frac{(1+F_1/3)}{(1+\alpha)}\right]\right\}$$

$$- \frac{\xi^2}{3} + \left(\frac{(1+F_o)(1+F_1/3)}{9(1+\alpha)^2} - \frac{(1+F_1/3)}{9a(1+\alpha)}\right) . \qquad (5.19)$$

Unfortunately, the mechanical application of Newton's approximation for finding solutions near $\xi = 1$ did not always converge reliably to the solution, as there was a tendency for a succession of wild overcorrections to be applied. A variety of checks was built into the programme to detect this behaviour, and a new initial guess at the solution was tried if the original guess

proved unsuitable. With these procedures the programme was made reliable.

In the limit $\omega\tau \to 0$, y_3^2 and y_0^2 both tend to $\frac{(1+F_0)(1+F_{1/3})}{3(1+\alpha)^2}$.

In order to obtain an accurate value for $(y_3 - y_0)$ (which was needed for evaluating C and D - see equation (5.14)), the computer was instructed to find

$$y_0^2 - \frac{(1+F_0)(1+F_{1/3})}{3(1+\alpha)^2} = -\frac{(1+F_{1/3})}{3(1+\alpha)} \frac{Z}{aZ+\omega}$$

which is accurate, and hence to find

$$y_3^2 - y_0^2 = \left(y_3^2 - \frac{(1+F_0)(1+F_{1/3})}{3(1+\alpha)^2} \right) - \left(y_0^2 - \frac{(1+F_0)(1+F_{1/3})}{3(1+\alpha)^2} \right).$$

Then $(y_3 - y_0)$ was evaluated in the form $\frac{y_3^2 - y_0^2}{y_3 - y_0}$.

When all the quantities described above were evaluated, the velocity and attenuation of the wave motion were calculated, and these quantities were printed out.

(d) Integrations

The integral defined by (5.13) had to be evaluated so as to give $\phi(y_2)$, $\phi(y_3)$, and $\phi(y_0)$; this presented several complications. Let us write

$$\phi(y) = \frac{y}{2\pi i} \int_0^1 \ln[\,] \frac{dx}{y^2 - x^2} \qquad \text{cf (5.13)}$$

as a convenient abbreviation. $\ln[\,]$ has an infinite gradient at $x = 1$, since it varies there like $\lambda + \frac{\mu}{\ln(1-x)}$.

This means that large errors would be incurred if a quadrature method were applied to the whole range of x at once. The range was therefore divided into two, and the part from $x = 0$ to $x = \frac{1}{2}$ was integrated. The first half of the remaining range ($x = \frac{1}{2}$ to $x = 3/4$) was next integrated, and so on until only 1/524288 of the range remained. A calculated end correction was applied to this portion, and the subdivision was continued until successive estimates of the integral were consistent.

Within each sub-range (e.g. $x = 0$ to $x = \frac{1}{2}$), $\ln[\,]$ was tabulated at 16 points. The imaginary part of the logarithm was checked for continuity at each step, and arrangements were made for subdividing the step in cases of doubt. If necessary a multiple of $2\pi i$ was added to the logarithm to achieve continuity; in this way the correct imaginary part was found. The integral over this sub-range was found by Simpson's rule, with a division of the sub-range into as many steps as were necessary to give a consistent result. As each ordinate was calculated, its logarithmic term was compared with the nearest tabulated value to make sure that the correct multiple of $2\pi i$ was added in. Since $\ln[\,]$ was common to $\phi(y_2)$, $\phi(y_3)$, etc., the integrals were evaluated simultaneously.

The convergence tests applied to the integration were fairly sophisticated, as the integration took longer than all other numerical operations together. Theoretically, halving the step-length in a quadrature by Simpson's rule should reduce the error in

the integral by a factor of about 8. This ideal situation may fail to be satisfied if the step-length is very large compared with some feature of the integrand, or if a limit is set by the accuracy with which the integrand can be calculated. A check was therefore made to see whether successive estimates X_1, X_2, X_3 of the integral were improving in accuracy by a factor of about 8, that is

$$\frac{\delta_3}{\delta_2} = \frac{|X_3 - X_2|}{|X_2 - X_1|} \sim \frac{1}{8}.$$

If the improvement was satisfactory, it was assumed that if a further reduction in step-length were performed, the integral X_4 obtained would satisfy

$$\delta_4 = |X_4 - X_3| \sim \delta_3/8,$$

so the probable error in the integral X_3 should not greatly exceed $\delta_3/7$. If δ_3/δ_2 was appreciably larger than 1/8, a larger error was estimated for X_3. Each integral was required in the first instance to have a fractional error less than 10^{-7}. Should this not be achieved in one or more of the integrals, a figure of merit was constructed according to the value of δ_3/δ_2. From this figure of merit, the computer "decided" whether to make a further reduction of the step-length, or whether to accept the accuracy attained.

It occasionally happened that the integrand of

$$\phi(y) = \frac{y}{2\pi i}\int_0^1 \ln[\,]\,\frac{dx}{y^2 - x^2}$$

could vary very rapidly over a small range of x. This occurred if the denominator $(y^2 - x^2)$ in the integrand approached zero very closely, which could happen if the number y had a very small imaginary part, and had a real part less than 1. y_2 and y_o could both satisfy this condition at various times. To overcome this difficulty a special routine was devised for integrating a range of x containing Re y, so that a very small step-length could be used over the region of greatest difficulty.

It can readily be shown from the argument principle that when $x \to 1$, $\ln [\,] \to -2n\pi i$, where n is the number of pairs of solutions possessed by $\Delta(s)$. By making the computer print out a table of $\ln [\,]$, we verified in special cases that the equations (3.41) et seq. gave the correct number of solutions, though no check on this was built into the programme.

To confirm that the integration routine was giving the accuracy claimed, we made the routine evaluate the integral

$$\frac{2y^2}{2\pi i}\int_0^1 \frac{\ln [\,]}{x}\,\frac{dx}{y^2-x^2}$$

which has all the important properties of the actual integral required. This check integral is known to be equal to $\ln G(s)$, so by evaluating the integral by quadrature and via $\ln G(s)$, we were able to check the accuracy of the quadrature. Sample results of this test are given in the table below.

	real part	imaginary	fractional error
by quadrature:	$-7{\cdot}1723834 \times 10^{-4}$	$-1{\cdot}2565745$	$1{\cdot}6 \times 10^{-7}$
by formula:	$-7{\cdot}1726192 \times 10^{-4}$	$-1{\cdot}2565745$	
by quadrature:	$11{\cdot}384765$	$-9{\cdot}2511863$	$7{\cdot}1 \times 10^{-9}$
by formula:	$11{\cdot}384764$	$-9{\cdot}2511860$	

In the second case, the special routine for dealing with a near-zero in $(y_2^2 - x^2)$ was used. The claimed error in the above examples was $4{\cdot}5 \times 10^{-8}$; it may be seen that the accuracy obtained was satisfactory.

(e) Calculation of A, B, C, and D

The next step in the calculation was to evaluate the quantities A, B, C, and D which are defined by (5.15). This involved first setting up various quantities of the form

$$\pm \sqrt{V \prod_i \frac{(y_2 - y_{oi})}{(y_2 + y_{oi})} \frac{(y_2 + 1)}{(y_2 - 1)}} \quad ;$$

the procedure for this was straightforward. (For definiteness, we give here the formulae for finding A only; to find C, similar expressions were used with y_3 in place of y_2.) It was necessary next to find the appropriate sign to be given to the square root, by finding the sign of $\sqrt{G(s_2)} / \sqrt{G(0)}$. This was done by defining $\Gamma(\xi)$ by

$$G(s) = \frac{(1+\alpha)^2 \prod_i y_{oi}^2}{(1+F_0)(1+F_1/3)(1+F_2/5)} \Gamma(\xi)$$

where $\xi = 1/\alpha s$

so that $$\Gamma(\xi) = -\frac{9F_2}{4} f(\xi) \prod_i \frac{(\xi^2 - 1)}{(\xi^2 - y_{oi}^2)} \qquad (5.20)$$

with $f(\xi)$ given by the function of (5.19). We thus had to find the sign of $\sqrt{\Gamma(y_2)}/\sqrt{\Gamma(\infty)}$ by requiring $\sqrt{\Gamma(\xi)}$ to be continuous between $\xi = y_2$ and $\xi = \infty$. For this test, ξ was given values of the form

$$\mathrm{Re}\ y_2 + i\, y\, \mathrm{Im}\ y_2$$

with y increasing from 1 to a large number; for each ξ, $\Gamma(\xi)$ was calculated, and a check was made to see whether $\sqrt{\Gamma(\xi)}$ was continuous in the latest step; the steps could be subdivided in cases of doubt. When $\Gamma(\xi)$ became close to $\Gamma(\infty)$, the check on the continuity of $\sqrt{\Gamma(\xi)}$ was stopped, as it was no longer necessary. An arbitrary sign was initially given to $\sqrt{\Gamma(y_2)}$, and from this the consistent sign of $\sqrt{\Gamma(\infty)}$ was found, so that the sign of $\sqrt{\Gamma(y_2)}/\sqrt{\Gamma(\infty)}$ was determined. By using (5.15), the appropriate sign for

$$\pm\sqrt{V \prod_i \frac{(y_2 - y_{oi})}{(y_2 + y_{oi})} \frac{(y_2 + 1)}{(y_2 - 1)}}$$

was found and A was completely evaluated. An exactly similar procedure was used for finding C. The signs of B and D presented no difficulty, for they could be found from A and C as indicated in equation (5.15).

(f) Calculation of (C - D)

Although A, B, C, and D were now found, the quantities required for evaluating the acoustic impedance were (A ± B) and (C ± D) (see equation (5.12)). Of these, (C - D) in particular could not always be found by a simple subtraction, as in the limit where F_2 was very small, C and D both tended to the same limiting value of -1. The programme was therefore provided with facilities for evaluating $(C^2 - D^2)$ in the form

$$\frac{C^2 - D^2}{U} = X(\sinh x \cos y + i \cosh x \sin y) + YZ(\cosh x \cos y + i \sinh x \sin y)$$

where $x + iy = 2\phi(y_3)$

$$X = \prod_i \frac{(y_3 - y_{oi})}{(y_3 + y_{oi})} \frac{(y_3 + 1)}{(y_3 - 1)} + \prod_i \frac{(y_3 + y_{oi})}{(y_3 - y_{oi})} \frac{(y_3 - 1)}{(y_3 + 1)}$$

$$Y = \frac{\prod_i (y_3 - y_{oi})(y_3 + 1) + \prod_i (y_3 + y_{oi})(y_3 - 1)}{\prod_i (y_3 - y_{oi})(y_3 + 1) \times \prod_i (y_3 + y_{oi})(y_3 - 1)}$$

$$Z = -2 y_3 \sum_i (y_{oi} - 1) \prod_{j \neq i} (y_3^2 - y_{oj}) .$$

(C - D) could now be found from $\frac{C^2 - D^2}{C + D}$. Similar expressions could be used if necessary to find (A ± B) and (C + D).

(g) Calculation of Z/ρ

The evaluation of the expressions for Z/ρ given by (5.12) was now straightforward, and presented no points of special difficulty.

(h) Calculation of f_j

Another piece of information which could be obtained from the analysis was the quantity f_j, which is the fraction of the liquid's velocity accounted for by the jth wave motion. In order to save machine time, f_j was not calculated for all cases, but the additional calculation was called in as required by setting a switch on the computer. When the routine was called in in this way, the integration routine was used for finding $\phi(y_{oj})$ as well as $\phi(y_2)$ and $\phi(y_3)$.

Next the computer calculated Λ_j defined by (5.17). This involved a straightforward assembly of products except for the quantity

$$\frac{f'(y_{oj})}{2y_{oj}} = \frac{\omega'}{2y_{oj}}\left\{\left[y_{oj}^2 - \left(\frac{(1+F_o)(1+F_1/3)}{3(1+\alpha)^2} - \frac{(1+F_1/3)}{3a(1+\alpha)} + \frac{(1-2a)}{3a}\right)\right](y_{oj}^2-1) + \frac{1}{3a}\left[\left(\frac{(1+F_o)(1+F_1/3)}{3(1+\alpha)^2}-1\right)(1-2a) + \frac{2}{3}\frac{(1+F_1/3)}{(1+\alpha)}\right]\right\}$$

$$-\omega\left[2y_{oj}^2 - \left(\frac{(1+F_o)(1+F_1/3)}{3(1+\alpha)^2} - \frac{(1+F_1/3)}{3a(1+\alpha)} + \frac{(1+\alpha)}{3a}\right)\right] - \frac{1}{3}\ .$$

$\frac{f'(y_{oj})}{2y_{oj}}$ was evaluated by means of the expression given here when $|y_{oj}|$ was less than 2, but in other cases, a power series in y_{oj}^{-2} was used to avoid loss of accuracy. The correct sign for Λ_j was found by the routine described above in (e), and the remainder of the calculation involved no special difficulty.

Usually it was convenient to calculate several values of Z/ρ over a range of temperatures, for the same values of the parameters F_o, F_1, F_2, τT^2, and the frequency $\omega/2\pi$. Then as each value of Z/ρ was calculated, the next temperature in the set was read in, and the

calculation was restarted at stage (b) (page 107). When all the temperatures in the set were dealt with, the programme was restarted from the beginning.

As a check against careless errors in programming, a large part of the calculation for one point was performed by hand with frequent comparisons against the computer's answers.

The calculation of one value of the acoustic impedance usually took about 2 minutes on the computer, but occasional points for which the integration presented some point of difficulty took up to 5 minutes. Obtaining the figures for one graph (e.g. Fig. 23, 24, or 25) took 20 - 30 minutes. All the theoretical curves given in this thesis were calculated with the same programme.

5.5 Results

Fig. 26 shows values of the absorption of sound and zero sound as a function of temperature for $F_1 = 3{\cdot}6$ and $F_2 = 0$, 4, and 10. The value of τT^2 has been made equal to $1{\cdot}55 \times 10^{-12}$ sec $^{\circ}K^2$ for the $F_2 = 0$ curve. In view of

$$\tau = \frac{5}{\rho v_F^2 (1 + F_1/3)} \frac{\eta}{(1 + F_2/5)} , \qquad (3.36)$$

we have reduced τT^2 to $\frac{1{\cdot}55 \times 10^{-12}}{1 + F_2/5}$ s $^{\circ}K^2$ for the other curves, in order to keep the assumed value of the viscosity the same. The peak in the absorption always occurs very close to $\omega\tau = 1$, so the

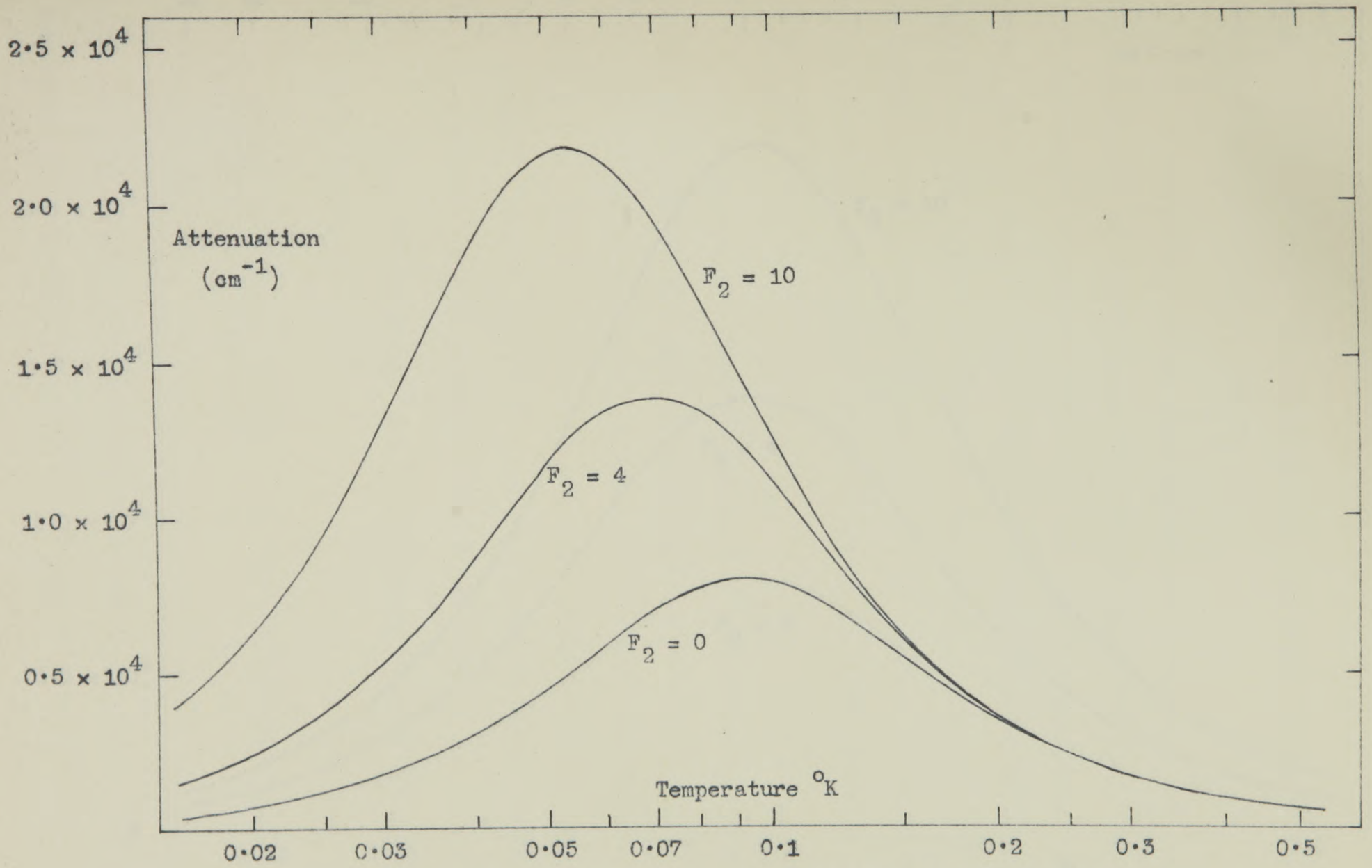

Fig. 26. Attenuation of the wave motion for various F_2

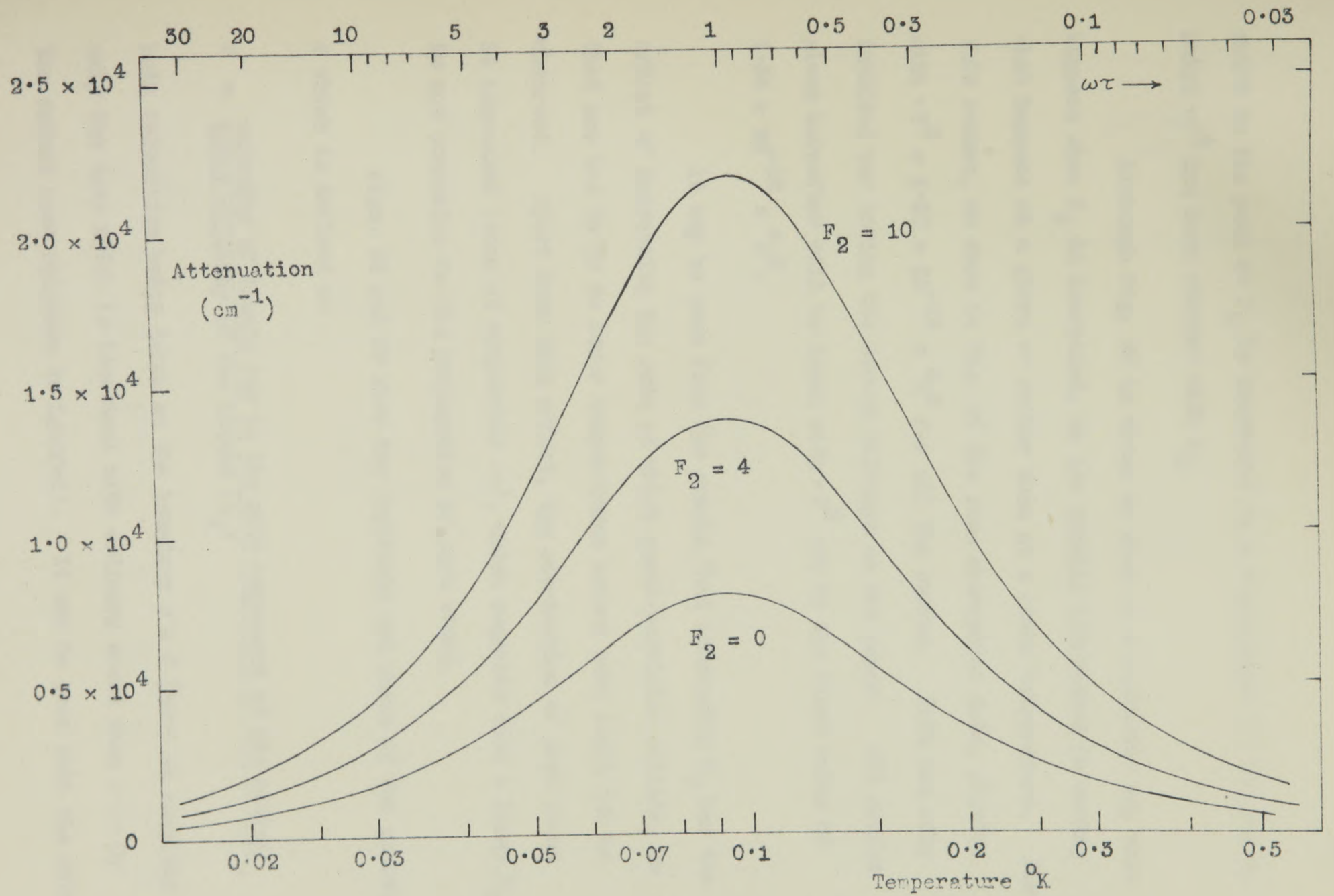

Fig. 27. Attenuation of the wave motion for various F_2.

shift in the peak as F_2 is increased is a consequence of the way in which τT^2 has been changed with F_2.

Although Fig. 26 is drawn to show in a realistic way what happens when F_2 is increased, we are usually interested in seeing what happens at a given $\omega\tau$ rather than at a given temperature. For this reason, we show in Fig. 27 the same absorption data, plotted with $\tau T^2 = 1{\cdot}35 \times 10^{-12}$ s $^{\circ}K^2$ for all the curves. This has only involved our moving the curves sideways on the paper. All graphs given hereafter will be drawn with τT^2 set to the fixed value of $1{\cdot}35 \times 10^{-12}$ s $^{\circ}K^2$.

It may be seen from the graphs that increasing F_2 has the effect of increasing the rate at which quasi-particles collide, so that one has to go to lower temperatures before zero sound can be observed. Apart from this effect, the attenuation of zero sound is increased (even at comparable $\omega\tau$), which suggests that a large F_2 is not conducive to the propagation of zero sound.

Figs. 28 and 29 show the amplitude and phase of the quantity f which is defined as

$$f = \frac{\text{velocity of liquid due to the wave component of its motion}}{\text{total velocity of the liquid } (u_z)},$$

both velocities being taken at the boundary $z = 0$ (here we consider only the wave which is identical with ordinary sound when $\omega\tau \to 0$; the second wave solution is ignored). It may be seen that the effect

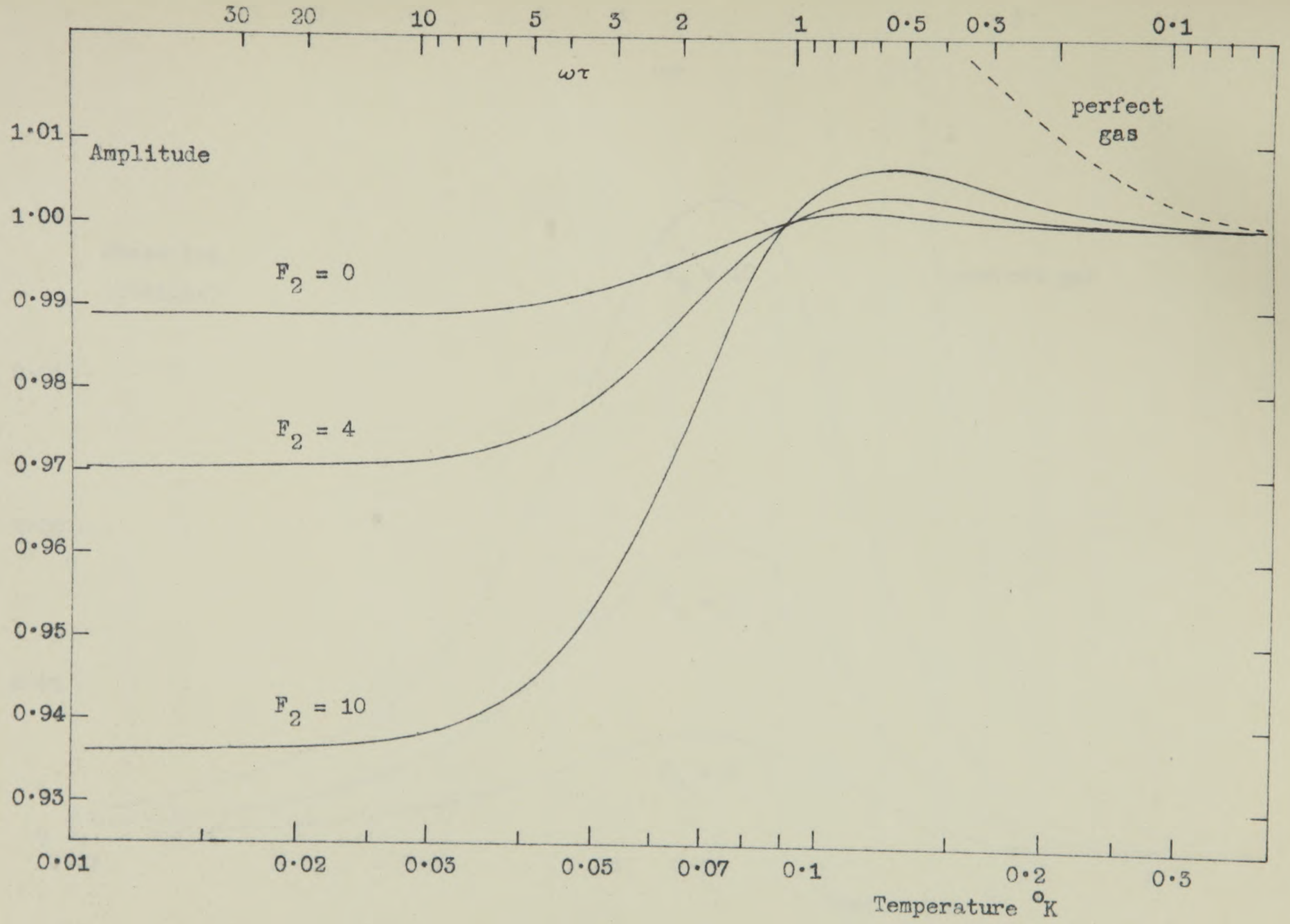

Fig. 28. Amplitude of the dominant wave motion ($F_o = 7{\cdot}1320$, $F_1 = 3{\cdot}6$)

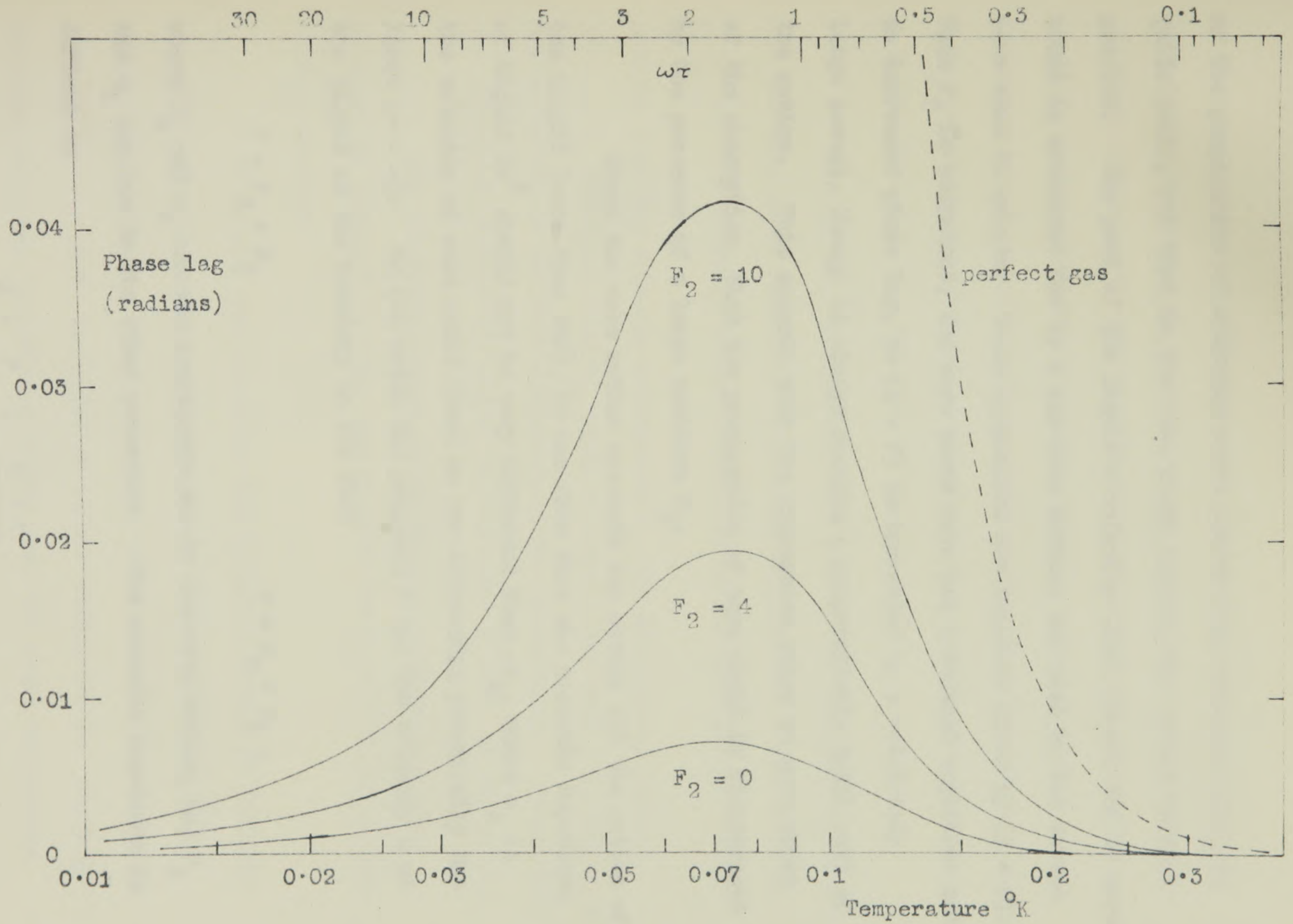

Fig. 29. Phase of the dominant wave motion ($F_o = 7{\cdot}1320$, $F_1 = 3{\cdot}6$)

on the propagation of ordinary sound produced by increase of F_2 is quite small, but that in the zero sound region, the effect is much greater. The part of the liquid's velocity which is not due to zero sound is accounted for by a gas-like motion, and also by the second wave when it exists; these components are together given by $(1 - f)$. When F_2 is increased, the zero sound wave has a reduced amplitude and an increased phase lag, so $(1 - f)$ is increased by a relatively large amount, though it always remains a comparatively small part of the motion. This accords with the discussion which we gave above of the absorption, that the propagation of zero sound is discouraged by the presence of a large positive F_2.

Since the wave motion accounts for nearly all the motion of the liquid (more than 90%), we can show that the acoustic impedance of liquid He^3 should not be very different from ρc_0, where c_0 is the velocity of zero sound (here we are discussing principally the limit $\omega\tau \to \infty$). We can write the pressure P and the velocity u of the liquid at the boundary in the form

$$P = P_0 + P_1 \qquad\qquad u = u_0 + u_1 ,$$

where P_0 and u_0 are the components due to the wave motion, and P_1 and u_1 are due to the other processes. The acoustic impedance is defined as

$$Z = \frac{P}{u} = \frac{P_0 + P_1}{u_0 + u_1} .$$

As the greater part of the motion is due to the wave, this is not very different from P_0/u_0, which is ρc_0 by (4.1). An order-of-magnitude estimate of P_1/u_1 may be obtained if we notice that the particle motion and the second wave solution have velocities of v_F or less, so $P_1/u_1\rho$ can hardly be greater than 60 - 75 m/s (in general P_1/u_1 is of course complex). We should therefore expect Z/ρ to be a little less than the velocity of zero sound.

In Fig. 30, we show the real part of the acoustic impedance for the same three values of F_2 as were used before. The velocity $\frac{\omega}{\mathrm{Re}\ k}$ is also shown by broken lines, and we see that Z/ρ is indeed smaller than the velocity as expected. The discrepancy between Z/ρ and c_0 increases with F_2, which is consistent with a reduction in the amplitude of the wave component of the disturbance. Presumably the agreement between Z/ρ and c_0 in the case $F_2 = 0$ is fortuitous.

All the graphs drawn so far in this section have been obtained by taking $F_1 = 5{\cdot}6$; the results for $F_1 = 5{\cdot}46$ are qualitatively similar.

It should also be noted that Landau's theory is strictly accurate only in the range of temperature below $0{\cdot}05^\circ$ - $0{\cdot}1^\circ$K. However this is not a rigid criterion, and it is not clear how far the theory can still be useful at higher temperatures. We have therefore included theoretical points over the whole temperature range in order to show the qualitative predictions of the theory.

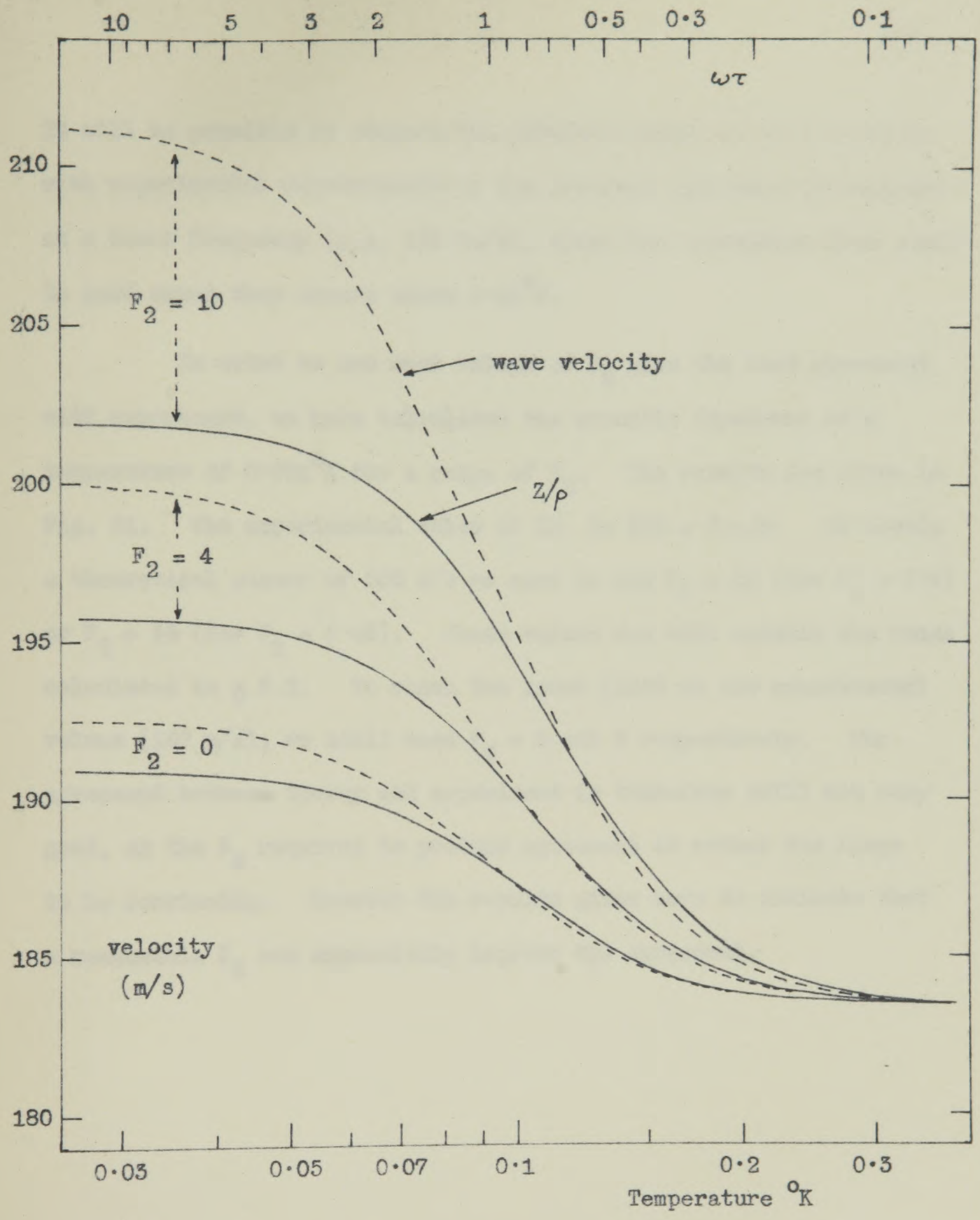

Fig. 30. Acoustic impedance, and the velocity of the dominant wave ($F_o = 7{\cdot}1320$, $F_1 = 3{\cdot}6$)

It will be possible to compare the detailed shape of the transition with experimental measurements if the acoustic impedance is measured at a lower frequency (e.g. 100 Mc/s), since the transition from sound to zero sound then occurs below $0{\cdot}05^{\circ}K$.

In order to see what values of F_2 give the best agreement with experiment, we have calculated the acoustic impedance at a temperature of $0{\cdot}001^{\circ}K$ for a range of F_2. The results are shown in Fig. 31. The experimental value of Z/ρ is 202 ± 5 m/s. To obtain a theoretical answer of 202 m/s we need to use $F_2 = 10$ (for $F_1 = 3{\cdot}6$) or $F_2 = 14$ (for $F_1 = 5{\cdot}46$). These values are well outside the range calculated in § 5.2. To reach the lower limit on the experimental values (197 m/s), we still need $F_2 = 5$ and 8 respectively. The agreement between theory and experiment is therefore still not very good, as the F_2 required to produce agreement is rather too large to be convincing. However the results given here do indicate that a reasonable F_2 can appreciably improve the agreement.

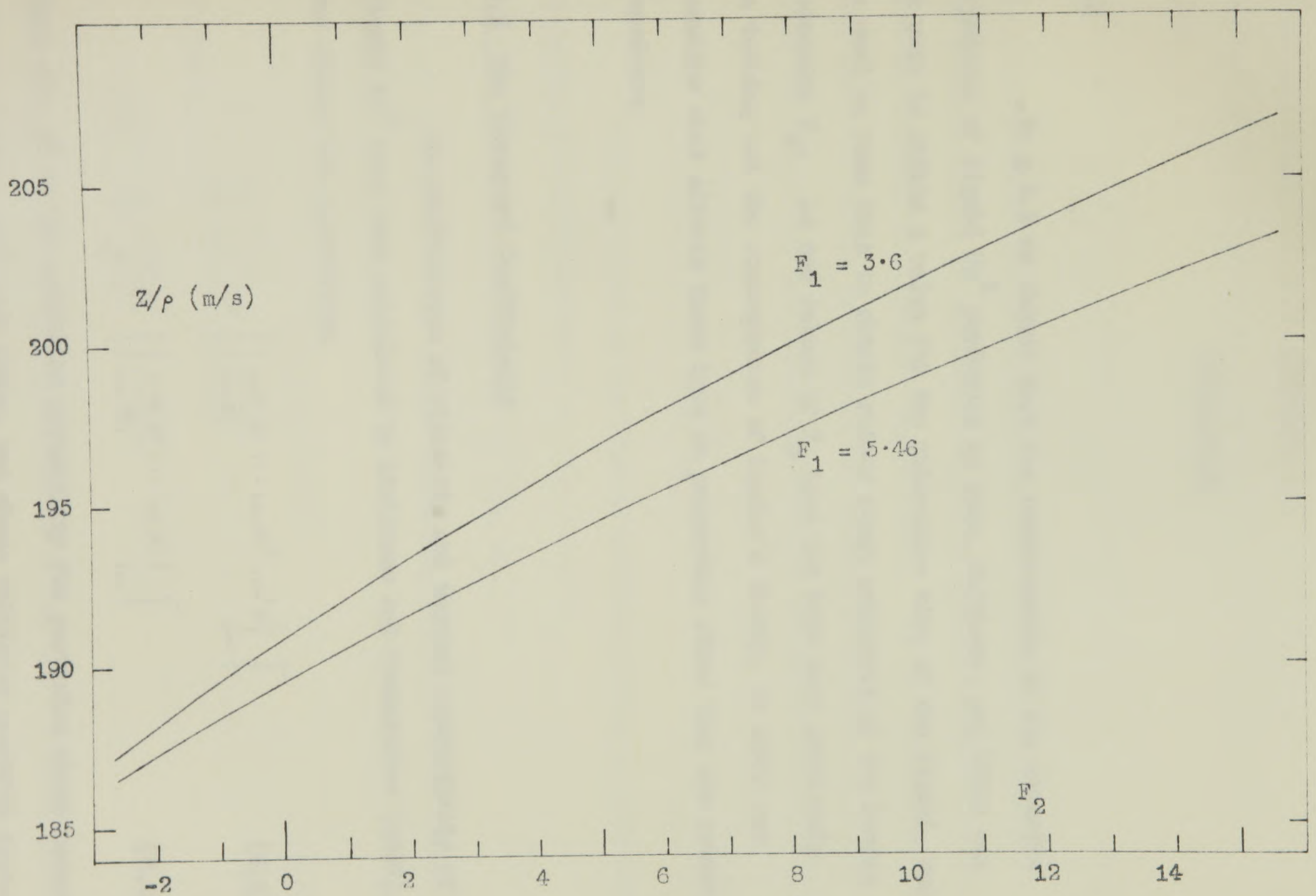

Fig. 31. Acoustic impedance at $0{\cdot}001^{o}K$ as a function of F_2

CHAPTER 6

Discussion

6.1

In § 5.2 we showed that the measurements of the acoustic impedance of liquid He^3 performed by Keen, Matthews, and Wilks can be used to obtain a value for the relaxation time of the liquid, and we went on from this to obtain rather rough estimates of the Landau parameter F_2. As our values of F_2 have not been used previously in working out the consequences of Landau's theory, we shall now consider what effects these have on properties other than the acoustic impedance.

6.2 The Transport Coefficients

The coefficients of viscosity and thermal conductivity of liquid He^3 have been calculated by Abrikosov and Khalatnikov (1957), who obtain the expressions

$$\eta = \frac{64}{45} \frac{\hbar^3 p_F^5}{m_p^{*4} k^2 T^2} \left\{ \left[\frac{w(\theta,\phi)}{\cos\theta/2} (1-\cos\theta)^2 \sin^2\phi \right]_{av} \right\}^{-1} \qquad (6.1)$$

$$K = \frac{8}{3} \frac{\pi^2 \hbar^3 p_F^3}{m_p^{*4} T} \left\{ \left[\frac{w(\theta,\phi)}{\cos\theta/2} (1-\cos\theta) \right]_{av} \right\}^{-1} . \qquad (6.2)$$

Here $w(\theta, \phi)$ is the collision probability for particles whose momenta make an angle θ with each other, and whose collision products appear

in a plane making an angle ϕ with the plane of incidence. The coefficient of diffusion has been calculated by Hone (1961) who obtains

$$D = \frac{32}{3} \frac{\pi^2 \hbar^6 p_F^2}{m_F^{*5} k^2 T^2} (1 + Z_0/4) \left\{ \left[\frac{w(\theta, \phi)}{\cos \theta/2} (1 - \cos\theta)(1 - \cos\phi) \right]_{av} \right\}^{-1}. \qquad (6.3)$$

The present writer has also calculated the collision probability for quasi-particles on the Fermi surface by methods similar to those used for finding the transport coefficients. As the calculation is long and is of little interest in the present discussion, we simply quote the result for the collision time τ_p = (collision probability)$^{-1}$:

$$\tau_F = 32 \frac{\pi^2 \hbar^6}{m_F^{*3} k^2 T^2} \left\{ \left[\frac{w(\theta, \phi)}{\cos \theta/2} \right]_{av} \right\}^{-1}. \qquad (6.4)$$

The magnitudes of the kinetic coefficients can be estimated by making the approximation

$$w(\theta, \phi) = w(\theta, 0).$$

$w(\theta, 0)$ is related to the forward scattering amplitude a for quasi-particles by the relation

$$w(\theta, o) = \frac{2\pi}{\hbar} [a(\theta)]^2. \qquad (6.5)$$

Following Landau (1959) we write

$$\left[\frac{\partial \tau}{\partial \varepsilon}\right]_\mu a(\theta) = A(\theta) = B(\theta) + C(\theta)\, \underline{\sigma}.\underline{\sigma}'$$

where $\underline{\sigma}$ and $\underline{\sigma}'$ are the spin orientations of the two colliding quasi-particles. In the same way the expansion of the complete inter-

action function $f(\underline{p},\underline{\sigma};\ \underline{p}',\ \underline{\sigma}')$ is

$$\left[\frac{\partial \tau}{\partial \varepsilon}\right]_{\varepsilon=\mu} f(\theta,\ \underline{\sigma},\underline{\sigma}') \quad = \quad F(\theta) \ + \ Z(\theta)\ \underline{\sigma}.\underline{\sigma}' .$$

Landau showed that

$$B_n \ = \ \frac{F_n}{1 + \frac{F_n}{2n+1}} \quad , \qquad C_n \ = \ \frac{Z_n}{1 + \frac{Z_n}{4(2n+1)}}$$

so that $w(\theta, 0)$ can be calculated from (6.5) when the F_n and Z_n are known.

In calculating $w(\theta,0)$ it is necessary to treat separately those collisions involving particles with parallel and antiparallel spins, and to calculate an average collision probability from the two separate contributions. This means that the Z_n have to be known as well as the F_n. The parameter Z_o is obtained from the magnetic susceptibility χ of liquid He^3 by the equation

$$\chi \ = \ \frac{3}{2}\frac{N\beta^2}{kT_F^{**}}$$

where $$kT_F^{**} \ = \ \frac{p_F^2}{2m_F^*}\ (1 + Z_o/4).$$

Experimental values of T_F^{**} are:

$0{\cdot}54^{\circ}K$ (Anderson, Hart, and Wheatley (1960));

$0{\cdot}45$ (Thomson, Meyer, and Adams (1962));

$0{\cdot}58$ (Beal (1964)).

We use the value $T_F^{**} = 0{\cdot}58^{\circ}K$. The scattering amplitude $A(\theta)$ must

be zero for a collision at $\theta = 0$ involving particles with parallel spins, so following Hone (1962), we use this condition to estimate C_1 by

$$\frac{C_1}{4} = -\left(B_0 + B_1 + B_2 + \frac{C_0}{4}\right).$$

With this convention we obtain the following tables for the transport coefficients.

$F_1 = 5{\cdot}46$

F_2 =	0	2	5	10		
ηT^2	2·44	8·32	5·23	1·45	micropoise $^oK^2$	
κT	86·7	169	96·0	52·3	erg cm^{-1} sec^{-1}	
DT^2	6·47	8·57	8·52	7·70	cm^2 sec^{-1} $^oK^2$	$(\times 10^{-6})$
$\tau_F T^2$	1·46	1·45	1·00	0·71	sec $^oK^2$	$(\times 10^{-12})$

$F_1 = 3{\cdot}6$

F_2 =	0	2	5	10		
ηT^2	1·10	2·34	3·20	2·71	micropoise $^oK^2$	
κT	45·7	83·3	101	87·5	erg cm^{-1} sec^{-1}	
DT^2	3·47	4·48	5·28	5·85	cm^2 sec^{-1} $^oK^2$	$(\times 10^{-6})$
$\tau_F T^2$	0·88	1·11	1·05	0·88	sec $^oK^2$	$(\times 10^{-12})$

These figures are to be compared with experimental values:

$\eta T^2 = 2{\cdot}7 - 4{\cdot}2$ micropoise $^oK^2$

$\kappa T = 48$ erg cm^{-1} sec^{-1}

$DT^2 = 1{\cdot}54 \times 10^{-6}$ cm^2 sec^{-1} $^oK^2$

$\tau_F T^2 = 1{\cdot}35 \times 10^{-12}$ sec $^oK^2$

It may be seen that the results are very sensitive to the value assumed for F_1, so that the transport coefficients may be changed by a factor of up to 2 by changing F_1 from 5·6 to 5·46. Also our results for the case $F_1 = 5{\cdot}46$ and $F_2 = 0$ are about 50% higher than those quoted by Hone (1962) due to a different choice of T_F^{**}. A further uncertainty amounting to perhaps a factor 2 is introduced by the use of the approximation $w(\theta, \phi) \simeq w(\theta, 0)$. It seems therefore that a comparison of predicted and observed transport coefficients cannot help us to put closer limits on F_2, until the other parameters are known more accurately. Meanwhile, we conclude that a value of F_2 between 0 and 5 does not lead to values for the transport coefficients which are inconsistent with the observed magnitudes.

6.3 The Specific Heat

In the first order, the specific heat of liquid He^3 is determined only by the parameter F_1, but when a second approximation is taken by evaluating the specific heat to order T^3, higher parameters become relevant.

The specific heat correct to order T^3 is

$$C = \frac{\pi^2 k^2 T}{3}\left[\frac{\partial \tau}{\partial \varepsilon}\right]_{\varepsilon=\mu}\left\{1 - \frac{3\pi^2 k^2 T^2}{10}\left(\frac{2m_F^*}{p_F^2}\right)^2(1+\phi) + O(T^4)\right\}. \qquad (6.6)$$

Here $\left[\frac{\partial \tau}{\partial \varepsilon}\right]_\mu = \frac{p_F m_F^*}{\pi^2 \hbar^3}$ is the density of states at the Fermi surface (evaluated at absolute zero) and ϕ is given by

$$\phi = \left[\frac{5}{12}p^2\frac{\partial^2 \mathcal{F}_0}{\partial p \partial p'} - \frac{p^2}{9}\frac{\partial}{\partial p}\left(\frac{\mathcal{F}_1}{p}\right) - \frac{7}{36}p^2\frac{\partial^2}{\partial p^2}\left(\frac{\mathcal{F}_1}{p}\right) - \frac{4}{27}\left\{p^2\frac{\partial}{\partial p}\left(\frac{\mathcal{F}_1}{p}\right)\right\}^2\right]_{p=p'=p_F} \qquad (6.7)$$

where $\mathcal{F}(p, \chi, p') = \left[\frac{\partial \tau}{\partial \varepsilon}\right]_{\varepsilon=\mu} f(\underline{p}, \underline{p}')$.

Richards (1965) calculates the specific heat to order T^3, but he only obtains the first term in ϕ; equation (6.7) is the complete expression, and it is exact if C is required to order T^3 only.

The derivatives of $\mathcal{F}(\underline{p}, \underline{p}')$ in equation (6.7) are not known, so ϕ can only be evaluated if we make an assumption about $\mathcal{F}(\underline{p}, \underline{p}')$. Richards makes the assumption that

$$\mathcal{F}(\underline{p}, \underline{p}') = \mathcal{F}(|\underline{p} - \underline{p}'|). \qquad (6.8)$$

Equation (6.8) is equivalent to assuming that

$$\left[\int g(\underline{p}, \underline{p}'', \underline{p}')\, \underline{p}''\, \frac{d\Omega''}{4\pi}\right]_{p''=p_F} = 0 \qquad (6.9)$$

for all $\underline{p}$, $\underline{p}'$, where $g(\underline{p}, \underline{p}', \underline{p}'')$ is the third derivative of the energy E, and is defined by

$$\delta f(\underline{p}, \underline{p}') = \int g(\underline{p}, \underline{p}', \underline{p}'')\, \delta n(\underline{p}'')\, d\tau''. \qquad (6.10)$$

By expanding $\mathcal{F}(|\underline{p}-\underline{p}'|)$ as a power series in $|\underline{p} - \underline{p}'|$, and by assuming also that the series $F(\chi) = \sum_n F_n P_n(\cos\chi)$ terminates at F_2, one finds after a lengthy substitution that

$$\phi = 3F_2 - \frac{4}{3}F_2^2 . \qquad (6.11)$$

In this approximation, ϕ can never be larger than 27/16 (when $F_2 = 9/8$) although the values obtained from experiment are in the range 8 - 30.

The above calculation is however not very realistic, because we have made the following assumptions in deriving (6.11):

(i) Landau's theory applies over the range of temperature where the T^3 term in the specific heat is appreciable;

(ii) $\mathcal{F}(\underline{p}, \underline{p}')$ has the property (6.8);

(iii) the series for $F(\chi)$ terminates at F_2.

The fact that Richards' values for ϕ estimated from the pressure dependence of F_0 and F_1 are large enough to account for the observed T^3 term in the specific heat suggests that assumption (i) is satisfied. There is however little justification for assumption (ii). Hence it is not clear how much the properties of equation (6.11) are due to the assumption that $\mathcal{F}(\underline{p}, \underline{p}') = \mathcal{F}(|\underline{p} - \underline{p}'|)$, and how much to the assumption that F_3, F_4 etc. are zero. The lack of agreement between the calculated and experimental values of ϕ must therefore unfortunately be regarded as inconclusive.

6.4 Transverse Waves

The equation giving the propagation constant k of transverse (m = 1) oscillations in He^3 is set up in a very similar way to that for longitudinal waves. The equation obtained by assuming that $F(\chi)$ contains terms up to F_2 only is

$$\omega(1-\xi^2) + \frac{1}{3} = \frac{\frac{2}{3}(1+\alpha)}{F_1/3 - \alpha + 4\alpha\xi^2(1+\alpha)} \qquad (6.12)$$

where $\xi = \dfrac{i\omega\tau - 1}{ik\tau v_F}$ $\qquad \alpha = \dfrac{1}{i\omega\tau - 1}$

$$\alpha = \frac{F_2/4}{1 + F_2/5} \qquad \omega = \frac{\xi}{2}\ln\left(\frac{\xi+1}{\xi-1}\right) - 1 .$$

In the limit $\omega\tau \to 0$, the propagation constant reduces to

$$k = \frac{\omega}{v_F}\sqrt{\frac{5}{2(1+F_1/3)(1+F_2/5)\omega\tau}}\,(1+i) = \sqrt{\frac{\omega\rho}{2\eta}}\,(1+i)$$

which is the expression obtained from hydrodynamics for a viscous wave in a fluid (cf section 3.2 where m = 1 waves were stated to be analogous to viscous waves).

In the limit $\omega\tau \to \infty$, the existence of a wave solution depends on the details of the interaction function $F(\chi)$. There will be a solution ("transverse zero sound") if

$$F_1 + \frac{3F_2}{1 + F_2/5} > 6. \qquad (6.13)$$

Taking our lowest estimate of F_1 (= 3·6), the condition (6.13) can be

can be satisfied if $F_2 > 0{\cdot}95$, while for $F_1 = 5{\cdot}46$, F_2 need only be $0{\cdot}19$ to satisfy (6.13). There is therefore a possibility that transverse zero sound may exist in liquid He^3 under the vapour pressure, but the uncertainty in the parameters prevents a definite prediction. The experiments of Anderson, Salinger, Steyert, and Wheatley (1961 b) show that F_1 increases considerably with pressure, rising to a value of about 10 in the region of 25 atmospheres. Therefore transverse zero sound should certainly be observable when the pressure is increased to a few atmospheres.

6.5 The Kapitza Boundary Resistance

The Kapitza boundary resistance between a solid and liquid He^3 has been calculated by Bekarevich and Khalatnikov (1961). They assume that the only mechanism for transferring heat from a solid to liquid He^3 is the radiation of acoustic energy by the solid. Thus if the solid boundary has r.m.s. velocity components U_z and U_x along the normal and transverse directions, the rate of energy transfer is

$$W = Z_l U_z^2 + Z_t U_x^2 \qquad (6.14)$$

where Z_l and Z_t are the acoustic impedances of liquid He^3 for longitudinal and transverse oscillations respectively. Khalatnikov calculates U_z^2 and U_x^2 by considering the reflection of longitudinal and transverse waves at the surface of the solid, and adds in a

separate contribution due to surface waves. Thus he finds

$$\left.\begin{aligned} U_z^2 &= \frac{4\pi^5}{15}\frac{(kT)^4}{\rho_s(2\pi\hbar c_t)^3}F \\ U_x^2 &= \frac{4\pi^5}{15}\frac{(kT)^4}{\rho_s(2\pi\hbar c_t)^3}\Phi \end{aligned}\right\} \qquad (6.15)$$

where ρ_s is the density of the solid, and c_t is the velocity of transverse waves in the solid. F and Φ are both numbers of the order of unity. It follows that the rate of energy transfer between a solid and liquid He^3 is equal to

$$W = \frac{4\pi^5}{15}\frac{(kT)^4}{\rho_s(2\pi\hbar c_t)^3}(Z_\ell F + Z_t \Phi)$$

when the solid is at temperature T. Energy must of course be transferred at this rate equally in both directions when the temperatures of liquid and solid are equal. When there is a temperature difference ΔT, a net flow of heat ΔW results, and a thermal boundary resistance R may be defined as

$$R = \frac{\Delta T}{\Delta W} = \frac{15}{16\pi^5}\frac{\rho_s}{k}\left(\frac{2\pi\hbar c_t}{kT}\right)^3\frac{1}{Z_\ell F + Z_t \Phi} . \qquad (6.16)$$

We must emphasize that in this section U_z and U_x have always been root mean square values. We use capital U's to denote r.m.s. values and small letters to denote amplitudes, so as to be consistent with our previous notation. In Bekarevich and Khalatnikov's notation,

$$\Pi_{33} = -3\frac{\rho}{m}\psi_{2n} = 3\frac{\rho}{m}p_F u_z a \qquad \text{or} \quad \frac{Z_\ell}{\rho} = 3\frac{p_F}{m}a$$

$$\Pi_{13} = -3\frac{\rho}{m}\psi_{2t} = 3\frac{\rho}{m}p_F u_{zc} b \qquad \text{or} \quad \frac{Z_t}{\rho} = 3\frac{p_F}{m}b .$$

Thus $$R = \frac{5}{16\pi^5}\frac{\rho_s}{k}\left(\frac{2\pi\hbar c_t}{kT}\right)^3 \frac{1}{aF + b\Phi}\,\frac{1}{\rho p_F/m} . \qquad (6.17)$$

The resistance given by (6.17) is half that given by Bekarevich and Khalatnikov in their equation (4.7). It would appear that a factor 2 has appeared in Bekarevich and Khalatnikov's calculation due to a confusion between r.m.s. and peak values of the velocities. Thus they write

$$W = \frac{1}{2}\frac{3\rho p_F}{m}\left[a|u_z|^2 + b|u_t|^2\right] \qquad (6.18)$$

explicitly saying that the $\frac{1}{2}$ at the front of this expression arises from averaging over the period of vibration. Therefore (6.18) is correct only if $|u_z|^2$ and $|u_t|^2$ are the peak values, but B and K proceed to substitute for them an expression which is true for r.m.s. values.

The quantity of greatest interest in the calculation is the value of the ratio

$$\frac{(T^3R)_{low\,T}}{(T^3R)_{high\,T}} .$$

At high temperatures, the transverse term in the energy transfer (6.14) is negligible, so that energy is transferred from solid to liquid in

the form of sound waves. Equation (6.16) reduces in this case to

$$(T^3R)_{high\,T} = \frac{15}{16\pi^5}\,\frac{\rho_s(2\pi\hbar c_t)^3}{k^4}\,\frac{1}{\rho c\,F}\,.$$

In the low-temperature case, we know that Z_1 is larger than (ρc) by a factor $\beta \sim 1{\cdot}1$. Thus

$$(T^3R)_{low\,T} = \frac{15}{16\pi^5}\,\frac{\rho_s(2\pi\hbar c_t)^3}{k^4}\,\frac{1}{\beta(\rho c)\,F + Z_t\,\Phi}\,,$$

$$\frac{(T^3R)_{low\,T}}{(T^3R)_{high\,T}} = \frac{(\rho c)}{\beta(\rho c) + Z_t\,\Phi/F}\,. \qquad (6.19)$$

This ratio is obviously less than 1, and is actually about 0·85. However by the inclusion of a spurious factor 2 and some rather rough arithmetic, Bekarevich and Khalatnikov make it about 3.

If the assumption that thermal transfer takes place by acoustic radiation is accepted, a measurement of $\frac{(T^3R)_{low\,T}}{(T^3R)_{high\,T}}$ amounts in effect to a measurement of $\beta = \frac{Z_{\omega\tau\to\infty}}{\rho c}$ with a correction to be applied for the transverse term. The theory given in chapters 4 and 5 of this thesis then applies, and β should be between 1·05 and 1·1.

The Kapitza boundary resistance has been measured in the temperature range $0{\cdot}06^\circ$ - $0{\cdot}6^\circ$K by Anderson, Connolly, and Wheatley (1964) who find that the product T^3R rises by a factor of about 5 between the high and low-temperature regions. Since the wavelength of the phonons responsible for thermal transfer is a function of

temperature, they consider the possible effect of surface roughness in accounting for this rise, but conclude that acoustic radiation is not the only mechanism of thermal transfer. Anderson, Connolly, and Wheatley also discuss the experiment of Keen, Matthews, and Wilks in terms of the Bekarevich-Khalatnikov theory, but as they use the equations given by B and K without removing the spurious factor 2, we disagree with their conclusions.

6.6 Conclusions

In the last few sections we have discussed the various properties of liquid He^3 which might be affected by including the parameter F_2 in the theory. In all cases except the acoustic impedance, we find that no improvement can be obtained, but this is due to the uncertainty in the other parameters, or to approximations in the theory, and in no case does the introduction of F_2 make the agreement between theory and experiment any worse. In the case of the acoustic impedance, the agreement between theory and experiment is appreciably improved by including F_2, though even here the agreement is still not perfect.

With an F_2 between 0 and 5 included in Landau's theory, the acoustic impedance predicted by the theory agrees with experiment to within 2 - 5% in the low temperature region. There is still however a small discrepancy, and the values of F_2 needed to remove

this are larger than are plausible (see § 5.2). The discrepancy could perhaps be removed by introducing a further parameter (F_3), but until an independent estimate of F_3 becomes available, it is not worthwhile to attempt this. It may be that agreement with experiment to better than 5% is all that can be expected from Landau's theory, in which case the situation can be regarded as satisfactory, but we feel that an attempt at obtaining a closer agreement was justified.

The experiment of Keen, Matthews, and Wilks was performed in an attempt at verifying Landau's prediction that zero sound should be observable in liquid He^3. The fact that the experiment gives results in quantitative agreement with the theory provides a valuable support to the theory, and it may well be justifiable to argue that if the theory gives good numerical predictions, it is probably also qualitatively correct. But the experiment does not provide direct evidence for zero sound, and it is of considerable interest to see if a more direct test can be devised.

The most obvious experiment to attempt is a measurement of the absorption of sound. If zero sound exists, the absorption should show a peak as in Figs. 15 and 16, and it should vary as T^2 on the low-temperature side of the peak. Unfortunately it is not immediately clear that the observation of this behaviour guarantees the existence of zero sound. Single quasi-particles excited by an oscillating boundary constitute a disturbance which travels into the liquid for a distance of about τv_F; as τ varies as T^{-2}, the atten-

uation of this disturbance decreases like T^2 as the temperature is reduced, that is it varies in the same way as that of zero sound. It is probable however that the effect of the single-particle motion on an acoustic receiver should be small if the receiver is separated from the transmitter by a distance greater than $2\pi v_p/\omega$. Under these circumstances, particles may bounce off the transmitter onto the receiver without colliding with other particles on the way. Particles travelling normally carry information which is out of date by one period when they reach the receiver. Particles moving at other angles carry information which is out of date by larger amounts, and so their effect on the receiver is to oppose the signal carried by the first particles. It is therefore to be expected that the signal transferred by the particle motion should vary with distance in a non-exponential manner, and in particular that it should die away very rapidly at large distances. The principal effect of zero sound should therefore be to effect a large decrease in the absorption compared with that of the particle motion alone, and it is this quantitative feature rather than the temperature dependence which should serve to identify zero sound. (In order to analyse measurements of the absorption coefficient, it is desirable to find an expression for the energy transfer by an extension of Bekarevich and Khalatnikov's calculation; this has not yet been done.)

REFERENCES

Abel, Anderson, and Wheatley	(1961)	Phys. Rev. Letters 7, 299.
Abrikosov and Khalatnikov	(1957)	Soviet Physics JETP 5, 887.
Abrikosov and Khalatnikov	(1958)	Soviet Phys. JETP 6, 84.
Abrikosov and Khalatnikov	(1959)	Rep. Prog. Phys. 22, 329.
Anderson, Connolly, and Wheatley	(1964)	to be published.
Anderson, Hart, and Wheatley	(1960)	Phys. Rev. Letters 5, 133.
Anderson, Reese, and Wheatley	(1963)	Phys. Rev. 130, 495.
Anderson, Salinger, Steyert, and Wheatley	(1961a)	Phys. Rev. Letters 6, 331.
Anderson, Salinger, Steyert, and Wheatley	(1961b)	Phys. Rev. Letters 7, 295.
Beal	(1964)	private communication.
Bekarevich and Khalatnikov	(1961)	Soviet Phys. JETP 12, 1187.
Bernardes and Brewer	(1962)	Revs. Mod. Phys. 34, 190.
Betts and Wilks	(1964)	to be published.
Brewer and Keyston	(1961)	Nature 191, 1261.
Brueckner and Gammel	(1958)	Phys. Rev. 109, 1040.
Carr and Strandenberg	(1962)	J. Phys. Chem. Solids 23, 925.
Hone	(1961)	Phys. Rev. 121, 669.
Hone	(1962)	Phys. Rev. 125, 1494.
Jacobsen	(1960a)	J. Acoust. Soc. Amer. 32, 949.
Jacobsen	(1960b)	Quantum Electronics, p. 468.
Keen, Matthews, and Wilks	(1963)	Phys. Letters 5, 5.

Landau	(1957a)	Soviet Phys. JETP 3, 920
Landau	(1957b)	Soviet Phys. JETP 5, 101
Landau	(1959)	Soviet Phys. JETP 8, 70.
Laquer, Sydoriak, and Roberts	(1959)	Phys. Rev. 113, 417.
McSkimin	(1956)	J. Acoust. Soc. Amer. 28, 484.
Moreno	(1948)	Microwave Transmission Design Data, p. 229.
Pochhammer	(1876)	J. f. Math. (Crelle), Bd 81, p.324.
Richards	(1963)	Phys. Rev. 132, 1867.
Rives and Meyer	(1961)	Phys. Rev. Letters 7, 217.
Salinger	(1961)	Report No. 1. under US Contract No. AT(11-1)-1056.
Sherman and Bdeskuty	(1960)	Ann. Phys. 9, 522.
Shiren	(1961)	Phys. Rev. Letters 6, 168.
Strongin, Zimmerman, and Fairbank	(1961)	Phys. Rev. Letters 6, 404.
Sykes	(1964)	private communication.
Thomson, Meyer, and Adams	(1962)	Phys. Rev. 125, 509.
Tolansky	(1960)	Surface Microphotography.
Waterman	(1959)	Phys. Rev. 113, 1240.
Wiener and Hopf	(1931)	Berliner Ber. Math. Phys. Klasse, p. 696.